

DESIGN OF SELF-ORGANIZING MAP TYPE ELECTROMAGNETIC  
TARGET CLASSIFIERS FOR DIELECTRIC SPHERES AND CONDUCTING  
AIRCRAFT TARGETS WITH INVESTIGATION OF THEIR NOISE  
PERFORMANCES

A THESIS SUBMITTED TO  
THE GRADUATE SCHOOL OF NATURAL AND APPLIED SCIENCES  
OF  
MIDDLE EAST TECHNICAL UNIVERSITY

BY

TUFAN TAYLAN KATILMIŞ

IN PARTIAL FULFILLMENT OF THE REQUIREMENTS FOR THE DEGREE  
OF  
MASTER OF SCIENCE  
IN  
ELECTRICAL AND ELECTRONICS ENGINEERING

NOVEMBER 2009

Approval of the thesis:

**DESIGN OF SELF-ORGANIZING MAP TYPE ELECTROMAGNETIC TARGET  
CLASSIFIERS FOR DIELECTRIC SPHERES AND CONDUCTING AIRCRAFT  
TARGETS WITH INVESTIGATION OF THEIR NOISE PERFORMANCES**

submitted by **TUFAN TAYLAN KATILMIŞ** in partial fulfillment of the requirements for the degree of Master of Science in **Electrical and Electronics Engineering Department, Middle East Technical University** by,

Prof. Dr. Canan Özgen \_\_\_\_\_  
Dean, Graduate School of **Natural and Applied Sciences**

Prof. Dr. İsmet Erkmn \_\_\_\_\_  
Head of Department, **Electrical and Electronics Engineering**

Prof. Dr. Gönül Turhan Sayan \_\_\_\_\_  
Supervisor, **Electrical and Electronics Engineering**

**Examining Committee Members:**

Prof. Dr. Mustafa Kuzuoğlu \_\_\_\_\_  
Electrical and Electronics Engineering Dept., METU

Prof. Dr. Gönül Turhan Sayan \_\_\_\_\_  
Electrical and Electronics Engineering Dept., METU

Prof. Dr. Kemal Leblebicioğlu \_\_\_\_\_  
Electrical and Electronics Engineering Dept., METU

Prof. Dr. Gülbin Dural \_\_\_\_\_  
Electrical and Electronics Engineering Dept., METU

Mustafa Seçmen, PhD. in EE \_\_\_\_\_  
METU-MEMS

**Date :** 19.11.2009

**I hereby declare that all information in this document has been obtained and presented in accordance with academic rules and ethical conduct. I also declare that, as required by these rules and conduct, I have fully cited referenced all material and results that are not original to this work.**

Name, Last name: Tufan Taylan KATILMIŞ

Signature :

## **ABSTRACT**

# **DESIGN OF SELF-ORGANIZING MAP TYPE ELECTROMAGNETIC TARGET CLASSIFIERS FOR DIELECTRIC SPHERES AND CONDUCTING AIRCRAFT TARGETS WITH INVESTIGATION OF THEIR NOISE PERFORMANCES**

KATILMIŞ, Tufan Taylan

M.S. Department of Electrical and Electronics Engineering

Supervisor :Prof. Dr. Gönül TURHAN SAYAN

November 2009, 147 pages

The Self-Organizing Map (SOM) is a type of neural network that forms a regular grid of neurons where clusters of neurons represent different classes of targets. The aim of this thesis is to design electromagnetic target classifiers by using the Self-Organizing Map (SOM) type artificial neural networks for dielectric and conducting objects with simple or complex geometries. Design simulations will be realized for perfect dielectric spheres and also for small-scaled aircraft targets modeled by thin conducting wires. The SOM classifiers will be designed by target features extracted from the scattered signals of targets at various aspects by using the Wigner distribution. Noise performance of classifiers will be improved by using slightly noisy input data in SOM training.

Keywords: Electromagnetic target classification, Self-Organizing Maps, Wigner-Ville distribution, feature extraction, noise analysis.

## ÖZ

# YALITKAN KÜRELER VE İLETKEN UÇAKLAR İÇİN ÖZ- ÖRGÜTLENMELİ HARİTA TİPİ ELEKTROMANYETİK HEDEF SINIFLANDIRICILARIN TASARIMI VE GÜRÜLTÜ PERFORMANSLARININ İNCELENMESİ

KATILMIŞ, Tufan Taylan

Y. Lisans, Elektrik ve Elektronik Mühendisliği Bölümü

Tez Yöneticisi : Prof. Dr. Gönül TURHAN SAYAN

Kasım 2009, 147 sayfa

Öz Örgütlenmeli Harita, haritadaki her nöronun bir sınıfı temsil ettiği, girdi verilerinden düzenli bir harita oluşturan yapay sinir ağı çeşididir. Bu tezin amacı, Öz Örgütlenmeli Harita tipi yapay sinir ağları kullanarak basit veya karmaşık geometrilere sahip yalıtkan ve iletken cisimler için elektromanyetik hedef sınıflandırıcılar tasarlamaktır. Tasarım benzetimleri mükemmel yalıtkan küreler ve ince iletken tellerle modellenmiş küçük ölçekli uçaklar için yapılacaktır. Öz örgütlenmeli haritaların tasarımında, hedeflerin çeşitli görüş açılarına ait saçınım işaretlerinden Wigner dağılımı kullanılarak çıkarılmış öznitelikler kullanılacaktır. SOM eğitiminde az gürültülü girdi verileri kullanarak, sınıflandırıcıların gürültü performanları iyileştirilecektir.

Anahtar sözcükler: Elektromanyetik hedef sınıflandırma, Öz Örgütlenmeli Harita, Wigner-Ville dağılımı, öznitelik çıkarımı.

To My Family

## ACKNOWLEDGEMENTS

I would like to express my deepest gratitude to my supervisor Prof. Dr. Gönül TURHAN SAYAN for her guidance, advices, and encouragements, insight throughout this thesis study. I would like to thank also for giving me the opportunity to work on this research topic.

My special thanks to M.Alper SELVER, H.Gökalp CİNBIŞ, Eda ÇETİNER and Burcu ELLİDÖRT for their support.

Lastly, I would like to express my gratitude to my parents, Jale -Yavuz KATILMIŞ and my sister, Pınar TÜRKDEMİR for their encouragement and support.

## TABLE OF CONTENTS

ABSTRACT .....	iv
ÖZ .....	v
ACKNOWLEDGEMENTS .....	vii
TABLE OF CONTENTS .....	viii
LIST OF TABLES .....	xi
LIST OF FIGURES .....	xiii
CHAPTERS	
1.INTRODUCTION .....	1
2.THEORY .....	5
2.1    Self Organizing Map Type Artificial Neural Networks .....	5
2.1.1.    Structure of Self Organizing Maps .....	6
2.1.2.    Kohonen Learning Algorithm .....	9
2.2    Target Feature Extraction Using Wigner Distribution .....	13
2.2.1.    Wigner Distrubution Based Feature Extraction Technique .....	14
3.DESIGN OF SOM CLASSIFIERS FOR DIELECTRIC SPHERES .....	18
3.1    Description of Electromagnetic Scattered Data of Dielectric Spheres and Simulation Parameters Used in Classifier Design and Testing.....	20
3.2    Design of SOM Classifiers for the Target Library TL1 of Two Dielectric Spheres .....	24
3.2.1.    Classifier Simulation #1: Design of a SOM Classifier Using Noise-Free Reference Data for the Target Library TL1 with Spheres S1 and S2 .....	25
3.2.2.    Classifier Simulation #2: Design of a SOM Classifier Using Slightly Noisy (SNR Level of 20 dB) Reference Data for the Target Library TL1 with spheres S1 and S2 .....	32



3.2.3. Classifier Simulation #3: Design of a SOM Classifier Using Moderately Noisy (SNR Level of 10 dB) Reference Data for the Target Library TL1 with spheres S1 and S2 .....	38
3.3 Design of SOM Classifiers for the Target Library TL2 of Three Dielectric Spheres .....	43
3.3.1. Classifier Simulation #4: Design of a SOM Classifier Using Noise-Free Reference Data for the Target Library TL2 with Spheres S1, S2 and S3 .....	44
3.3.2. Classifier Simulation #5: Design of a SOM Classifier Using Slightly Noisy (SNR Level of 20 dB) Reference Data for the Target Library TL2 of Spheres S1, S2 and S3.....	50
3.3.3. Classifier Simulation #6: Design of a SOM Classifier Using Moderately Noisy (SNR Level of 10 dB) Reference Data for the Target Library TL2 of Spheres S1, S2 and S3 .....	54
3.4 Design of SOM Classifiers for the Target Library TL3 of Four Dielectric Spheres .....	57
3.4.1. Classifier Simulation #7: Design of a SOM Classifier Using Noise-Free Reference Data for the Target Library TL3 with spheres S1, S2, S3 and S4 ....	58
3.4.2. Classifier Simulation #8: Design of a SOM Classifier Using Slightly Noisy (SNR Level of 20 dB) Reference Data for the Target Library TL3 with Spheres S1, S2, S3 and S4 .....	64
4.DESIGN OF SOM CLASSIFIERS FOR SMALL-SCALE MODEL AIRCRAFT ...	70
4.1 Description of Electromagnetic Scattered Data of Small Scale Aircraft and Simulation Parameters Used in Classifier Design and Testing.....	72
4.2 Design of SOM Classifiers for the Target Library TL4 of Two Small Scale Aircraft .....	74
4.2.1. Classifier Simulation #9: Design of a SOM Classifier Using Noise-Free Reference Data for the Target Library TL4 with Two Aircraft .....	75
4.2.2. Classifier Simulation #10: Design of a SOM Classifier Using Slightly Noisy (SNR Level of 20 dB) Reference Data for the Target Library TL4 with Two Aircraft.....	82

4.2.3. Classifier Simulation #11: Design of a SOM Classifier Using Moderately Noisy (SNR Level of 10 dB) Reference Data for the Target Library TL4 with Two Aircraft.....	87
4.3 Design of SOM Classifiers for the Target Library TL5 of Three Small-Scale Aircraft.....	93
4.3.1. Classifier Simulation #12: Design of a SOM Classifier Using Noise-Free Reference Data for the Target Library TL5 with Three Aircraft.....	95
4.3.2. Classifier Simulation #13: Design of a SOM Classifier Using Slightly Noisy (SNR Level of 20 dB) Reference Data for the Target Library TL5 with Three Aircraft.....	101
4.3.3. Classifier Simulation #14: Design of a SOM Classifier Using Moderately Noisy (SNR Level of 10 dB) Reference Data for the Target Library TL5 with Three Aircraft.....	107
4.4 Design of SOM Classifiers for the Target Library TL6 of Four Small Scale Aircraft.....	113
4.4.1. Classifier Simulation #15: Design of a SOM Classifier Using Noise-Free Reference Data for the Target Library TL6 with Four Aircraft.....	114
4.4.2. Classifier Simulation #16: Design of a SOM Classifier Using Slightly Noisy (SNR Level of 20 dB) Reference Data for the Target Library TL6 with Four Aircraft.....	120
4.4.3. Classifier Simulation #17: Design of a SOM Classifier Using Moderately Noisy (SNR Level of 10 dB) Reference Data for the Target Library TL6 with Four Aircraft.....	126
5.CONCLUSION.....	133
REFERENCES.....	139
APPENDIX.....	143

## LIST OF TABLES

Table 3.1 Descriptions of target libraries containing the same size lossless dielectric spheres with different permittivity values $\varepsilon = \varepsilon_0 \varepsilon_r$ .....	32
Table 3.2 Correct decision rates for the Classifier #1 at different testing SNR levels for each type of cluster boundary.....	43
Table 3.3. Correct decision rates for the Classifier #2 at different testing SNR levels. ....	49
Table 3.4. Correct decision rates for the Classifier #3 at different testing SNR levels for each type of cluster boundary.....	53
Table 3.5 Correct decision rates for the Classifier #4 at different testing SNR levels. ....	61
Table 3.6 Correct decision rates for Classifier #5 at different testing SNR levels. ...	66
Table 3.7 Correct decision rates for the Classifier #7 at different testing SNR levels. ....	75
Table 3.8 Correct decision rates for the Classifier #8 at different testing SNR levels. ....	80
Table 4.1 Descriptions of target libraries containing small-scale aircraft targets.....	82
Table 4.2 Dimensions of the small-scale aircraft targets used in Chapter 4. ....	83
Table 4.3 Correct decision rates for the Classifier #9 at different testing SNR levels for two different $\theta$ range .....	93
Table 4.4 Correct decision rates for the Classifier #10 at different testing SNR levels for two different $\theta$ range. ....	98
Table 4.5 Correct decision rates for the Classifier #11 at different testing SNR levels for two different $\theta$ range .....	104
Table 4.6 Correct decision rates for the Classifier #12 at different testing SNR levels for two different $\theta$ range .....	112
Table 4.7 Correct decision rates for the Classifier #13 at different testing SNR levels for two different $\theta$ range. ....	118

Table 4.8 Correct decision rates for the Classifier #14 at different testing SNR levels for two different $\theta$ range. ....	124
Table 4.9 Correct decision rates for the Classifier #15 at different testing SNR levels for two different $\theta$ range. ....	131
Table 4.10 Correct decision rates for the Classifier #16 at different testing SNR levels for two different $\theta$ range. ....	137
Table 4.11 Correct decision rates for the Classifier #17 at different testing SNR levels for two different $\theta$ range. ....	143

## LIST OF FIGURES

Figure 2.1. Two dimensional lattice structures of SOM. ....	7
Figure 2.2 Different Types Of SOM Output Maps (reproduced from Demo #3 of The SOM Toolbox 2 of [18]). ....	8
Figure 2.3 Three possible functions for learning rate: Linear (red), power series (black) and inverse-of-time (blue). (The figure is reproduced from Demo #3 of the SOM Toolbox 2 of [18]). ....	10
Figure 2.4 The four neighborhood functions (a) bubble, (b) gaussian, (c) cut gaussian and (d) epanechicov. ....	11
Figure 3.1 (a) Problem geometry used to synthesize electromagnetic signals scattered from dielectric spheres. (b) Scattered response of the sphere S2, at $\theta=75$ degrees aspect angle with SNR = 20 dB SNR level. (c) LTFV of sphere S2, at the reference aspect angle $\theta =75^\circ$ for 20 dB SNR level. ....	20
Figure 3.2 The CCF versus $q^*$ plot generated to determine the optimal late-time design interval for the target library TL1 in the case of noise-free classifier design. ....	22
Figure 3.3 The CCF versus $q^*$ plot generated to determine the optimal late-time design interval for the target library TL2 in the case of (a) SNR level of 20 dB and (b) SNR level of 10 dB classifier designs. ....	23
Figure 3.4 SOM output trained by the noise-free WD-based late time energy feature vectors of the dielectric spheres S1 and S2. ....	27
Figure 3.5 Winning neuron locations for the training features of spheres S1 (blue circles), S2 (magenta crosses) and three possible boundary curves to	

separate the cluster regions for S1 and S2 over the SOM output grid for the Classifier #1.....	28
Figure 3.6 SOM Classifier #1 tested by noise-free feature vectors of the spheres S1 (blue circles) and S2 (magenta crosses), using three different cluster boundaries drawn by Rule 1 (red curve), Rule 2 (orange curve) and Rule 3 (black curve).....	28
Figure 3.7 SOM Classifier #1 tested by noisy feature vectors of spheres S1 (blue circles) and S2 (magenta crosses) at 20 dB SNR level, using three different cluster boundaries drawn by Rule 1 (red curve), Rule 2 (orange curve) and Rule 3 (black curve).....	29
Figure 3.8 SOM Classifier #1 tested by noisy feature vectors of spheres S1 (blue circles) and S2 (magenta crosses) at 15 dB SNR level, using three different cluster boundaries drawn by Rule 1 (red curve), Rule 2 (orange curve) and Rule 3 (black curve).....	30
Figure 3.9 SOM Classifier #1 tested by noisy feature vectors S1 (blue circles) and S2 (magenta crosses) at 10 dB SNR level, using three different cluster boundaries drawn by Rule 1 (red curve), Rule 2 (orange curve) and Rule 3 (black curve).....	30
Figure 3.10 Correct classification rates computed for the Classifier #1 at various testing SNR levels at all aspects for different cluster boundaries, red curve for Rule 1, orange curve for Rule 2 and black curve for Rule 3. .....	31
Figure 3.11 SOM output trained by slightly noisy (at the SNR level of 20 dB) WD- based late time energy feature vectors of the dielectric spheres S1 and S2. ....	33
Figure 3.12 Winning neuron locations for the training features of spheres S1 (blue circles) and S2 (magenta crosses) and the boundary curve to separate the cluster regions for S1 and S2 over the SOM output grid for the Classifier #2. ....	34
Figure 3.13 SOM Classifier #2 tested by noise-free feature vectors of spheres S1 (blue circles) and S2 (magenta crosses).....	35

Figure 3.14 SOM Classifier #2 tested by noisy feature vectors of spheres S1 (blue circles) and S2 (magenta crosses) at 20 dB SNR level. ....	35
Figure 3.15 SOM Classifier #2 tested by noisy feature vectors of spheres S1 (blue circles) and S2 (magenta crosses) at 15 dB SNR level. ....	36
Figure 3.16 SOM Classifier #2 tested by noisy feature vectors of spheres S1 (blue circles) and S2 (magenta crosses) at 10 dB SNR level. ....	36
Figure 3.17 Correct classification rates computed for the Classifier #2 at various testing SNR levels. ....	37
Figure 3.18. SOM output trained by noisy (at SNR level of 10 dB) WD-based late time energy feature vectors of the dielectric spheres S1 and S2. ....	38
Figure 3.19. Winning neuron locations for the training features of spheres S1 (blue circles) and S2 (magenta crosses) and the boundary curve to separate the cluster regions for S1 and S2 over the SOM output grid for the Classifier #3. ....	39
Figure 3.20. SOM Classifier #3 tested by noise-free feature vectors of spheres S1 (blue circles) and S2 (magenta crosses). ....	39
Figure 3.21. SOM Classifier #3 tested by noisy feature vectors of spheres S1 (blue circles) and S2 (magenta crosses) at 20 dB SNR level. ....	40
Figure 3.22. SOM Classifier #3 tested by noisy feature vectors of S1 (blue circles) and S2 (magenta crosses) at 15 dB SNR level. ....	40
Figure 3.23. SOM Classifier #3 tested by noisy feature vectors of spheres S1 (blue circles) and S2 (magenta crosses) at 10 dB SNR level. ....	41
Figure 3.24. Correct classification rates computed for the Classifier #3 at various testing SNR levels ....	42
Figure 3.25. Correct classification rates computed for the Classifier #1, Classifier #2 and Classifier #3 at various testing SNR levels for the aspect range $15^\circ < \theta < 165^\circ$ ....	42
Figure 3.26 The CCF versus $q^*$ plot generated to determine the optimal late-time design interval for the target library TL2 in the case of noise-free classifier design. ....	43

Figure 3.27 The CCF versus $q^*$ plot generated to determine the optimal late-time design interval for the target library TL2 in the case of (a) SNR level of 20 dB and (b) SNR level of 10 dB classifier designs. ....	44
Figure 3.28 SOM output trained by the noise-free WD-based late time energy feature vectors of the dielectric spheres S1,S2 and S3.....	45
Figure 3.29 Winning neuron locations for the training features of spheres S1 (blue circles), S2 (magenta crosses) and S3 (red plus signs) over the SOM output grid for the Classifier #4. ....	46
Figure 3.30 SOM Classifier #4 tested by noise-free feature vectors of spheres S1 (blue circles), S2 (magenta crosses) and S3 (red plus signs). ....	46
Figure 3.31 SOM Classifier #4 tested by noisy feature vectors of spheres S1 (blue circles), S2 (magenta crosses) and S3 (red plus signs) at 20 dB SNR level. ....	47
Figure 3.32 SOM Classifier #4 tested by noisy feature vectors of spheres S1 (blue circles), S2 (magenta crosses) and S3 (red plus signs) at 15 dB SNR level. ....	48
Figure 3.33 SOM Classifier #4 tested by noisy feature vectors of spheres S1 (blue circles), S2 (magenta crosses) and S3 (red plus signs) at 10 dB SNR level. ....	48
Figure 3.34 Correct classification rates computed for the Classifier #4 at various testing SNR levels. ....	49
Figure 3.35 SOM output trained by slightly noisy (SNR Level of 20 dB) WD-based late time energy feature vectors of the dielectric spheres S1, S2 and S3. ....	50
Figure 3.36 Winning neuron locations for the training features for spheres S1 (blue circles), S2 (magenta crosses) and S3 (red plus signs) over the SOM output grid for Classifier #5. ....	51
Figure 3.37 SOM Classifier #5 tested by noise-free feature vectors of spheres S1 (blue circles), S2 (magenta crosses) and S3 (red plus sign).....	52



Figure 3.38 SOM Classifier #5 tested by noisy feature vectors of spheres S1 (blue circles), S2 (magenta crosses) and S3 (red plus sign) at 20 dB SNR level.....	52
Figure 3.39 SOM Classifier #5 tested by noisy feature vectors of spheres S1 (blue circles), S2 (magenta crosses) and S3 (red plus signs) at 15 dB SNR level.....	53
Figure 3.40 SOM Classifier #5 tested by noisy feature vectors of spheres S1 (blue circles), S2 (magenta crosses) and S3 (red plus signs) at 10 dB SNR level.....	53
Figure 3.41 Correct classification rates computed for Classifier #5 at various testing SNR levels.....	54
Figure 3.42. SOM output trained by noisy (SNR Level of 10 dB) WD-based late time energy feature vectors of the dielectric spheres S1,S2 and S3.....	55
Figure 3.43 Winning neuron locations for the training features for S1, S2 and S3 over the SOM output grid for the Classifier #6.....	56
Figure 3.44 Correct classification rates computed for the Classifier #4 (noise-free design), Classifier # 5 (design at 20 dB SNR) and Classifier #6 (design at 10 dB SNR) at various testing SNR levels for aspect angles $5^\circ \leq \theta \leq 179^\circ$ .....	57
Figure 3.45 The CCF versus $q^*$ plot generated to determine the optimal late-time design interval for the target library TL3 in the case of (a) noise-free and (b) slightly noisy (SNR level of 20 dB) classifier designs.....	58
Figure 3.46 SOM output trained by the noise-free WD-based late time energy feature vectors of the dielectric spheres S1, S2, S3 and S4. ....	59
Figure 3.47 Cluster boudaries and winning neuron locations for the training features for S1 (blue circles), S2 (magenta crosses), S3 (red plus signs), S4 (black triangles) over the SOM output grid for Classifier #7. ....	60
Figure 3.48 SOM Classifier #7 tested by noise-free feature vectors of the spheres S1 (blue circles), S2 (magenta crosses), S3 (red plus signs), S4 (black triangles).....	61

Figure 3.49 SOM Classifier #7 tested by noisy feature vectors of the spheres S1 (blue circles), S2 (magenta crosses), S3 (red plus signs), S4 (black triangles) at 20 dB SNR level.....	61
Figure 3.50 SOM Classifier #7 tested by noisy feature vectors of the spheres S1 (blue circles), S2 (magenta crosses), S3 (red plus signs), S4 (black triangles) at 15 dB SNR level.....	62
Figure 3.51 SOM Classifier #7 tested by noisy feature vectors of the spheres S1 (blue circles), S2 (magenta crosses), S3 (red plus signs), S4 (black triangles) at 10 dB SNR level.....	62
Figure 3.52 Correct classification rates computed for the Classifier #7 at various testing SNR levels. ....	63
Figure 3.53 SOM output trained by slightly noisy (SNR Level of 20 dB) WD-based late time energy feature vectors of the dielectric spheres S1,S2,S3 and S4. ....	64
Figure 3.54 Winning neuron locations for the training features of the spheres S1 (blue circles), S2 (magenta crosses), S3 (red plus signs), S4 (black triangles) over the SOM output grid for the Classifier #8. ....	65
Figure 3.55 SOM Classifier #8 tested by noise-free feature vectors of the spheres S1 (blue circles), S2 (magenta crosses), S3 (red plus signs), S4 (black triangles).....	66
Figure 3.56 SOM Classifier #8 tested by noisy feature vectors of the spheres S1 (blue circles), S2 (magenta crosses), S3 (red plus signs), S4 (black triangles) at 20 dB SNR level.....	66
Figure 3.57 SOM Classifier #8 tested by noisy feature vectors of the spheres S1 (blue circles), S2 (magenta crosses), S3 (red plus signs), S4 (black triangles) at 15 dB SNR level.....	67
Figure 3.58 SOM Classifier #8 tested by noisy feature vectors of the spheres S1 (blue circles), S2 (magenta crosses), S3 (red plus signs), S4 (black triangles) at 10 dB SNR level.....	67
Figure 3.59 Correct classification rates computed for the Classifier #8 at various testing SNR levels. ....	68

Figure 3.60 Correct classification rates computed for the Classifier #7, Classifier # 8 at various testing SNR levels. ....	69
Figure 4.1 Problem geometry for aircraft library where the vector $\vec{k}$ denotes the propagation direction of incident plane wave. ....	72
Figure 4.2 The CCF versus $q^*$ plot generated to determine the optimal late-time design interval for the target library TL4 in the case of noise-free classifier design. ....	75
Figure 4.3 The CCF versus $q^*$ plots generated to determine the optimal late-time design interval for the target library TL4 in the case of (a) SNR=20 dB and (b) SNR=10 dB noise levels. ....	75
Figure 4.4 SOM output trained by the noise-free WD-based late time energy feature vectors of the small scale aircraft AC1 and AC2. ....	76
Figure 4.5 Winning neuron locations for the training features and the boundary curve to separate the cluster regions AC1 (blue circles) and AC2 (magenta crosses) over the SOM output grid for the Classifier #9. ....	77
Figure 4.6 SOM Classifier #9 tested by noise-free feature vectors of aircraft AC1 (blue circles) and AC2 (magenta crosses). ....	77
Figure 4.7 SOM Classifier #9 tested by noisy feature vectors of aircraft AC1 (blue circles) and AC2 (magenta crosses) at 20 dB SNR level. ....	78
Figure 4.8 SOM Classifier #9 tested by noisy feature vectors of aircraft AC1 (blue circles) and AC2 (magenta crosses) at 15 dB SNR level. ....	79
Figure 4.9 SOM Classifier #9 tested by noisy feature vectors of aircraft AC1 (blue circles) and AC2 (magenta crosses) at 10 dB SNR level. ....	79
Figure 4.10 SOM Classifier #9 tested by noisy feature vectors of aircraft AC1 (blue circles) and AC2 (magenta crosses) at 5 dB SNR level. ....	80
Figure 4.11 SOM Classifier #9 tested by noisy feature vectors of aircraft AC1 (blue circles) and AC2 (magenta crosses) at 0 dB SNR level. ....	80
Figure 4.12 Correct classification rates computed for the Classifier #9 at various testing SNR levels for two different $\theta$ range. ....	81

Figure 4.13 Winning neuron locations for the training features and the boundary curve to separate the cluster regions AC1 (blue circles) and AC2 (magenta crosses) over the SOM output grid for the Classifier #10..	82
Figure 4.14 SOM Classifier #10 tested by noise-free feature vectors of aircraft AC1 (blue circles) and AC2 (magenta crosses).....	83
Figure 4.15 SOM Classifier #10 tested by noisy feature vectors of aircraft AC1 (blue circles) and AC2 (magenta crosses) at 20 dB SNR level.....	84
Figure 4.16 SOM Classifier #10 tested by noisy feature vectors of aircraft AC1 (blue circles) and AC2 (magenta crosses) at 15 dB SNR level.....	84
Figure 4.17 SOM Classifier #10 tested by noisy feature vectors of aircraft AC1 (blue circles) and AC2 (magenta crosses) at 10 dB SNR level.....	85
Figure 4.18 SOM Classifier #10 tested by noisy feature vectors of aircraft AC1 (blue circles) and AC2 (magenta crosses) at 5 dB SNR level.....	85
Figure 4.19 SOM Classifier #10 tested by noisy feature vectors of aircraft AC1 (blue circles) and AC2 (magenta crosses) at 0 dB SNR level.....	86
Figure 4.20 Correct classification rates computed for the Classifier #10 at various testing SNR levels for two different $\theta$ range.....	86
Figure 4.21 SOM output trained by noisy (SNR Level of 10 dB) WD-based late time energy feature vectors of the small scale aircraft AC1 and AC2.....	87
Figure 4.22 Winning neuron locations for the training features and the boundary curve to separate the cluster regions AC1 and AC2 over the SOM output grid for the Classifier #11. ....	88
Figure 4.23 SOM Classifier #11 tested by noise-free feature vectors of aircraft AC1 (blue circles) and AC2 (magenta crosses).....	89
Figure 4.24 SOM Classifier #11 tested by noisy feature vectors of aircraft AC1 (blue circles) and AC2 (magenta crosses) at 20 dB SNR level.....	89
Figure 4.25 SOM Classifier #11 tested by noisy feature vectors of aircraft AC1 (blue circles) and AC2 (magenta crosses) at 15 dB SNR level.....	90
Figure 4.26 SOM Classifier #11 tested by noisy feature vectors of aircraft AC1 (blue circles) and AC2 (magenta crosses) at 10 dB SNR level.....	90

Figure 4.27 SOM Classifier #11 tested by noisy feature vectors of aircraft AC1 (blue circles) and AC2 (magenta crosses) at 5 dB SNR level.....	91
Figure 4.28 SOM Classifier #11 tested by noisy feature vectors of aircraft AC1 (blue circles) and AC2 (magenta crosses) at 0 dB SNR level.....	91
Figure 4.29 Correct classification rates computed for the Classifier #11 at various testing SNR levels for two different $\theta$ range.....	92
Figure 4.30 Correct classification rates computed for the Classifier #9, Classifier #10 and Classifier #11 at various testing SNR levels. ....	93
Figure 4.31 The CCF versus $q^*$ plot generated to determine the optimal late-time design interval for the target library TL5 in the case of noise-free classifier design.....	94
Figure 4.32 The CCF versus $q^*$ plot generated to determine the optimal late-time design interval for the target library TL5 in the case of (a) SNR level of 20 dB and (b) SNR level of 10 dB designs.....	94
Figure 4.33 SOM output trained by noise-free WD-based late time energy feature vectors of the small scale aircraft AC1, AC2 and AC4. ....	95
Figure 4.34 Winning neuron locations for the training features and the boundary curve to separate the cluster regions AC1 (blue circles), AC2 (magenta crosses) and AC4 (red plus signs) over the SOM output grid for the Classifier #12.....	96
Figure 4.35 SOM Classifier #12 tested by noise-free feature vectors of the aircraft AC1 (blue circles), AC2 (magenta crosses) and AC4 (red plus signs). ....	97
Figure 4.36 SOM Classifier #12 tested by noisy feature vectors of the aircraft AC1 (blue circles), AC2 (magenta crosses) and AC4 (red plus signs) at 20 dB SNR level. ....	97
Figure 4.37 SOM Classifier #12 tested by noisy feature vectors of the aircraft AC1 (blue circles), AC2 (magenta crosses) and AC4 (red plus signs) at 15 dB SNR level. ....	98

Figure 4.38 SOM Classifier #12 tested by noisy feature vectors of the aircraft AC1 (blue circles), AC2 (magenta crosses) and AC4 (red plus signs) at 10 dB SNR level. ....	98
Figure 4.39 SOM Classifier #12 tested by noisy feature vectors of the aircraft AC1 (blue circles), AC2 (magenta crosses) and AC4 (red plus signs) at 5 dB SNR level. ....	99
Figure 4.40 SOM Classifier #12 tested by noisy feature vectors of the aircraft AC1 (blue circles), AC2 (magenta crosses) and AC4 (red plus signs) at 0 dB SNR level. ....	99
Figure 4.41 Correct classification rates computed for the Classifier #12 at various testing SNR levels for two different $\theta$ range.....	100
Figure 4.42 SOM output trained by slightly noisy (SNR Level of 20 dB) WD-based late time energy feature vectors of the small scale aircraft AC1, AC2 and AC4. ....	101
Figure 4.43 Winning neuron locations for the training features of the aircraft AC1 (blue circles), AC2 (magenta crosses) and AC4 (red plus signs) over the SOM output grid for the Classifier #13.....	102
Figure 4.44 SOM Classifier #13 tested by noise-free feature vectors of the aircraft AC1 (blue circles), AC2 (magenta crosses) and AC4 (red plus signs). ....	103
Figure 4.45 SOM Classifier #13 tested by noisy feature vectors of the aircraft AC1 (blue circles), AC2 (magenta crosses) and AC4 (red plus signs) at 20 dB SNR level. ....	103
Figure 4.46 SOM Classifier #13 tested by noisy feature vectors of the aircraft AC1 (blue circles), AC2 (magenta crosses) and AC4 (red plus signs) at 15 dB SNR level. ....	104
Figure 4.47 SOM Classifier #13 tested by noisy feature vectors of the aircraft AC1 (blue circles), AC2 (magenta crosses) and AC4 (red plus signs) at 10 dB SNR level. ....	104

Figure 4.48 SOM Classifier #13 tested by noisy feature vectors of the aircraft AC1 (blue circles), AC2 (magenta crosses) and AC4 (red plus signs) at 5 dB SNR level. ....	105
Figure 4.49 SOM Classifier #13 tested by noisy feature vectors of the aircraft AC1 (blue circles), AC2 (magenta crosses) and AC4 (red plus signs) at 0 dB SNR level. ....	105
Figure 4.50 Correct classification rates computed for the Classifier #13 at various testing SNR levels for two different $\theta$ range.....	106
Figure 4.51 SOM output trained by noisy (SNR Level of 10 dB) WD-based late time energy feature vectors of the small scale aircraft AC1, AC2 and AC4. ....	107
Figure 4.52 Winning neuron locations for the training features of the aircraft AC1 (blue circles), AC2 (magenta crosses) and AC4 (red plus signs) over the SOM output grid for the Classifier #14.....	108
Figure 4.53 SOM Classifier #14 tested by noise-free feature vectors of the aircraft AC1 (blue circles), AC2 (magenta crosses) and AC4 (red plus signs). ....	109
Figure 4.54 SOM Classifier #14 tested by noisy feature vectors of the aircraft AC1 (blue circles), AC2 (magenta crosses) and AC4 (red plus signs) at 20 dB SNR level. ....	109
Figure 4.55 SOM Classifier #14 tested by noisy feature vectors of the aircraft AC1 (blue circles), AC2 (magenta crosses) and AC4 (red plus signs) at 15 dB SNR level. ....	110
Figure 4.56 SOM Classifier #14 tested by noisy feature vectors of the aircraft AC1 (blue circles), AC2 (magenta crosses) and AC4 (red plus signs) at 10 dB SNR level. ....	110
Figure 4.57 SOM Classifier #14 tested by noisy feature vectors of the aircraft AC1 (blue circles), AC2 (magenta crosses) and AC4 (red plus signs) at 5 dB SNR level. ....	111

Figure 4.58 SOM Classifier #14 tested by noisy feature vectors of the aircraft AC1 (blue circles), AC2 (magenta crosses) and AC4 (red plus signs) at 0 dB SNR level. ....	111
Figure 4.59 Correct classification rates computed for the Classifier #14 at various testing SNR levels for two different $\theta$ range.....	112
Figure 4.60 The CCF versus $q^*$ plot generated to determine the optimal late-time design interval for the target library TL6 in the case of noise-free classifier design.....	114
Figure 4.61 The CCF versus $q^*$ plot generated to determine the optimal late-time design interval for the target library TL6 in the case of (a) SNR=20 dB and (b) SNR=10 dB classifier design simulations.....	114
Figure 4.62 SOM output trained by noise-free WD-based late time energy feature vectors of the small scale aircraft AC1, AC2, AC3 and AC4.....	115
Figure 4.63 Winning neuron locations for the training features and the boundary curve to separate the cluster regions for the aircraft AC1 (blue circles), AC2 (magenta crosses), AC3 (red plus signs) and AC4 (black triangles) over the SOM output grid for the Classifier #15. ....	116
Figure 4.64 SOM Classifier #15 tested by noise-free feature vectors of the aircraft AC1 (blue circles), AC2 (magenta crosses), AC3 (red plus signs) and AC4 (black triangles). ....	116
Figure 4.65 SOM Classifier #15 tested by noisy feature vectors of the aircraft AC1 (blue circles), AC2 (magenta crosses), AC3 (red plus signs) and AC4 (black triangles) at 20 dB SNR level.....	117
Figure 4.66 SOM Classifier #15 tested by noisy feature vectors of the aircraft AC1 (blue circles), AC2 (magenta crosses), AC3 (red plus signs) and AC4 (black triangles) at 15 dB SNR level.....	117
Figure 4.67 SOM Classifier #15 tested by noisy feature vectors of the aircraft AC1 (blue circles), AC2 (magenta crosses), AC3 (red plus signs) and AC4 (black triangles) at 10 dB SNR level.....	118



Figure 4.68 SOM Classifier #15 tested by noisy feature vectors of the aircraft AC1 (blue circles), AC2 (magenta crosses), AC3 (red plus signs) and AC4 (black triangles) at 5 dB SNR level.....	118
Figure 4.69 SOM Classifier #15 tested by noisy feature vectors of the aircraft AC1 (blue circles), AC2 (magenta crosses), AC3 (red plus signs) and AC4 (black triangles) at 0 dB SNR level.....	119
Figure 4.70 Correct classification rates computed for the Classifier #15 at various testing SNR levels for different $\theta$ range.....	120
Figure 4.71 SOM output trained by slightly noisy (SNR Level of 20 dB) WD-based late time energy feature vectors of the small scale aircraft AC1, AC2, AC3 and AC4.....	121
Figure 4.72 Winning neuron locations for the training features of the aircraft AC1 (blue circles), AC2 (magenta crosses), AC3 (red plus signs) and AC4 (black triangles) over the SOM output grid for the Classifier #16. .	121
Figure 4.73 SOM Classifier #16 tested by noise-free feature vectors of the aircraft AC1 (blue circles), AC2 (magenta crosses), AC3 (red plus signs) and AC4 (black triangles). .....	122
Figure 4.74 SOM Classifier #16 tested by noisy feature vectors of the aircraft AC1 (blue circles), AC2 (magenta crosses), AC3 (red plus signs) and AC4 (black triangles) at 20 dB SNR level.....	123
Figure 4.75 SOM Classifier #16 tested by noisy feature vectors of the aircraft AC1 (blue circles), AC2 (magenta crosses), AC3 (red plus signs) and AC4 (black triangles) at 15 dB SNR level.....	123
Figure 4.76 SOM Classifier #16 tested by noisy feature vectors of the aircraft AC1 (blue circles), AC2 (magenta crosses), AC3 (red plus signs) and AC4 (black triangles) at 10 dB SNR level.....	124
Figure 4.77 SOM Classifier #16 tested by noisy feature vectors of the aircraft AC1 (blue circles), AC2 (magenta crosses), AC3 (red plus signs) and AC4 (black triangles) at 5 dB SNR level.....	124

Figure 4.78 SOM Classifier #16 tested by noisy feature vectors of the aircraft AC1 (blue circles), AC2 (magenta crosses), AC3 (red plus signs) and AC4 (black triangles) at 0 dB SNR level.....	125
Figure 4.79 Correct classification rates computed for the Classifier #16 at various testing SNR levels for different $\theta$ range .....	126
Figure 4.80 SOM output trained by noisy (SNR Level of 10 dB) WD-based late time energy feature vectors of the small scale aircraft AC1, AC2,AC3 and AC4. ....	127
Figure 4.81 Cluster boundaries and the winning neuron locations for the training features of the aircraft AC1 (blue circles), AC2 (magenta crosses), AC3 (red plus signs) and AC4 (black triangles) over the SOM output grid for the Classifier #17. ....	128
Figure 4.82 SOM Classifier #17 tested by noise-free feature vectors of the aircraft AC1 (blue circles), AC2 (magenta crosses), AC3 (red plus signs) and AC4 (black triangles) . ....	128
Figure 4.83 SOM Classifier #17 tested by noisy feature vectors of the aircraft AC1 (blue circles), AC2 (magenta crosses), AC3 (red plus signs) and AC4 (black triangles) at 20 dB SNR level.....	129
Figure 4.84 SOM Classifier #17 tested by noisy feature vectors of the aircraft AC1 (blue circles), AC2 (magenta crosses), AC3 (red plus signs) and AC4 (black triangles) at 15 dB SNR level.....	129
Figure 4.85 SOM Classifier #17 tested by noisy feature vectors of the aircraft AC1 (blue circles), AC2 (magenta crosses), AC3 (red plus signs) and AC4 (black triangles) at 10 dB SNR level.....	130
Figure 4.86 SOM Classifier #17 tested by noisy feature vectors of the aircraft AC1 (blue circles), AC2 (magenta crosses), AC3 (red plus signs) and AC4 (black triangles) at 5 dB SNR level.....	130
Figure 4.87 SOM Classifier #17 tested by noisy feature vectors of the aircraft AC1 (blue circles), AC2 (magenta crosses), AC3 (red plus signs) and AC4 (black triangles) at 0 dB SNR level.....	131

Figure 4.88 Correct classification rates computed for the Classifier #17 at various testing SNR levels for different  $\theta$  range..... 132

## **CHAPTER 1**

### **INTRODUCTION**

Radar target identification has been an active research area for over half a century [1] as accurate and fast recognition of targets is an important problem especially for military applications. All the characteristic information of an electromagnetic scatterer (i.e. the target) is implicitly contained in its scattered response signals. For that reason, the raw database needed by an electromagnetic target classifier must contain scattered signatures for each library target over a proper bandwidth [2]. However, target recognition from scattered electromagnetic fields is a very difficult problem to solve, not only because scattering mechanisms are very complicated even for geometrically simple targets, but also due to the fact that such data are highly frequency, aspect and polarization dependent [1-5]. A feasible target classifier must be based on a proper feature extraction technique to obtain aspect and polarization invariant target features. Correct classification rate of a target classifier can be maximized as a result of training by such special target features. It must be also emphasized that extracted features must be highly sensitive to geometrical and material properties such as size, shape and electrical parameters (permittivity, permeability, conductivity) of individual targets to discriminate similar objects from each other.

Another complication in target recognition is the presence of noise contaminating scattered signals. In general, any unwanted signal component is considered to be noise. Recognition of targets becomes more difficult as the level of noise contamination in the available electromagnetic scattered database signals gets

higher [4, 6, 29]. The contamination may be simply due to additive Gaussian noise or it may be due to clutter type noise caused by the signals scattered by some other objects around. In this thesis, only the effects of additive Gaussian noise will be investigated on the performance of target recognition at various signal-to-noise ratio (SNR) levels.

There are various techniques suggested for target classification in electromagnetic target recognition literature such as the techniques based on the use of natural resonance frequencies of a target [1-7], artificial neural network (ANN) based techniques [7-13], time-frequency analysis based techniques [3-4, 6-9] and statistical signal processing based techniques [4, 6, 11, 29]. In particular, use of Artificial Neural Network (ANN) based target classification techniques in target recognition, has been a popular approach since late 1980's. ANN's are composed of a large number of highly interconnected parallel processing elements (neurons) working in coordination to learn certain patterns contained in the training data. Learning algorithms used to train ANNs may be either supervised or unsupervised. Self-organizing map (SOM) type neural networks learn in an unsupervised manner.

A SOM output can be considered as a topographic map of input data where each neuron in the network represents a class of inputs, so it is considered as an attractive tool for target classification [14-17]. As it is mentioned above, a SOM learns without any form of supervision. In other words, when an input data vector is fed into a SOM, the class information of the input is not provided. However, this information is acquired eventually as a result of the cluster formation capability of the SOM [18, 21-24]. The output of a SOM is a grid composed of neurons. Each neuron has a weight vector, which is assigned randomly at the beginning of the training phase and updated at each iteration of the learning process. The length of weight vectors are the same as the length of the training input vectors. In SOM based electromagnetic classifier design problems, the

length of the input vectors (and hence the length of the weight vectors) is usually the same as the length of the time-domain scattered signal [7, 8, 13]

In this thesis, SOM type electromagnetic classifiers will be designed for two different types of targets. First, a set of dielectric spheres of the same size but of different relative permittivity values will be used as library targets. Secondly, target classifiers will be designed for a set of small-scaled aircraft which are modeled by perfectly conducting thin wires [19]. The SOM classifiers will be trained by target feature vectors which are extracted from scattered signals of such targets by using a Wigner Distribution (WD) based target feature computation technique [3, 4, 20]. The resulting input feature vectors are called late-time feature vectors (LTFVs) as they are extracted over an optimal late-time interval [4].

Evaluation of the classifier accuracy under noisy testing conditions is a very important issue. Therefore, all of the SOM based classifiers designed in this thesis are thoroughly tested at various signal to noise ratio (SNR) levels. Also, various SOM classifiers are designed in this thesis by using slightly and/or moderately noisy training input data to improve the classifier accuracy at lower SNR testing conditions.

The organization of the rest of the thesis is as follows:

Chapter 2 gives the theory and design steps of the SOM based classifiers including an outline of the WD based feature extraction technique.

Chapter 3 presents eight different classifier design simulations for various target libraries composed of only dielectric spheres. Classifiers designed under

difference noise conditions will be tested at various SNR levels to evaluate noise performances of the resulting SOM classifiers.

Nine different SOM classifiers are designed in Chapter 4 for various target libraries of small-scale model aircraft. Noise performances of all these classifiers will be evaluated at different SNR levels both in the classifier design phase and in the test phase.

Finally, the concluding remarks and suggestions for future study will be outlined in Chapter 5.

There is also an Appendix containing a sample MATLAB code used to design and test SOM classifiers.

## **CHAPTER 2**

### **THEORY**

In this chapter, theoretical background of the SOM (Self-Organizing Map) based classifier design problem will be presented with a special emphasis on the issue of target feature extraction. Firstly, the basic properties of SOM type artificial neural networks will be discussed. SOM design parameters will be defined. Next, the use of Wigner Distribution based feature extraction process will be outlined.

#### **2.1 Self Organizing Map Type Artificial Neural Networks**

Artificial Neural Networks (ANNs) are information processing devices which are inspired by the biological learning processes that are believed to take place in human brain. An ANN is, in general, composed of a large number of highly interconnected parallel processing elements (neurons) working in coordination to solve specific problems through learning. ANNs, like people, learn by examples. Learning in an ANN is accomplished by exposing the network to training inputs which are randomly selected from an available training database. With their ability to learn and generalize, ANNs can be used in specific applications such as pattern recognition, speech processing, data classification, microwave circuit design and electromagnetic target recognition.

Type of an ANN is determined by its network topology and its learning rules. ANNs are categorized according to their learning strategy as supervised or



unsupervised neural networks. In the case of supervised ANNs, such as multi-layer perceptrons, available training inputs are provided together with their class information. Conversely, in the case of unsupervised ANNs, no class information is provided during training [14]. The Self-Organising Map (SOM) type neural network is a well-known unsupervised ANN, which acquires the class information of training inputs by itself during the training phase through cluster formation [14-18, 21-24]. Electromagnetic target classifiers to be designed in this thesis use the SOM type ANNs as the basic signal processing tool. Basic topological structure of the SOM together with its design parameters and its learning algorithm will be described in the following subsections.

#### 2.1.1. Structure of Self Organizing Maps

The Self-Organizing Map type artificial neural network technique discussed in this thesis, is one of the most important model of unsupervised learning ANN class, which is introduced by Kohonen [14,15]. SOM type ANNs can be used in applications such as vector quantization, speech processing, robotics, control, statistical pattern recognition, radar classification and image compression.

A SOM algorithm creates a mapping from a high dimensional vector space onto a low dimensional grid. SOM consists of neurons organized on a regular low dimensional grid such as the hexagonal and rectangular grids shown in Figure 2.1. Each neuron  $i$  of the SOM has an associated  $d$ -dimensional vector  $m_i = [m_{i1}, m_{i2}, \dots, m_{id}]$ , where  $d$  is equal to the dimension of the input vectors. The neurons are connected to adjacent neurons by a neighborhood relation [16, 17]. The number of map units (i.e. neurons), which typically varies from a few dozen up to several thousand depending upon the application in hand, determines the accuracy and generalization capability of SOM [17].

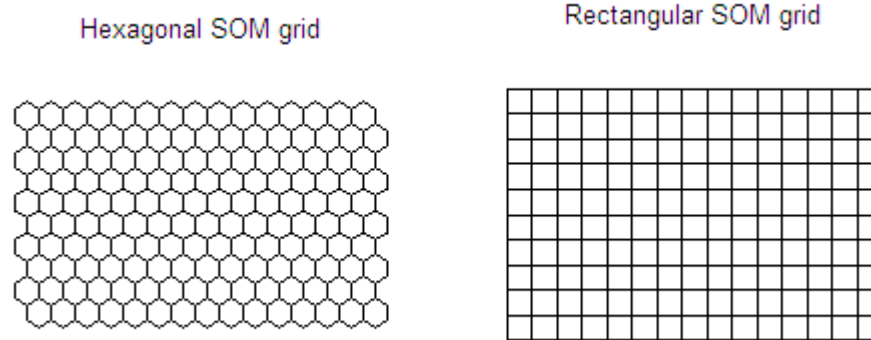


Figure 2.1. Two dimensional lattice structures of SOM.

During training, neurons of the SOM grid are exposed to each available input according to an unsupervised learning rule. When the training is over, each neuron is tuned to a specific signal or classes of pattern through this unsupervised learning process. The coordinates of a neuron in the network then correspond to a particular domain of input signal patterns. Each neuron or local neuron group acts like a separate decoder for the same input. Then, the interpretation of the input information is provided by the presence or absence of an active response at that location, rather than the exact input-output signal transformations or magnitude of the response [14, 15]. Different types of SOM output grids are shown in Figure 2.1 and Figure 2.2. In two dimensional case, the neurons of the map can be arranged either on a rectangular or a hexagonal lattice as shown in Figure 2.1. If the sides of the map are connected to each other, the global shape of the map becomes a cylinder or a toroid, as shown in Figure 2.2.

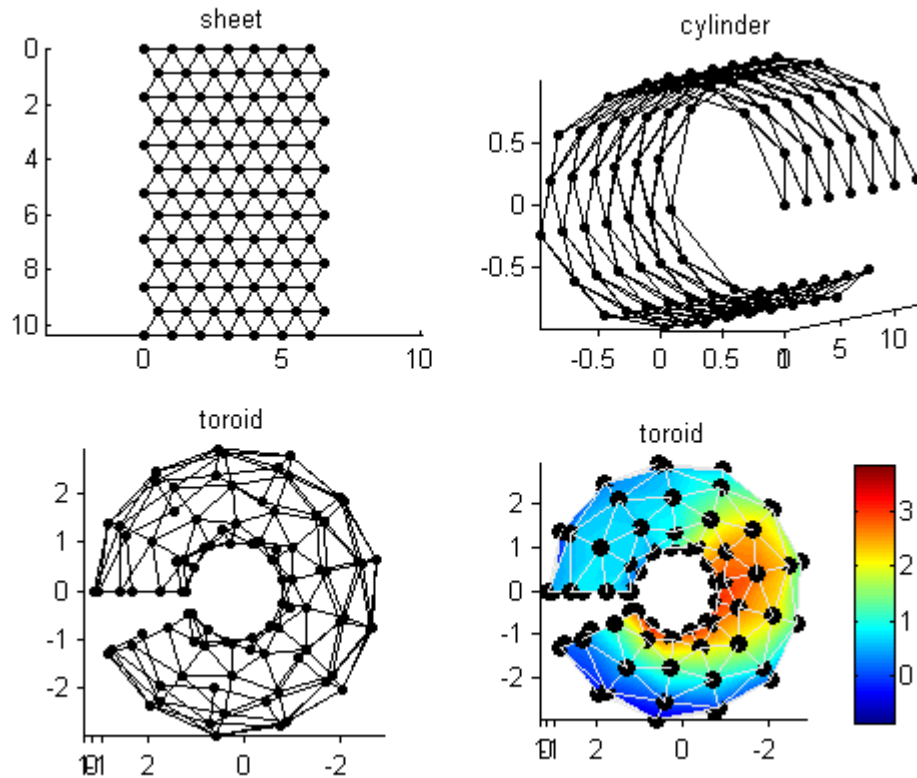


Figure 2.2 Different Types Of SOM Output Maps (reproduced from Demo #3 of The SOM Toolbox 2 of [18]).

In the classical SOM, the number of neurons and their topological relations are fixed from the beginning. There are three issues which need to be a priori decided: dimensions of the map grid, map lattice and shape. The number of neurons should usually be selected as big as possible, with the neighborhood size controlling the smoothness and generalization of the mapping. However, as the size of the map increases, the computational load of the training phase becomes too heavy for most applications. In our simulations, dimensions of the map grids will be selected as  $[12 \times 12]$ ,  $[21 \times 21]$ ,  $[30 \times 30]$  in 2-target, 3-target and 4-target applications and a sheet-shaped map grid with rectangular lattice will be used.

### 2.1.2. Kohonen Learning Algorithm

The Kohonen model consists of two groups of units: input units (input vectors) and hidden units (neurons with weight vectors) on the map. Initially, there is no connection between the input vectors and neurons [14]. Ordering the weight vectors of the neurons in such way that they will represent the similarities of the input vectors is accomplished by using the Kohonen's learning algorithm.

The first step in constructing a SOM is to initialize the weight vectors prior to training. Initial values are assigned to each vector of the SOM grid. The SOM is, in general, very robust with respect to initialization but a properly accomplished initialization may allow the algorithm to converge faster to a good solution. In this thesis work, random initialization is used in all SOM simulations where the weight vectors are initialized with small random values.

After initialization, training part of Kohonen Learning algorithm is started. The SOM is trained iteratively. In each training step, one sample vector  $\mathbf{x}$  from the input data set is chosen randomly and the distances between this input vector and all the weight vectors of the SOM grid are calculated using some distance measure. The winning neuron, denoted by the index  $c$ , is the unit whose weight vector  $\mathbf{m}_c$  is closest to the input vector  $\mathbf{x}$ . The similarity is usually defined by means of a distance measure, typically the Euclidian distance [18]. Formally, the winning neuron is defined as the neuron for which

$$\|\mathbf{x} - \mathbf{m}_c\| = \min_i \{\|\mathbf{x} - \mathbf{m}_i\|\} \quad (2.1)$$

where  $\|\cdot\|$  is the Euclidian distance. After finding the winning neuron, the weight vectors of the SOM neurons are updated. The SOM update rule for the weight vector of the unit  $i$  is given as

$$\mathbf{m}_i[n + 1] = \mathbf{m}_i[n] + a[n]h_{ci}[r[n]](\mathbf{x}[n] - \mathbf{m}_i[n]) \quad (2.2)$$

where  $n$  denotes iteration number,  $a[n]$  is the learning rate and  $h_{ci}[r[n]]$  is the neighborhood function centered at the winning neuron  $c$ , with neighborhood radius  $r[n]$ . The critical distinguishing feature of Kohonen Learning Model, is that the other neurons physically close to the winning neuron are also trained at weaker learning levels. So, the choice of training parameters, the learning rate and the neighborhood function, are important for successful learning. The values of weight vectors are usually very small at the beginning of the training, but during the iterations of training, the weights adapt themselves to the input vectors according to the learning rule stated in Equation (2.2) for specified types and values of the learning rate and the neighborhood function [18].

Learning rate  $a[n]$ , which defines the intensity of the neuron weight adaptation, is a decreasing function of iteration. Three well-known learning rate functions; linear, inverse-of-time, and a power series are illustrated in Figure 2.3. Learning rate is a critical variable as it controls the rate of evolution of vectors. Initial learning rate is the starting value of learning rate at the training phase. Linear learning rate function with 0.5 initial learning rate will be used in all simulations to be presented in this thesis.

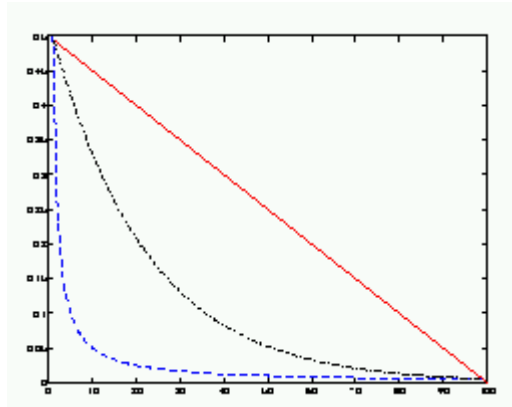


Figure 2.3 Three possible functions for learning rate: Linear (red), power series (black) and inverse-of-time (blue). (The figure is reproduced from Demo #3 of the SOM Toolbox 2 of [18]).

The choice for the neighborhood function determines how strongly the neurons are connected to each other in a given SOM grid. The Gaussian neighborhood function, which will be used in our simulations, is defined as;

$$h_{ci}[r[n]] = \exp\left(-\frac{\|r_c - r_i\|^2}{2\sigma^2[n]}\right) \quad (2.3)$$

where  $r_i$  is the location of the unit  $c$  on the map grid and  $r_c$  is the winning neuron location at which the neighborhood function is centered and the  $\sigma[n]$  is the neighborhood radius at the  $n^{th}$  iteration. Notice that this is a function of distance  $\|r_c - r_i\|$  between map units on the SOM grid.

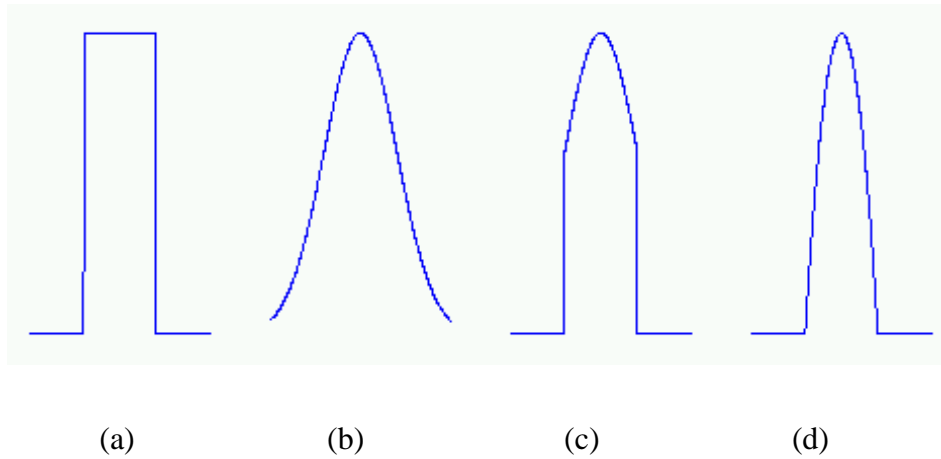


Figure 2.4 The four neighborhood functions (a) bubble, (b) gaussian, (c) cut gaussian and (d) epanechicov.

Typically, the neighborhood radius is decreased with increasing number of iterations. Larger neighborhood radius means that the training takes place at a more global level. It is preferred to have larger values of the neighborhood radius during the early training of the network so that the topological ordering of the network can be possible. Subsequent reduction of neighborhood radius then helps to refine the cluster formation. This interplay determines the accuracy and generalization capability of the SOM [14-18].

Maximum iteration number used in the training phase is an important parameter. During the training phase of SOM, training vectors are selected in random order for updating the weights of the map. Using each and every training vector only once corresponds to a complete iteration in SOM training phase. Maximum iteration number is set to 500 epochs in all design simulations in this thesis. This means that the whole database will be introduced to the SOM grid 500 times, but the individual training vectors of the database will be applied for training in a random order within each iteration.

SOM training is usually performed in two phases; the ordering phase and the convergence phase. In the former phase, relatively large values for the initial learning rate and for the neighborhood radius are used. In the latter phase, both learning rate and neighborhood radius assume smaller and smaller values as the training process continues.

As SOM is an unsupervised learning algorithm, there have to be no supervision provided during the training phase. Once the training parameters are fixed at the beginning and the SOM grid is initialized by assigning completely random weight vectors to all neurons, there will be no further control on any of the training steps in the SOM classifier design simulations.

Design of an electromagnetic target classifier using the SOM technique is a very challenging problem especially when the scattering objects are very similar to each other. The aspect and polarization dependent scattered signals of electromagnetic targets must be processed first for the extraction of proper target features. Then, the resulting aspect and polarization invariant features can be used as input vectors to train SOM classifiers. The next section will present an outline for the Wigner Distribution based target feature extraction technique which is used in this thesis successfully.

## 2.2 Target Feature Extraction Using Wigner Distribution

Although the main emphasis of this thesis is not the Wigner Distribution based feature extraction technique, the basic theory behind this approach will be outlined in this section for the sake of completeness.

In Chapter 3 and Chapter 4, classifier design simulations will be presented for two different classes of electromagnetic targets, dielectric spheres and conducting small-scaled model aircraft, respectively. The input data vectors used to train the SOM based classifiers need to be extracted from time-domain scattered target responses of such targets by using the Wigner Distribution (WD) for efficient SOM training. The need for this preprocessing can be explained as follows: As mentioned in the Introduction chapter, electromagnetic target classification from scattered target signatures is a very challenging pattern recognition problem where the patterns to be classified are not only functions of time and frequency but they are also strong functions of aspect angles and polarization. A successful feature extraction technique must produce target features with low aspect/polarization sensitivity so that signals scattered from the same target at different angles can be closely matched with each other. Also, the extracted features must be highly sensitive to geometrical and physical properties of the associated target to be able to discriminate this target from the other similar targets of concern [4]. System poles (called also as complex natural resonance frequencies) of a given target are determined by the geometrical and electrical properties of that target and they characterize this target in an aspect and polarization invariant manner. Therefore, target features related to system poles are, in general, found quite useful in electromagnetic target recognition problems [1-5] and the WD based target feature extraction technique has been demonstrated recently to be very successful in characterizing electromagnetic scatterers [3, 6].



### 2.2.1. Wigner Distribution and the Formation of Late-Time Feature Vectors

In this thesis, the input vectors which are used to train the SOM based target classifiers are obtained as follows: First, a raw database of time-domain scattered signals are generated for each library target at a set of pre-determined aspect angles. Each of these signals are recorded over a common time span and their spectra are generated over the same frequency bandwidth. Total energy of each scattered signal is also normalized to unity prior to the computation of their Wigner-Ville distributions. The Wigner-Ville distribution is a real-valued, quadratic time–frequency representation preserving time shifts and frequency shifts of the signal and its output represents an approximate energy density function over the joint time-frequency plane. The auto-WD of a given time domain signal  $x(t)$  is expressed as [20];

$$W_x(t, f) = \int_{\tau} x(t + \frac{\tau}{2})x^*(t - \frac{\tau}{2})e^{-j2\pi f\tau} d\tau \quad (2.4)$$

where the superscript (\*) denotes complex conjugation. The integral of WD output,  $W_x(t, f)$ , computed over frequency corresponds to the signal's instantaneous power as

$$\int_f W_x(t, f)df = |x(t)|^2 \quad (2.5)$$

Similarly, the integral of  $W_x(t, f)$  computed over time gives the spectral energy density of the signal as

$$\int_t W_x(t, f)dt = P_x(f) = |X(f)|^2 \quad (2.6)$$

where  $X(f)$  is the Fourier transform of the signal  $x(t)$ . The WD output does not give an exact time-frequency energy density function defined at every point in the time-frequency plane. As explained by the uncertainty principle, it is not possible to have infinite resolution in both time and frequency simultaneously [20]. Accordingly, the WD outputs contain very strong and highly oscillatory

interference terms that may seriously deteriorate the identification capability of the classifier. Due to these oscillatory interference terms, the WD outputs may have negative values which cannot be interpreted as energy density terms. Therefore, these non-physical negative values in the WD output matrix are simply replaced by zeros to obtain a modified WD output as;

$$\widetilde{W}_x(t, f) = \frac{W_x(t, f) + |W_x(t, f)|}{2} \quad (2.7)$$

as suggested in [3].

The modified auto WD output is further processed to obtain a partitioned energy density vector which is indirectly related to target poles. In obtaining this target feature for a given target at a given aspect, the total time span  $T_0$  of the scattered target signal is divided into  $Q$  time bands (each having equal lengths of  $T_0/Q$  seconds) as the first step. Spectral distribution of partial energy packets confined to each of these non-overlapping subintervals is computed to construct an intermediate feature vector. The amount of signal energy contributed to subinterval  $q$  by a spectral component at  $f = f_m = \frac{(m-1)}{2T_0}$  [3, 4] is;

$$E_q(f_m) = \int_{(q-1)\Delta}^{q\Delta} W_x(t, f_m) dt \quad \text{for } q = 1, 2, 3 \dots Q \quad (2.8)$$

where  $\Delta = \frac{T_0}{Q}$  and,  $m = 1, 2, \dots, \frac{N}{2}$ .

As all the scattered signals  $x(t)$  are real-valued, the WD output matrix has even symmetry with respect to frequency. Therefore it is enough to process only half of the WD output matrix for non-zero frequency samples, i.e. for,  $m = 1, 2, \dots, \frac{N}{2}$ .

Then, the spectral distribution of the partial signal energy confined to the subinterval  $q$  can be expressed in vector form as [4];

$$\overline{E}_q = \left[ E_q(f_1) \ E_q(f_2) \ \dots \ E_q\left(f_{\frac{N}{2}}\right) \right] \quad (2.9)$$

As there are  $Q$  non-overlapping time bands altogether, the partitioned energy density vector  $\overline{E}$  is formed as

$$\overline{E} = [ \overline{E}_1 \ \overline{E}_2 \ \dots \ \overline{E}_Q ] \quad (2.10)$$

having the length of  $(\frac{N}{2} * Q)$ .

This operation is performed over the total time span of input signals. To capture the behavior of natural resonance components in the late-time region, only a couple of successive partitions of  $\overline{E}$  vector can be used to construct the corresponding late-time feature vector (LTFV). If we choose two successive time bands ( $q$  and  $q + 1$ ) or ( $q - 1$  and  $q$ ) for feature vector construction to include the pair  $\overline{E}_q$  and  $\overline{E}_{q+1}$  or the pair  $\overline{E}_{q-1}$  and  $\overline{E}_q$ , the resulting energy feature vector contains information also about the real parts of the natural resonance frequencies. The resulting 2-band aspect dependent feature vectors are called Late-Time Feature Vectors (LTFV). One of the most important steps of the classifier design is the selection of the optimal late-time interval for classification. In other words, we need to determine the late-time interval index  $q^*$  which corresponds to two successive time bands ( $q$  and  $q + 1$ ) or, ( $q - 1$  and  $q$ ). The value of  $q^*$  can be determined by maximizing the Correct Classification Factor (CCF) given in Equation (2.11) for a pre-selected  $Q$  value [4]. The value of the parameters  $Q$  and  $q^*$  of classifier design are decided by using scattered data only at the reference aspects.

$$CCF(q^*) = \frac{1}{M_{tar} K^2} \sum_{i,j} r_{i,j}^{matched} - \frac{1}{(M_{tar}^2 - M_{tar}) K^2} \sum_{i,j} r_{i,j}^{mismatched} \quad (2.11)$$

where  $M_{tar}$  is the number of targets and  $K$  is the number of reference aspects,  $r_{i,j}^{matc\ hed}$  is the correlation coefficient between any two LTFVs which belong to the same target at different aspects,  $r_{i,j}^{mismatch\ hed}$  is the correlation coefficient between any two LTFVs which belong to different targets. The index  $q^*$  is chosen from the possible values  $q^* = 1, 2, \dots, Q-1$ .

In the classifier design simulations of this thesis, the first step of target classifier design will be the computation of the optimal late-time design interval by using the previously computed partitioned energy density vectors [4, 6]. The optimal design interval is also a function of the SNR level of the database signals. Therefore, determination of the optimal design interval should be repeated all over again for each SNR design level before the late-time feature vectors are computed. Then, these LTFVs can be used to train the SOM classifiers as to be demonstrated in the application chapters.

## CHAPTER 3

### DESIGN OF SOM CLASSIFIERS FOR DIELECTRIC SPHERES

In this chapter, SOM type electromagnetic target classifiers will be designed for three different target libraries TL1, TL2 and TL3 which contain two, three and four dielectric spheres, respectively, as shown in Table 3.1. The lossless dielectric spheres S1, S2, S3 and S4 are very similar to each other as they have exactly the same shape and the same size with radii of 10 cm and their relative permittivity values  $\epsilon_r = 3, 4, 5, 6$  are all close to each other. Although these spheres have simple geometrical features, they are challenging targets as electromagnetic waves can penetrate into such perfect dielectric objects to create very complicated internal resonance mechanisms. Therefore, late-time scattered signals of these dielectric spheres may contain many damped sinusoidal signal components corresponding to a large number of complex conjugate target pole pairs. For each given dielectric sphere, its system poles are located quite densely along pole strings in the complex frequency plane [25, 26]. When the spheres are very similar to each other (as in the case of targets S1, S2, S3 and S4) certain pole values of one sphere may be very close to the pole values of other targets. This situation complicates the classification problem.

As discussed in Chapter 2, target classifiers will be designed by training self-organizing maps by means of Wigner Distribution (WD) based target feature vectors which are indirectly related to the aspect and polarization invariant system poles of the library targets [4]. The SOM Toolbox 2.0 developed by J. Vesanto

et.al will be utilized for sequential SOM training [20]. A couple of simple MATLAB codes developed during this thesis study will be used for classifier testing and for displaying the results in user friendly forms.

For any given target library, the SOM classifier will be first designed by using noise-free reference data at a chosen set of reference aspect angles. Then, the resulting classifier will be tested for its accuracy rate at the signal-to-noise ratio (SNR) levels of infinity (the noise-free testing database case), 20 dB, 15 dB and 10 dB to see if this classifier is robust under noisy testing conditions. If the noise performance of the SOM classifier is not found satisfactory, the design procedure will be repeated all over again by using slightly noisy (with SNR=20 dB) and moderately noisy (with SNR=10 dB) reference data. In each case, the resulting classifier will be tested against the same noisy feature database at the SNR levels of infinity, 20 dB, 15 dB and 10 dB. Usefulness of designing SOM classifiers by using noisy reference data will be evaluated based on the comparisons of resulting noise performances.

Table 3.1 Descriptions of target libraries containing the same size lossless dielectric spheres with different permittivity values  $\varepsilon = \varepsilon_0 \varepsilon_r$ .

Target Library	Targets
TL1	S1 (r=10 cm , $\varepsilon_r = 3$ ), S2 (r=10 cm , $\varepsilon_r = 4$ )
TL2	S1 (r=10 cm , $\varepsilon_r = 3$ ), S2 (r=10 cm , $\varepsilon_r = 4$ ), S3 (r=10 cm , $\varepsilon_r = 5$ )
TL3	S1 (r=10 cm , $\varepsilon_r = 3$ ), S2 (r=10 cm , $\varepsilon_r = 4$ ), S3 (r=10 cm , $\varepsilon_r = 5$ ), S4 (r=10 cm , $\varepsilon_r = 6$ )

### 3.1 Description of Electromagnetic Scattered Data of Dielectric Spheres and Simulation Parameters Used in Classifier Design and Testing

Time response waveforms of the dielectric spheres S1, S2, S3 and S4 are analytically synthesized in response to a plane wave excitation that is linearly polarized in x-direction and propagates in z-direction as described in Figure 3.1.a.

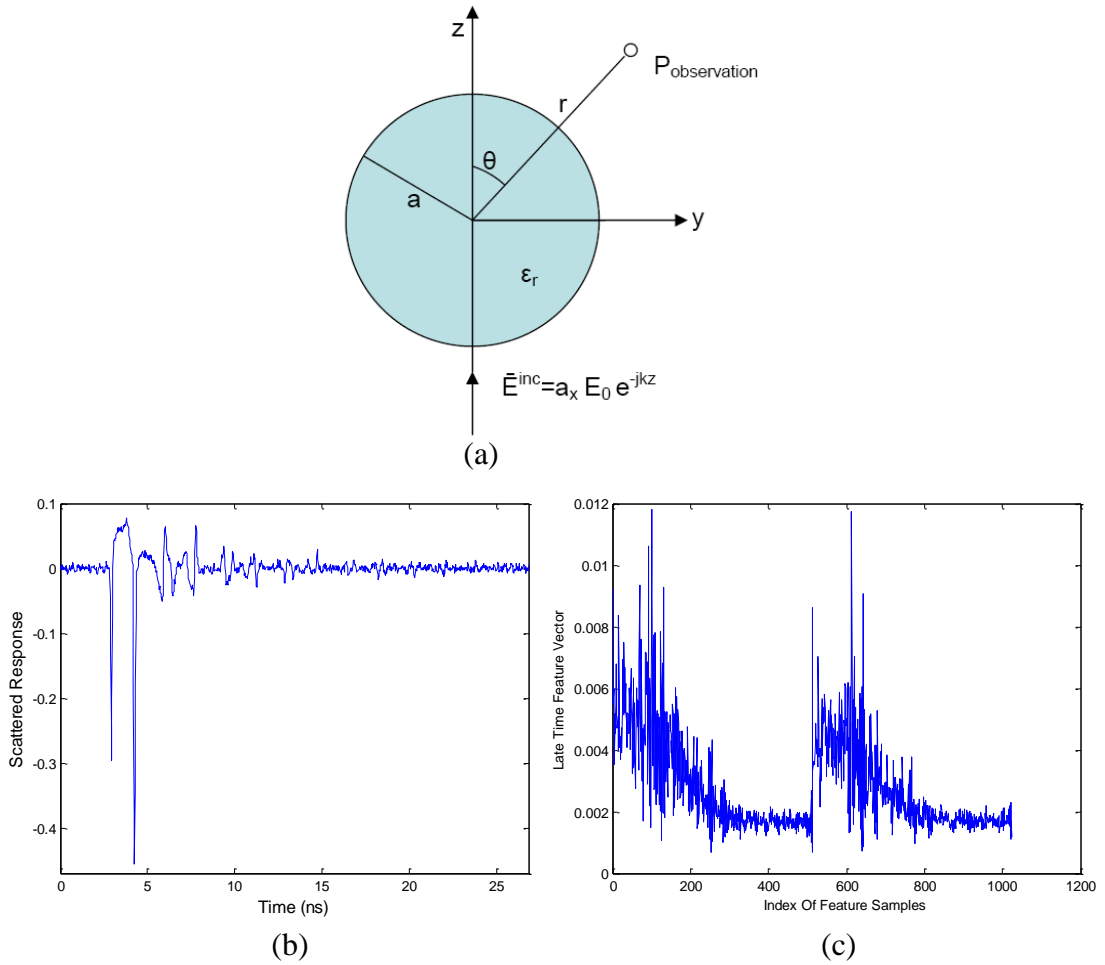


Figure 3.1 (a) Problem geometry used to synthesize electromagnetic signals scattered from dielectric spheres. (b) Scattered response of the sphere S2, at  $\theta=75$  degrees aspect angle with SNR = 20 dB SNR level. (c) LTFV of sphere S2, at the reference aspect angle  $\theta =75^\circ$  for 20 dB SNR level.

These far field scattered responses are computed at the  $\Phi = \pi / 2$  plane for different values of the angle  $\theta$  in the frequency domain over a bandwidth from zero to 19.1 GHz with frequency steps of  $\Delta f$  37.3 MHz (i.e. at 512 frequency sample points) by using the analytical solutions provided in the reference [26]. These computations are performed at 13 different values of the bistatic aspect angle  $\theta_b$ , where  $\theta_b = 180^\circ - \theta$  and the angle  $\theta$  assumes the values  $\theta = 5^\circ, 15^\circ, 30^\circ, 45^\circ, 60^\circ, 75^\circ, 90^\circ, 105^\circ, 120^\circ, 135^\circ, 150^\circ, 165^\circ$  and  $179^\circ$ . Corresponding time domain responses of the library targets are computed by using the Inverse Fast Fourier Transformation (IFFT) of the windowed frequency-domain data at 1024 sample points in time over a total time span of  $T_0 = 26.8 \text{ nsec}$ . As an example, Figure 3.1.b shows the scattered time-domain response of the target S2 at  $\theta = 75^\circ$  for SNR=20 dB level.

Generally, a very large-size reference database is needed for training neural network based electromagnetic target classifiers at many different target aspects. For example, use of training data at more than 30 or 40 aspects are reported in literature to design neural network classifiers over an aspect range of only 90 degrees [27]. However, this need is conveniently eliminated in the present thesis work as a result of the special feature extraction technique applied prior to SOM training. A total of only six reference aspects, which corresponds to  $\theta = 5^\circ, 30^\circ, 75^\circ, 105^\circ, 135^\circ, 179^\circ$  are used in designing classifiers through SOM training. These reference aspects are chosen to span the total  $\theta$  range of 180 degrees in angular steps of about 30-40 degrees for efficient characterization of targets in this aspect dependent problem. The rest of the scattered database (at non-reference aspects) is used for performance testing only.

As discussed in Chapter 2, the first step of target classifier design is to extract the WD based target feature vectors (LTFVs) over a common optimal late-time interval for each target at each reference aspect. Then, these normalized LTFVs are used to train the SOM. Selection of an optimal late-time interval for feature



extraction is a very important step. After the computation of discrete Wigner-Ville distributions and the corresponding energy density vectors for each reference scattered signal, the optimal late-time interval can be selected by using the optimization approach outlined in Chapter 2. This critical design interval is affected by the SNR level of the signals in the reference database. For example, combination of the late-time bands 11 and 12 are chosen (out of  $Q=16$  equally-wide non-overlapping time intervals) to determine the optimal design interval [16.8-20.1] nsec in the case of noise-free classifier design for the library target TL1 based on the correct classification factor (CCF) versus interval index ( $q^*$ ) plot shown in Figure 3.2. The CCF values of this plot are computed for each time interval index  $q^*=1, \dots, Q-1$  by using Equation 2.11 as discussed in Chapter 2.

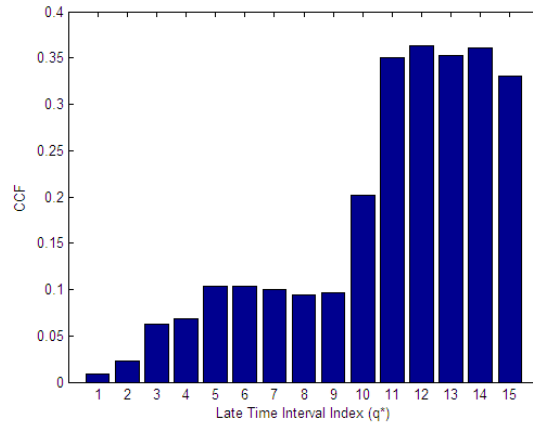


Figure 3.2 The CCF versus  $q^*$  plot generated to determine the optimal late-time design interval for the target library TL1 in the case of noise-free classifier design.

For the classifiers designed for the target library TL1 with noisy reference databases at the SNR levels of 20 dB and 10 dB, the optimal late-time design intervals are found to be [16.8-20.1] nsec and [9.8-13.0] nsec, respectively, based on the CCF versus  $q^*$  plots shown in parts (a) and (b) of Figure 3.3.

After selecting the optimal design interval and computing the late-time feature vectors (LTFVs) over this interval, the reference feature database of the classifier is constructed as the collection of all these LTFVs, which will be used to train the SOM classifier. As an example, LTFV of sphere S2, at the reference aspect angle  $\theta=75^\circ$  for 20 dB SNR level, extracted over the optimal late time interval [16.8-20.1] is shown in Figure 3.1.c.

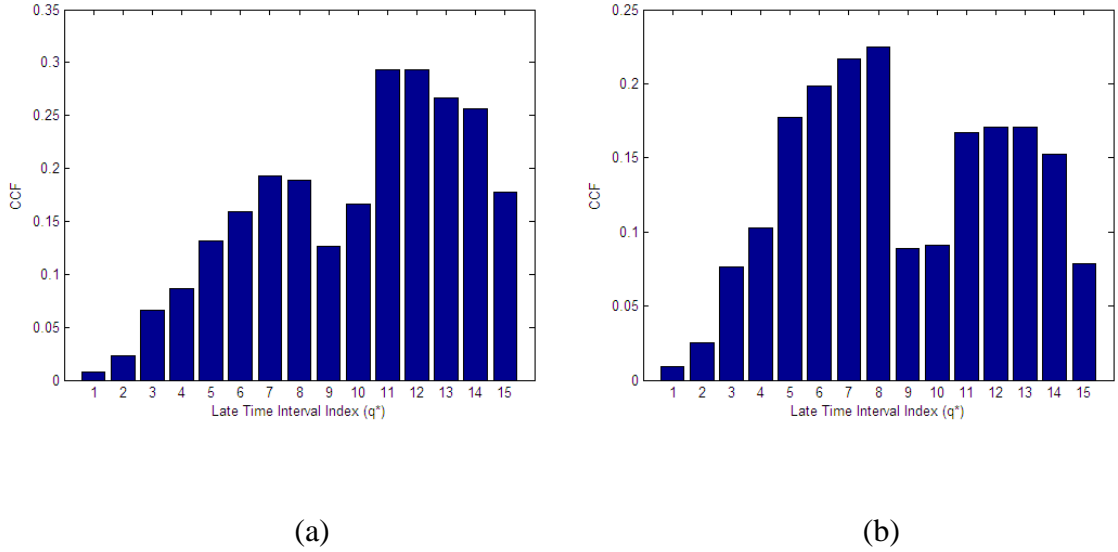


Figure 3.3 The CCF versus  $q^*$  plot generated to determine the optimal late-time design interval for the target library TL2 in the case of (a) SNR level of 20 dB and (b) SNR level of 10 dB classifier designs.

As mentioned in Chapter 2, a SOM consists of neurons organized on a regular low-dimensional grid and there are important structural parameters involved in SOM training. Before reporting the details of SOM classifier design and test simulations for different target libraries, it would be better to outline the common types and/or common values of the structural parameters used in SOM training. Size of the SOM grid and radius of the neighborhood function may change from one design simulation to another but the other SOM parameters will remain the same for all simulations to be reported in this chapter.

Firstly, the SOM is initialized with randomly generated weight vectors assigned to each and every neuron over a planar square grid of size  $N$  by  $N$ . The length of each weight vector is equal to the length of the WD based feature vectors (LTFVs) of the feature database. In this chapter, WD based target features have the length 1024 for all dielectric spheres at all target aspects. After the initialization, sequential SOM training will be accomplished in two steps; target features at the reference aspects  $\theta = 30^\circ, 75^\circ, 105^\circ,$  and  $135^\circ$  will be used in the first step of training and then, those at reference aspects  $\theta = 5^\circ$  and  $179^\circ$  will be added to training feature database in the second step. Based on experience, this two-step training is found useful to improve the performance of classifier at those aspects close to  $\theta = 0^\circ$  and  $180^\circ$  boundaries.

Also, the maximum number of iterations will be 500 epochs, initial learning rate will be 0.5, and the Gaussian type neighborhood function is used in all design simulations.

### **3.2 Design of SOM Classifiers for the Target Library TL1 of Two Dielectric Spheres**

In this subsection, three different SOM classifiers will be designed for the simplest target library of only two dielectric spheres S1 ( $r=10$  cm,  $\epsilon =3$ ), S2 ( $r=10$  cm,  $\epsilon =4$ ). The first classifier will be designed by using noise-free reference data and it will be tested at all non-reference aspects for the SNR levels of infinity, 20 dB, 15 dB and 10 dB. Secondly, slightly noisy reference data at 20 dB SNR level will be used in SOM training. The resulting classifier will also be tested at the SNR levels of infinity, 20 dB, 15 dB, 10 dB. Finally, the similar classifier design and test simulations will be repeated while using the reference data at a moderate noise level of 10 dB for SOM training.

### 3.2.1. **Classifier Simulation #1: Design of a SOM Classifier Using Noise-Free Reference Data for the Target Library TL1 with Spheres S1 and S2**

As indicated in Section 3.1, this classifier is designed over the late-time interval [16.8-20.1] nsec using noise-free scattered data of spheres S1 and S2 at the reference aspects  $\theta = 5^\circ, 30^\circ, 75^\circ, 105^\circ, 135^\circ, 179^\circ$ . The LTFV features extracted for both dielectric spheres at these bistatic aspects are used to train a SOM grid of size [12x12]. The SOM is initialized randomly at the beginning and the radius of the Gaussian neighborhood function is chosen to decrease from 7 to 3 during iterations. Sequential training of the SOM is completed after 500 epochs. During this training, a total of 12 training features (for 2 targets at 6 reference aspects) are selected in random order to train the self organizing map. When the training phase is completed, the resulting SOM output with  $12 \times 12 = 144$  weight vectors (each having the length of 1024) is saved as the classifier design matrix of size  $144 \times 1024$ . Figure 3.4 shows the contour plot of the norms of the trained weight vectors over the SOM grid of size  $12 \times 12$ . It is seen in this figure that two separate cluster regions are formed at the lower-left and the upper-right corners of the SOM output grid corresponding to the targets S1 and S2, respectively. The cluster region for the target S1, for example, is formed by the weight vectors whose distances to the LTFVs of the target S1 at all reference aspects are very small. This fact is more clearly shown in Figure 3.5 where the winning neuron locations for the training target features belonging to each dielectric sphere are marked on this SOM output. Although two different cluster regions can be clearly observed on this SOM output map, it is still necessary to draw the boundary curve separating these two regions over the map. In fact, there is no definite rule to divide the whole map into two well-defined regions as “the S1 region” and “the S2 region”. Such a separation is needed, however, during the test phase to classify an “unknown” target. When a scattered signal is received from a test target, the first thing to do is to extract the late-time feature vector (LTFV) from this test signal

over the previously selected optimal late-time design interval. Then, the distance of this feature vector to each weight vector is computed (in the L2 norm sense) at 144 neuron locations. The target cluster region containing the winning test neuron determines the class of this test target.

Among many others, three rules can be defined to determine the cluster boundary for the SOM output as shown in Figure 3.5:

- i) Rule 1: The cluster boundary is drawn as the dot-dashed red curve which passes through the neuron locations with smallest norm values.
- ii) Rule 2: The cluster boundary is drawn as the dashed orange curve which passes through the midpoints of closest training winning neurons from different clusters. For example, one such midpoint is obtained for the neuron locations for  $S1/5^0$  and  $S2/179^0$  training features. Another example point on the border curve is the midpoint of winning neurons for  $S1/30^0$  and  $S2/179^0$  training features.
- iii) Rule 3: Cluster boundary curves drawn in black leave a wide neutral region in between two target cluster regions. These black boundaries pass through neuron locations at which the weight norms do not have to be very close to the absolute minimum but they need to be sufficiently small. Obviously, “sufficiently small” is a vague definition and depends on the subjective decision of the designer.

While testing the performance of Classifier #1 designed in this first simulation, all three of the cluster boundaries shown in Figure 3.5 will be used to compute the corresponding accuracy rates of the classifier to choose the best fitting boundary curve.

The SOM based Classifier #1 is tested first with noise-free target features at seven non-reference aspects. Locations of the winning neurons for these tests are marked in Figure 3.6 with a correct decision rate of 93 percent based on the black cluster boundary. The only incorrect classification decision is made for the sphere S1 at 15 degrees aspect angle. As a matter of fact, the winning neuron for this test feature falls in the neutral region in between the two target cluster regions. Therefore, the target is not incorrectly labeled but the classifier can not classify this target with certainty. The accuracy rate of 100 percent is obtained, on the other hand, based on the orange and red cluster boundaries.

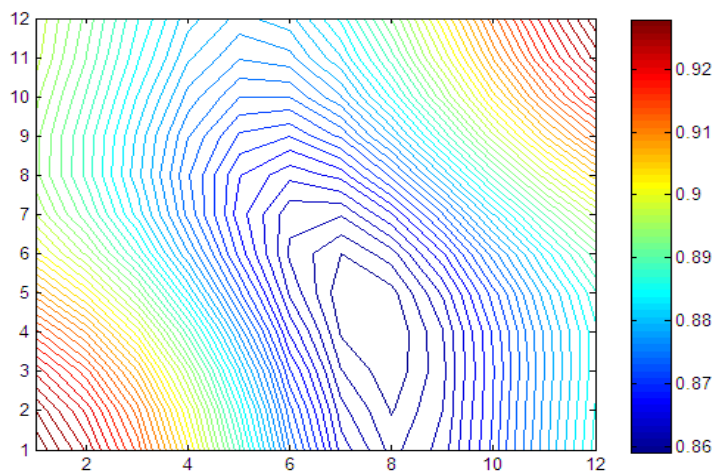


Figure 3.4 SOM output trained by the noise-free WD-based late time energy feature vectors of the dielectric spheres S1 and S2.

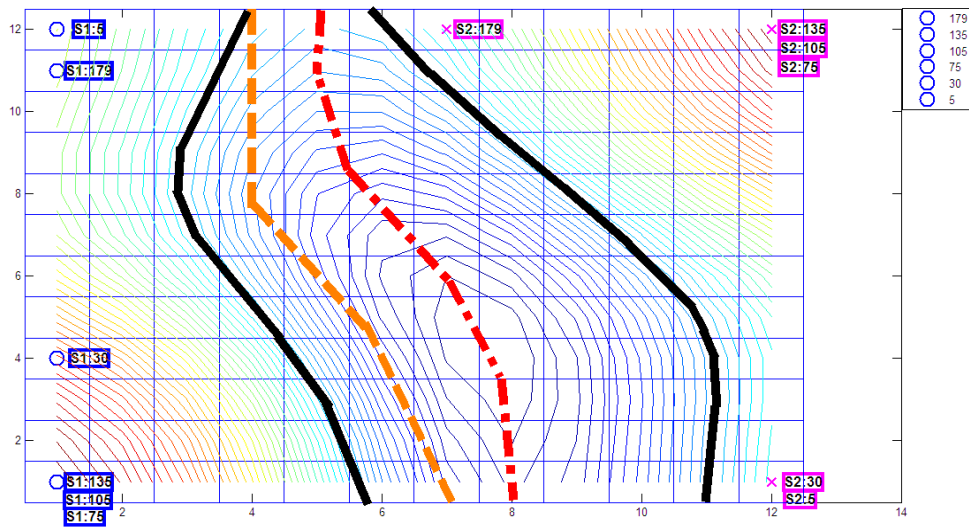


Figure 3.5 Winning neuron locations for the training features of spheres S1 (blue circles), S2 (magenta crosses) and three possible boundary curves to separate the cluster regions for S1 and S2 over the SOM output grid for the Classifier #1.

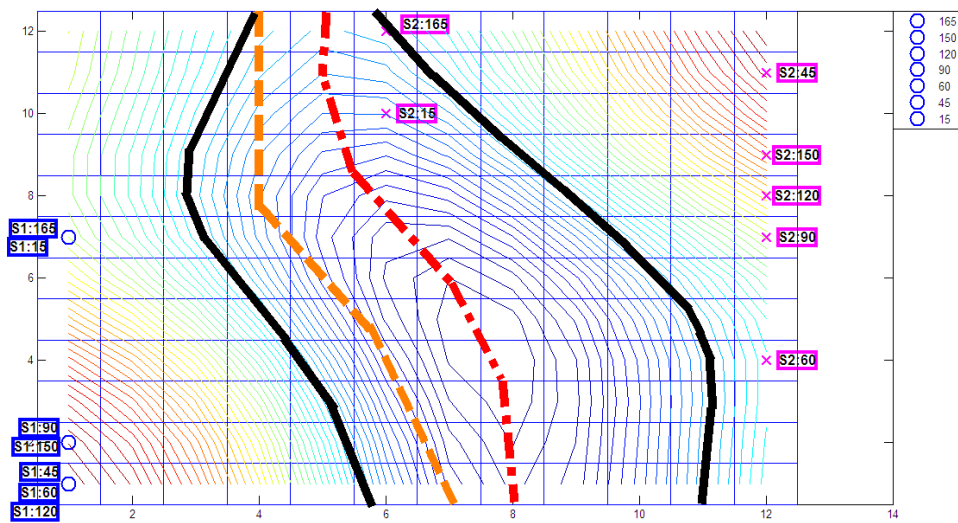


Figure 3.6 SOM Classifier #1 tested by noise-free feature vectors of the spheres S1 (blue circles) and S2 (magenta crosses), using three different cluster boundaries drawn by Rule 1 (red curve), Rule 2 (orange curve) and Rule 3 (black curve).

Next, the Classifier #1 is tested by noisy feature vectors at 20 dB, 15 dB and 10 dB SNR levels. As the feature vectors at reference aspects are not the same as their noise-free counterparts anymore, Classifier #1 is tested with a total of 26 noisy features (for two targets at 13 aspects) under noisy conditions. Locations of the testing winning neurons are marked in Figure 3.7, Figure 3.8 and Figure 3.9 for the SNR levels of 20 dB, 15 dB and 10 dB, respectively. The correct classification rates computed at each testing SNR level for each type of cluster boundary are listed in Table 3.2 and also plotted in Figure 3.10. Table 3.2 also gives the accuracy rates obtained over a restricted bistatic aspect range excluding  $\theta = 5, 15, 165$  and  $179$  degree cases because most of the classification errors occur at those aspects close to the ends of the overall aspect range. In general, the accuracy rate of the classifier decreases as the testing SNR level gets smaller, as expected.

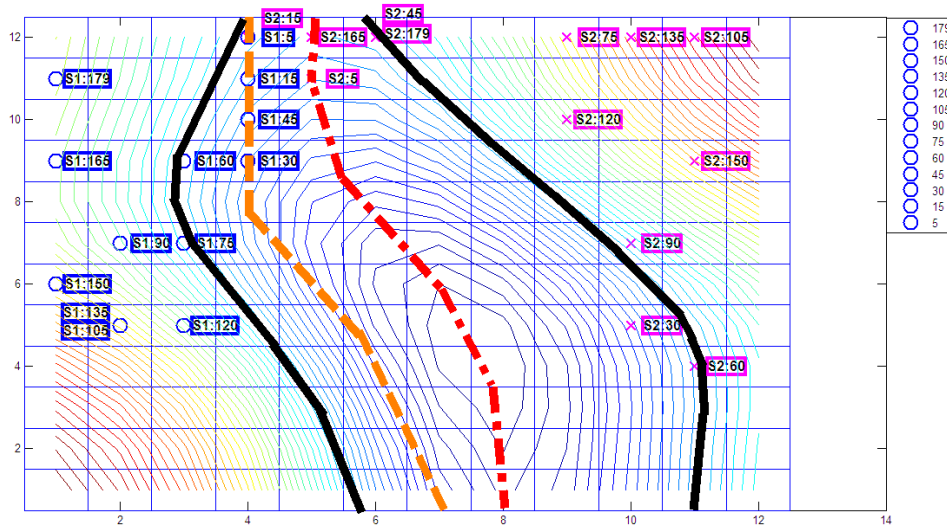


Figure 3.7 SOM Classifier #1 tested by noisy feature vectors of spheres S1 (blue circles) and S2 (magenta crosses) at 20 dB SNR level, using three different cluster boundaries drawn by Rule 1 (red curve), Rule 2 (orange curve) and Rule 3 (black curve).



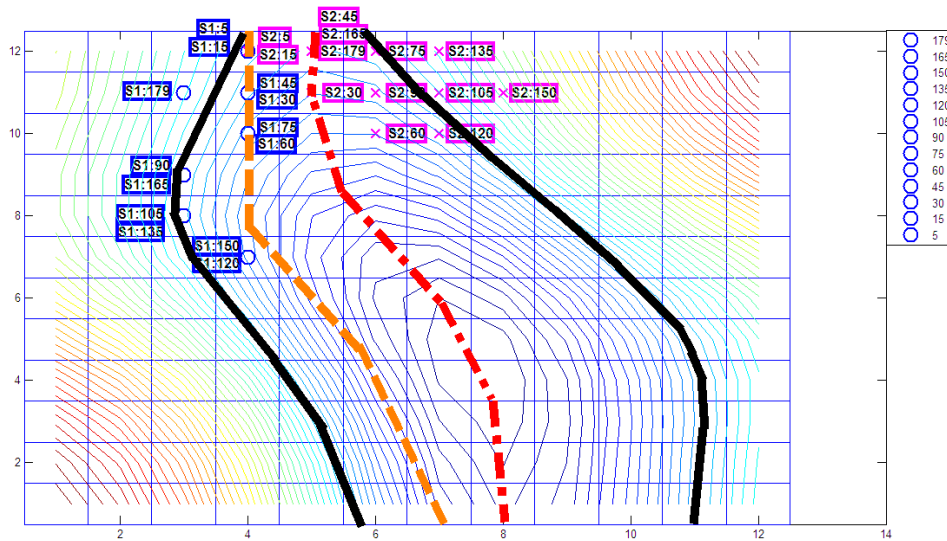


Figure 3.8 SOM Classifier #1 tested by noisy feature vectors of spheres S1 (blue circles) and S2 (magenta crosses) at 15 dB SNR level, using three different cluster boundaries drawn by Rule 1 (red curve), Rule 2 (orange curve) and Rule 3 (black curve).

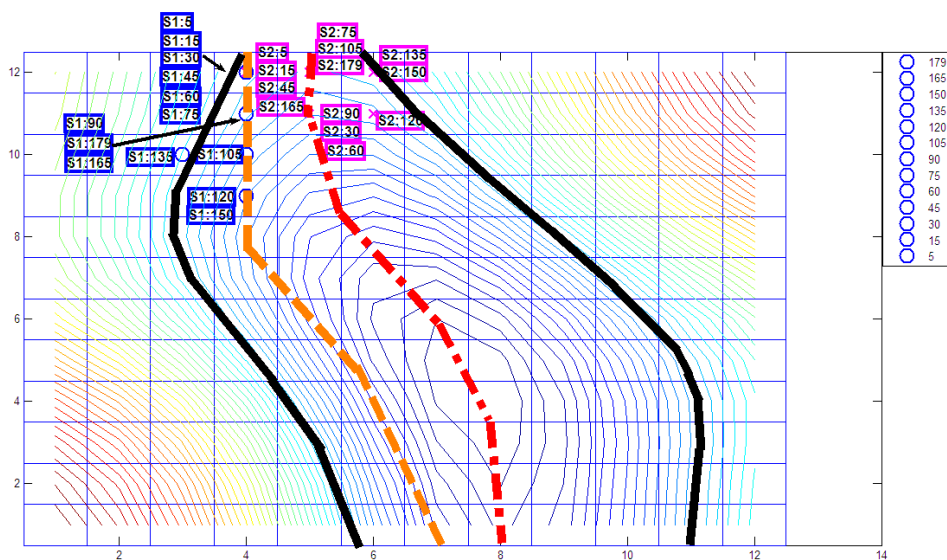


Figure 3.9 SOM Classifier #1 tested by noisy feature vectors S1 (blue circles) and S2 (magenta crosses) at 10 dB SNR level, using three different cluster boundaries drawn by Rule 1 (red curve), Rule 2 (orange curve) and Rule 3 (black curve).

Table 3.2 Correct decision rates for the Classifier #1 at different testing SNR levels for each type of cluster boundary.

SNR	Type Of Cluster Boundaries and $\theta$ Ranges					
	For $5^\circ \leq \theta \leq 179^\circ$			For $15^\circ < \theta < 165^\circ$		
	Black	Orange	Red	Black	Orange	Red
Noise Free	93	100	100	100	100	100
20 dB	46	77	88	56	89	100
15 dB	15	69	84	17	78	88
10 dB	4	38	62	6	50	67

As it seen clearly from Figure 3.10 and Table 3.2, the SOM based Classifier #1, which is designed by noise-free reference data, can successfully discriminate the spheres S1 and S2 under low noise testing conditions but its performance degrades as the testing SNR decreases. In the next section, a new classifier will be designed for the same target library TL1 (of dielectric spheres S1 and S2) by using slightly noisy reference data at 20 dB SNR level to improve the classification performance at lower testing SNR values.

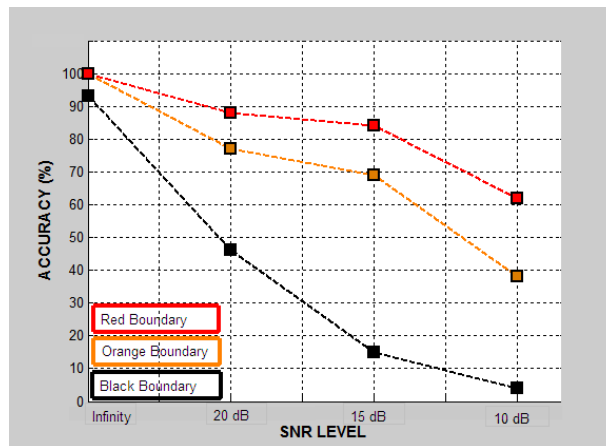


Figure 3.10 Correct classification rates computed for the Classifier #1 at various testing SNR levels at all aspects for different cluster boundaries, red curve for Rule 1, orange curve for Rule 2 and black curve for Rule 3.

It is also concluded based on the results shown in Figure 3.10 and Table 3.2 that the best way to separate target clusters on the SOM output grid is to use a locus of neurons with minimum weight norms. In cases when this is not possible, the cluster boundaries can be constructed by using the midpoints of closest training winning neurons of different target clusters. These approaches will be used in the classifier design simulations in the rest of this thesis.

**3.2.2. Classifier Simulation #2: Design of a SOM Classifier Using Slightly Noisy (SNR Level of 20 dB) Reference Data for the Target Library TL1 with spheres S1 and S2**

The classifier of this simulation is designed over the late-time interval [16.8-20.1] nsec using slightly noisy (SNR level of 20 dB) scattered data of spheres S1 and S2 at the reference aspects  $\theta = 5^\circ, 30^\circ, 75^\circ, 105^\circ, 135^\circ, 179^\circ$ , with the same design parameters used in Classifier Simulation #1. The optimal late-time intervals of the first and second classifier design simulations are turned out to be the same. When the training phase is completed, the resulting SOM output with  $12 \times 12 = 144$  weight vectors (each having the length of 1024) is saved as the classifier design matrix of size  $144 \times 1024$ . Figure 3.11 shows the contour plot of the norms of the trained weight vectors over the SOM grid of size  $12 \times 12$ .

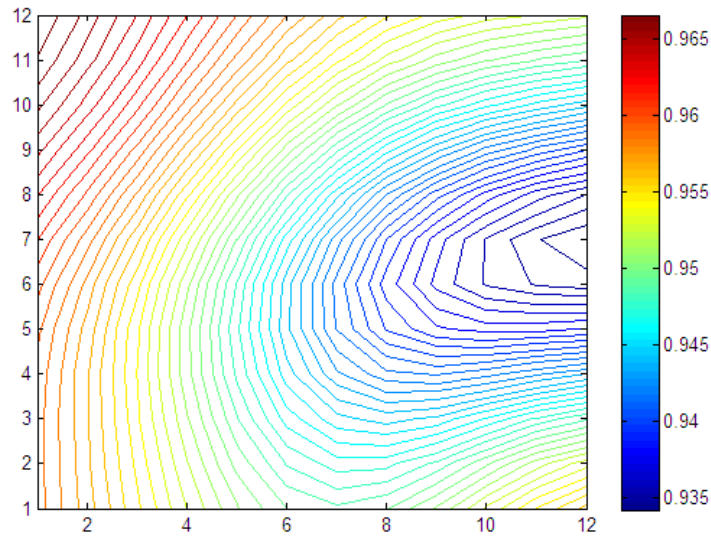


Figure 3.11 SOM output trained by slightly noisy (at the SNR level of 20 dB) WD-based late time energy feature vectors of the dielectric spheres S1 and S2.

It is seen in Figure 3.11 that, it is difficult to separate cluster regions by using neuron locations with smallest norm values only, so the cluster boundary is instead constructed by using the midpoints of closest training winning neurons of different target clusters also in other words, the Rule 1 and the Rule 2 are used together in selecting the cluster boundary in this design example. The winning neuron locations for the training target features belonging to each dielectric sphere are marked on the SOM output in Figure 3.12.

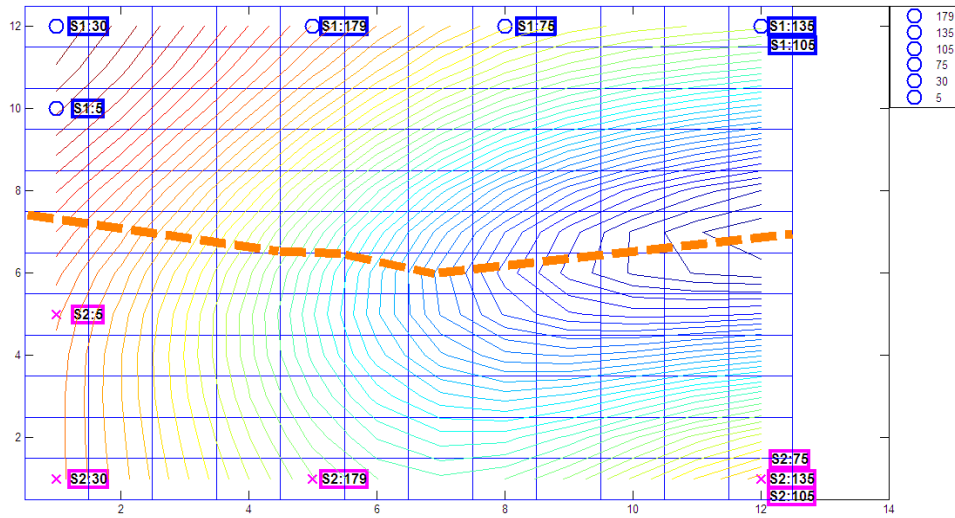


Figure 3.12 Winning neuron locations for the training features of spheres S1 (blue circles) and S2 (magenta crosses) and the boundary curve to separate the cluster regions for S1 and S2 over the SOM output grid for the Classifier #2.

Next, the Classifier #2 is tested with a total of 26 features (for two targets at 13 aspects) under noise free and noisy conditions with SNR level of 15 dB and 10 dB. It is also, tested with SNR level of 20 dB noisy target features at seven non-reference aspects. Locations of the testing winning neurons are marked in Figure 3.13, Figure 3.14, Figure 3.15, and Figure 3.16 for the SNR levels of infinity, 20 dB, 15 dB and 10 dB, respectively. The correct classification rates computed at each testing SNR level for each type of cluster boundary are listed in Table 3.3 and also plotted in Figure 3.17 Table 3.3 also gives the accuracy rates obtained over a restricted bistatic aspect range excluding  $\theta = 5, 15, 165$  and  $179$  degree cases.

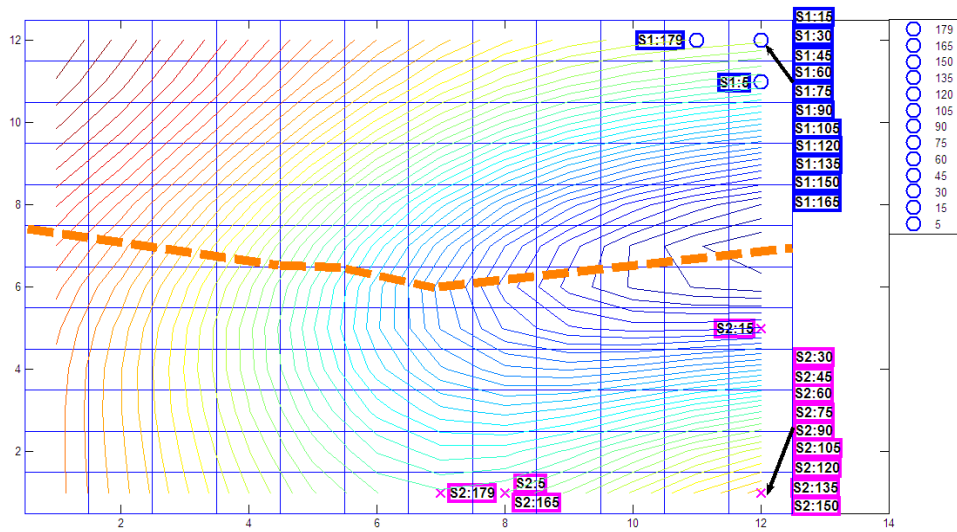


Figure 3.13 SOM Classifier #2 tested by noise-free feature vectors of spheres S1 (blue circles) and S2 (magenta crosses).

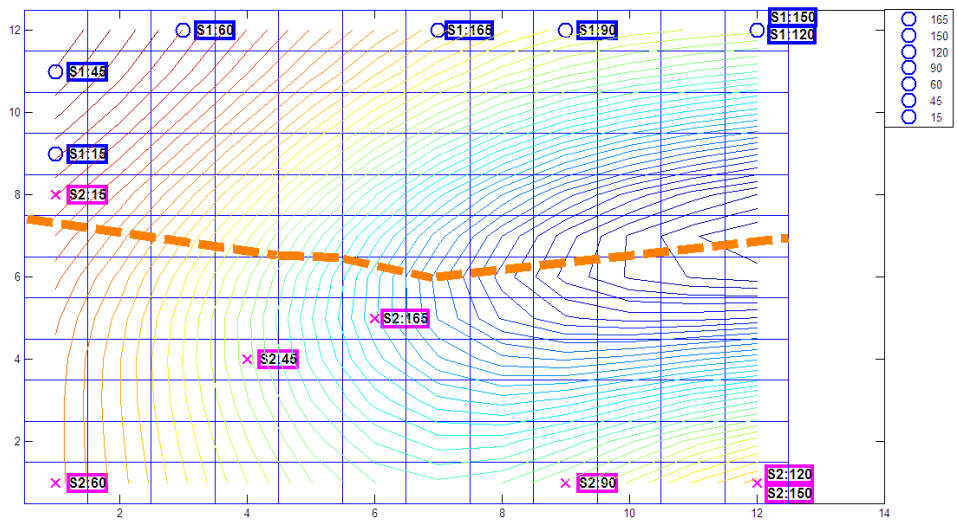


Figure 3.14 SOM Classifier #2 tested by noisy feature vectors of spheres S1 (blue circles) and S2 (magenta crosses) at 20 dB SNR level.

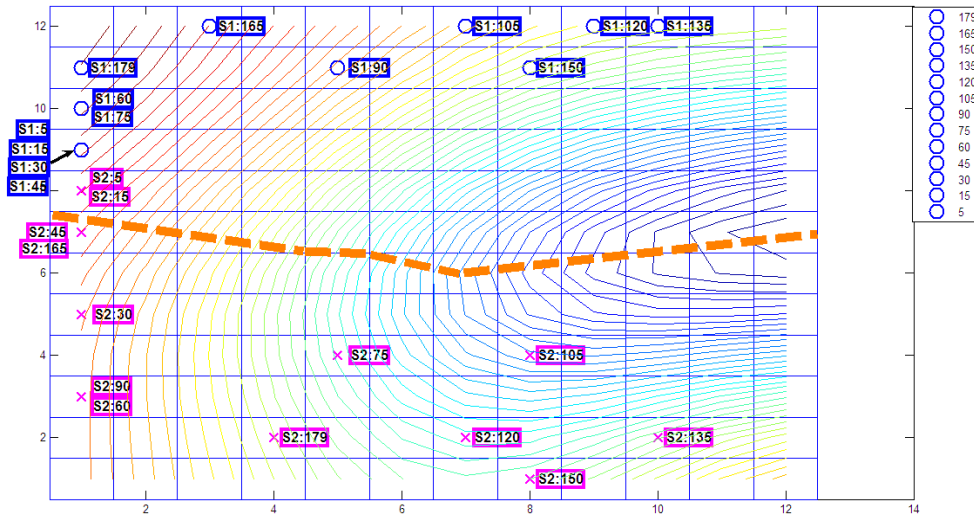


Figure 3.15 SOM Classifier #2 tested by noisy feature vectors of spheres S1 (blue circles) and S2 (magenta crosses) at 15 dB SNR level.

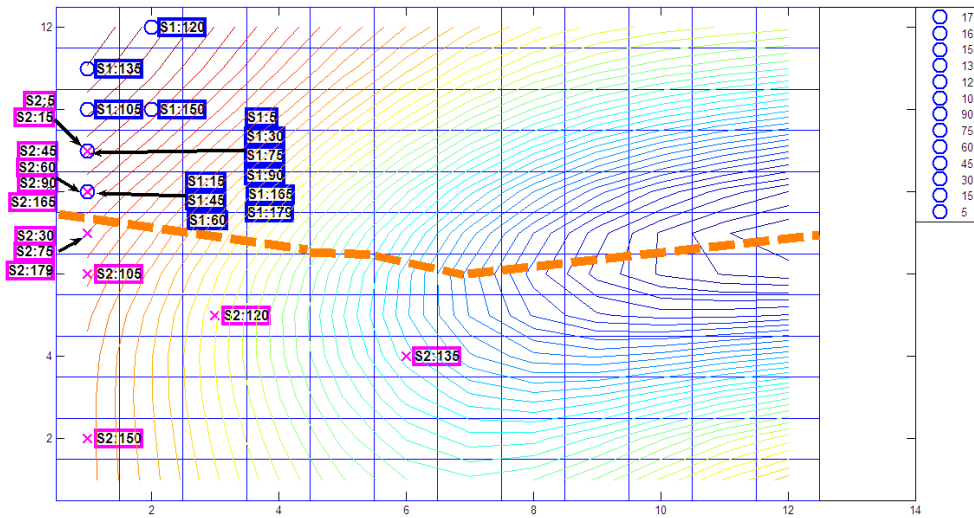


Figure 3.16 SOM Classifier #2 tested by noisy feature vectors of spheres S1 (blue circles) and S2 (magenta crosses) at 10 dB SNR level.

Table 3.3. Correct decision rates for the Classifier #2 at different testing SNR levels.

SNR	Type Of $\theta$ Ranges	
	For $5^\circ \leq \theta \leq 179^\circ$	For $15^\circ < \theta < 165^\circ$
Noise Free	100	100
20 dB	93	100
15 dB	92	100
10 dB	77	83

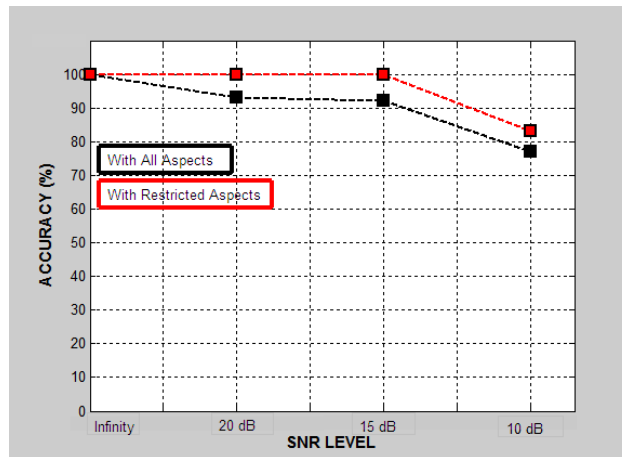


Figure 3.17 Correct classification rates computed for the Classifier #2 at various testing SNR levels.

Based on the correct decision rates reported in Table 3.2 and Table 3.3, it is clearly seen that Classifier #2 displays a much better noise performance as compared to Classifier #1. Using slightly noisy data in SOM classifier design helps improving the classifier performance.



### 3.2.3. Classifier Simulation #3: Design of a SOM Classifier Using Moderately Noisy (SNR Level of 10 dB) Reference Data for the Target Library TL1 with spheres S1 and S2

The optimal late-time interval is found to be [9,8-13.0] nsec for the design of Classifier #3 while using noise-free scattered data of spheres S1 and S2 at the reference aspects  $\theta = 5^\circ, 30^\circ, 75^\circ, 105^\circ, 135^\circ, 179^\circ$ . After the classifier training phase is completed, the resulting SOM output with  $12 \times 12 = 144$  weight vectors (each having the length of 1024) is saved as the classifier design matrix of size  $144 \times 1024$ . Figure 3.18 shows the contour plot of the norms of the trained weight vectors over the SOM grid of size  $12 \times 12$ .

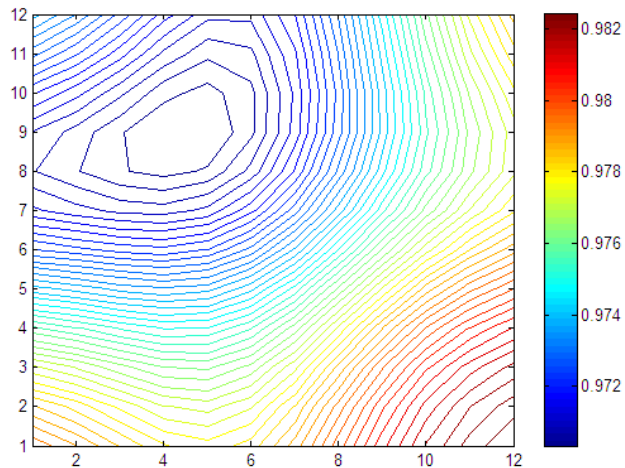


Figure 3.18. SOM output trained by noisy (at SNR level of 10 dB) WD-based late time energy feature vectors of the dielectric spheres S1 and S2.

The cluster boundary is constructed by using the midpoints of closest training winning neurons of different targets as shown in Figure 3.19. The winning neuron locations for the training target features belonging to each dielectric sphere are marked on the SOM output shown in this figure. Then, the Classifier #3 is tested at the SNR level of infinity, 20 dB, 15 dB and 10 dB. Locations of the testing

winning neurons are shown in Figure 3.20, Figure 3.21, Figure 3.22, and Figure 3.23 for these SNR levels, respectively. The correct classification rates computed at each testing SNR level for Classifier #3 are listed in Table 3.4 and plotted in Figure 3.24

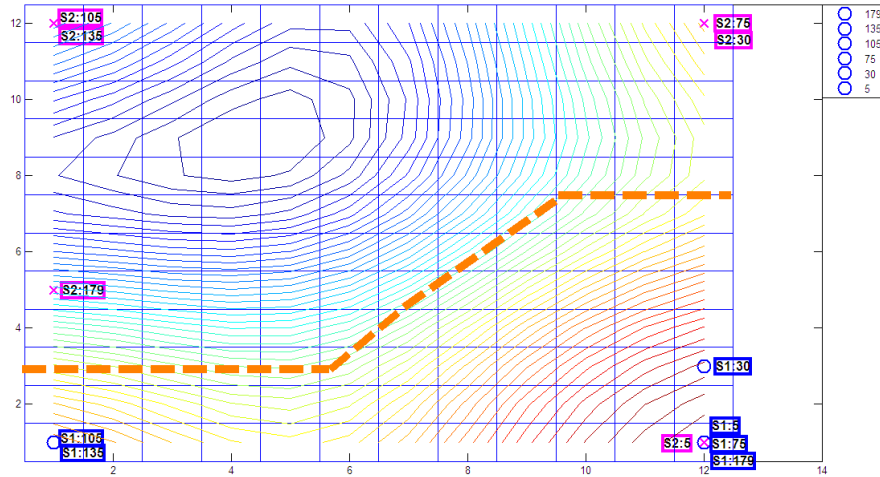


Figure 3.19. Winning neuron locations for the training features of spheres S1 (blue circles) and S2 (magenta crosses) and the boundary curve to separate the cluster regions for S1 and S2 over the SOM output grid for the Classifier #3.

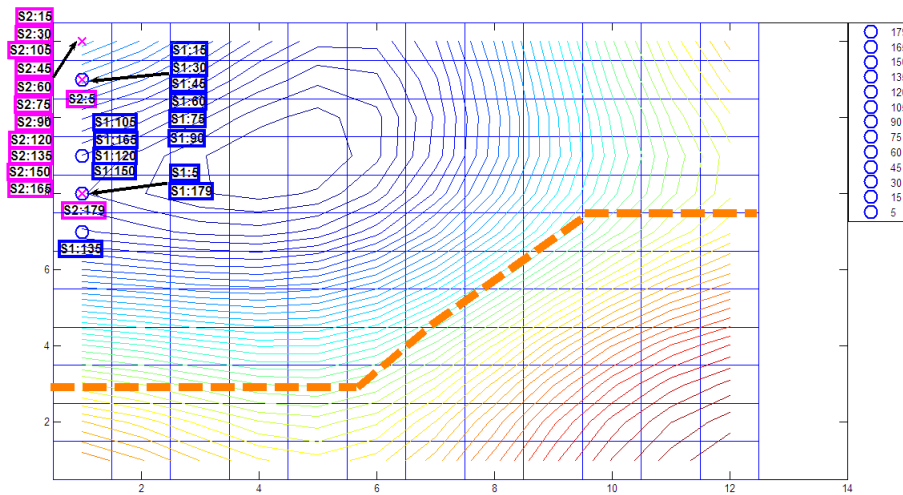


Figure 3.20. SOM Classifier #3 tested by noise-free feature vectors of spheres S1 (blue circles) and S2 (magenta crosses).

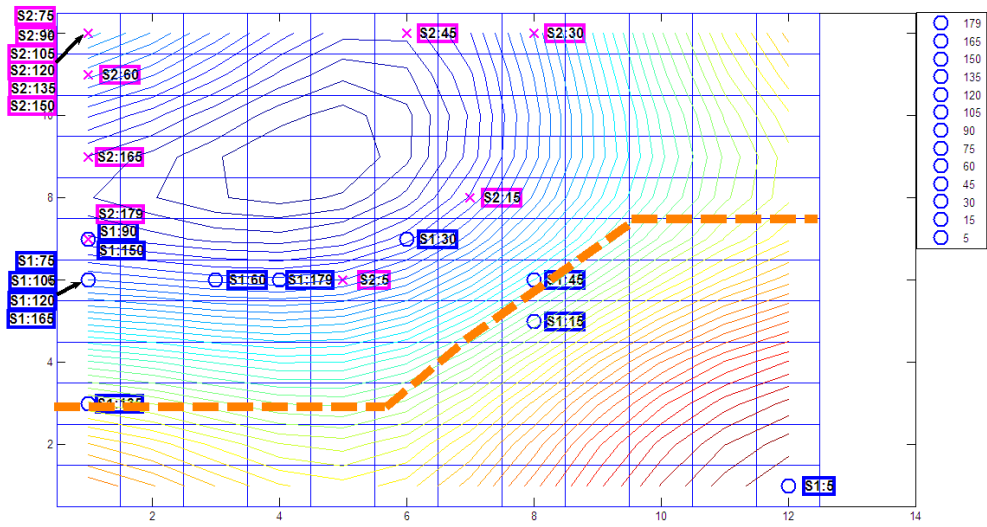


Figure 3.21. SOM Classifier #3 tested by noisy feature vectors of spheres S1 (blue circles) and S2 (magenta crosses) at 20 dB SNR level.

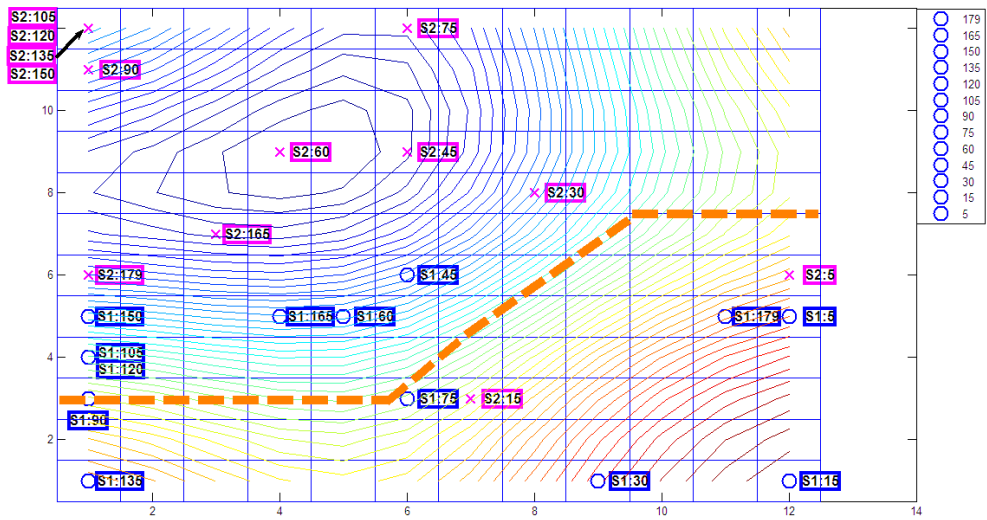


Figure 3.22. SOM Classifier #3 tested by noisy feature vectors of S1 (blue circles) and S2 (magenta crosses) at 15 dB SNR level.

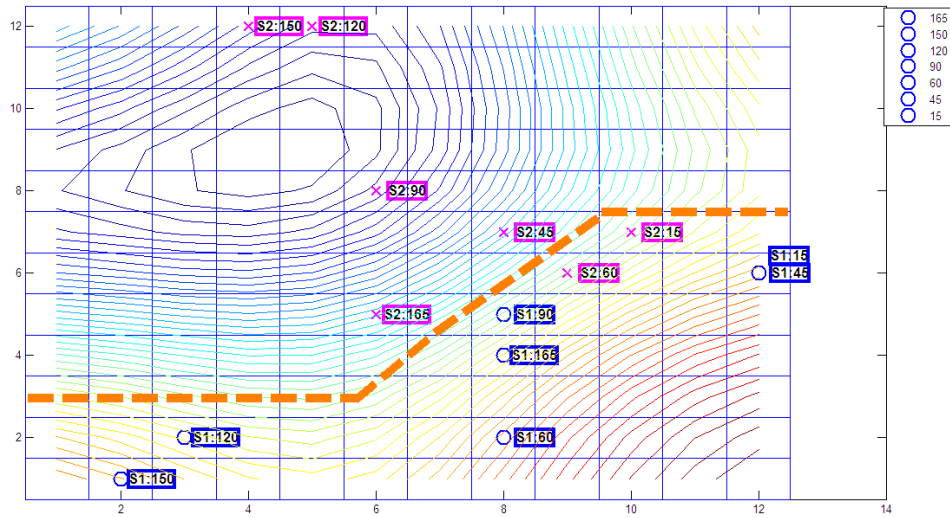


Figure 3.23. SOM Classifier #3 tested by noisy feature vectors of spheres S1 (blue circles) and S2 (magenta crosses) at 10 dB SNR level.

Table 3.4. Correct decision rates for the Classifier #3 at different testing SNR levels for each type of cluster boundary.

SNR	Type Of $\theta$ Range	
	For $5^\circ \leq \theta \leq 179^\circ$	For $15^\circ < \theta < 165^\circ$
Noise Free	50	50
20 dB	58	50
15 dB	65	72
10 dB	86	92

Correct classification rate of Classifier #3 is found acceptable only at the design SNR of 10 dB as shown in Table 3.4. When this classifier is tested by noise-free data, the accuracy rate turned out to be only 50 percent. Therefore, we can conclude that too much noise in training data results in an unsuccessful SOM classifier design.

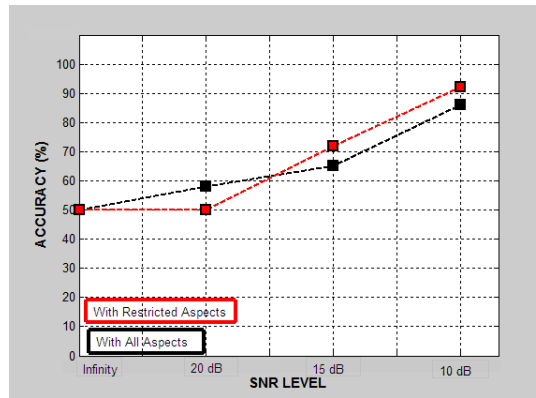


Figure 3.24. Correct classification rates computed for the Classifier #3 at various testing SNR levels

Finally, the correct classification rates of all three classifiers, Classifier #1 (designed by noise-free data), Classifier #2 (designed by slightly noisy data at 20 dB SNR level) and Classifier #3 (designed by moderately noisy data at 10 dB SNR level) are compared in Figure 3.25. Classifier #2 turns out to be the best classifier while Classifier #3 is found almost useless. The accuracy rates of Classifier #1 and Classifier #2 degrades as the testing SNR gets smaller as expected.

In conclusion, design of a SOM classifier with slightly noisy reference data is found useful in the 2-target classifiers of this section.

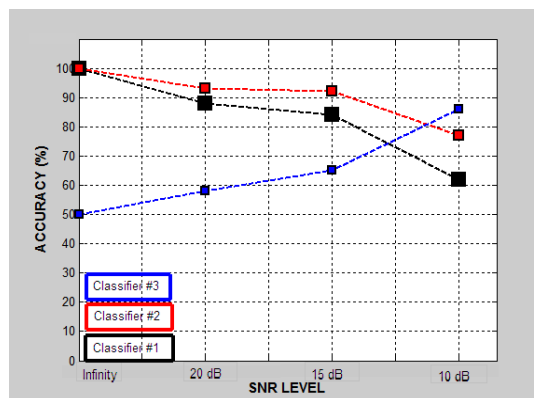


Figure 3.25. Correct classification rates computed for the Classifier #1, Classifier # 2 and Classifier #3 at various testing SNR levels for the aspect range  $5^\circ < \theta < 179^\circ$

### 3.3 Design of SOM Classifiers for the Target Library TL2 of Three Dielectric Spheres

In this subsection, three different SOM classifiers will be designed for the target library TL2 which contains three dielectric spheres S1 ( $r=10$  cm,  $\epsilon=3$ ), S2 ( $r=10$  cm,  $\epsilon=4$ ) and S3 ( $r=10$  cm,  $\epsilon=5$ ). The first classifier will be designed by using noise-free reference data and it will be tested at the SNR levels of infinity, 20 dB, 15 dB and 10 dB. Secondly, slightly noisy reference data at 20 dB SNR level will be used in SOM training. The resulting classifier will also be tested at the SNR levels of infinity, 20 dB, 15 dB, 10 dB. Finally, the similar classifier design and test simulations will be repeated while using the reference data at a moderate noise level of 10 dB for SOM training.

The optimal late-time intervals for classifier design are determined based on the CCF versus  $q^*$  plots shown in Figure 3.26 for noise-free design case, in Figure 3.27.(a) for SNR=20 dB design and in Figure 3.27.(b) for SNR=10 dB design. The resulting design intervals are found to be [16.8-20.1] nsec for both noise free and SNR=20 dB cases. The optimal interval shifts to [9.8-13.0] nsec for classifier design at 10 dB SNR.

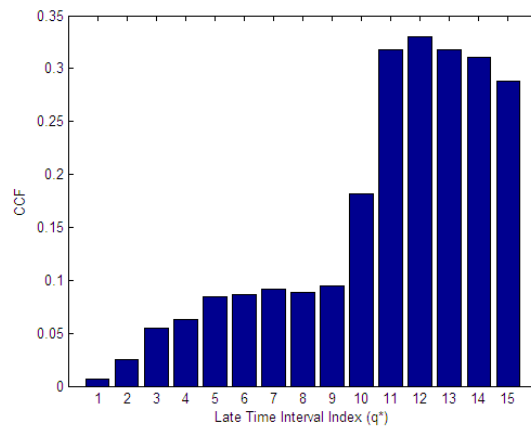


Figure 3.26 The CCF versus  $q^*$  plot generated to determine the optimal late-time design interval for the target library TL2 in the case of noise-free classifier design.

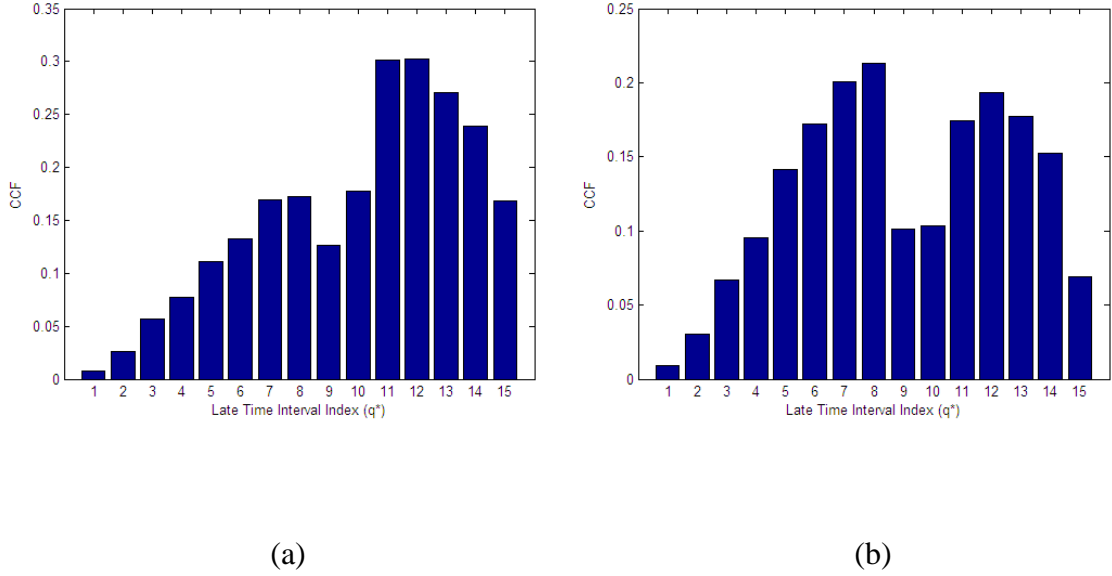


Figure 3.27 The CCF versus  $q^*$  plot generated to determine the optimal late-time design interval for the target library TL2 in the case of (a) SNR level of 20 dB and (b) SNR level of 10 dB classifier designs.

### 3.3.1. Classifier Simulation #4: Design of a SOM Classifier Using Noise-Free Reference Data for the Target Library TL2 with Spheres S1, S2 and S3

This classifier is designed over the late-time interval [16.8-20.1] nsec using noise-free scattered data of spheres S1, S2 and S3 at the reference aspects  $\theta = 5^\circ, 30^\circ, 75^\circ, 105^\circ, 135^\circ, 179^\circ$ . The LTFV features extracted for all three dielectric spheres at these reference aspects are used to train a SOM grid of size [21x21]. The SOM is initialized randomly at the beginning and the radius of the Gaussian neighborhood function is chosen to decrease from 10 to 7 during iterations. Sequential training of the SOM is completed after 500 epochs. During this training, a total of 18 training features (for 3 targets at 6 reference aspects) are selected in random order to train the self organizing map. When the training phase is completed, the resulting SOM output with  $21 \times 21 = 441$  weight vectors (each

having the length of 1024) is saved as the classifier design matrix of size 441x1024. Figure 3.28 shows the contour plot of the norms of the trained weight vectors over the SOM grid of size 21x21 .

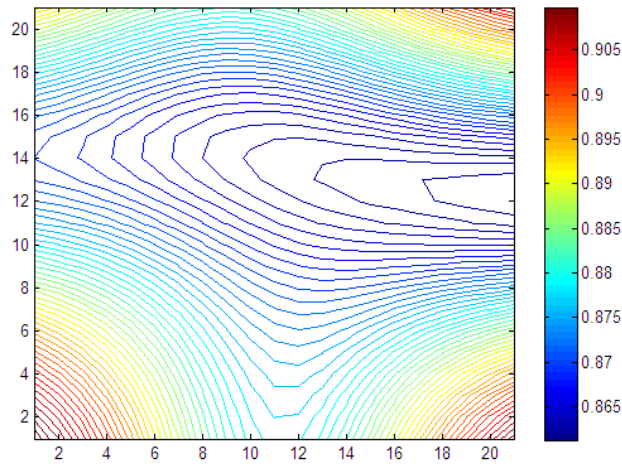


Figure 3.28 SOM output trained by the noise-free WD-based late time energy feature vectors of the dielectric spheres S1,S2 and S3.

It is seen in this figure that three separate cluster regions are formed at the lower-left and lower-right corners and along the upper side of the SOM output grid corresponding to the targets S3, S2 and S1, respectively. The winning neuron locations for the training target features belonging to each dielectric sphere are marked on the SOM output map as shown in Figure 3.29. The cluster boundary is conveniently constructed by using the locus of neurons with minimum weight norms as shown in this figure.

The SOM based Classifier #4 is tested first with noise-free target features at seven non-reference aspects. Locations of the winning neurons for these tests are marked in Figure 3.30 with a correct decision rate of 100 percent.



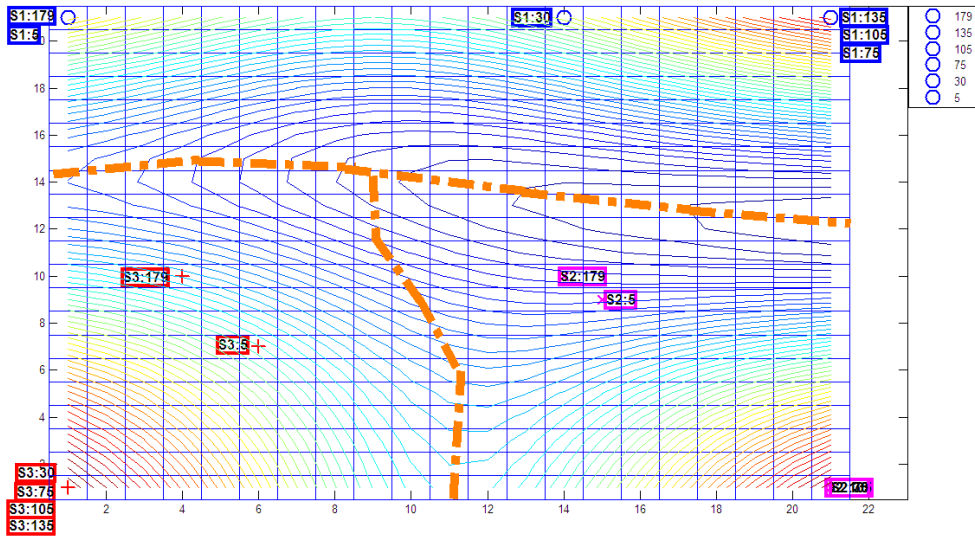


Figure 3.29 Winning neuron locations for the training features of spheres S1 (blue circles), S2 (magenta crosses) and S3 (red plus signs) over the SOM output grid for the Classifier #4.

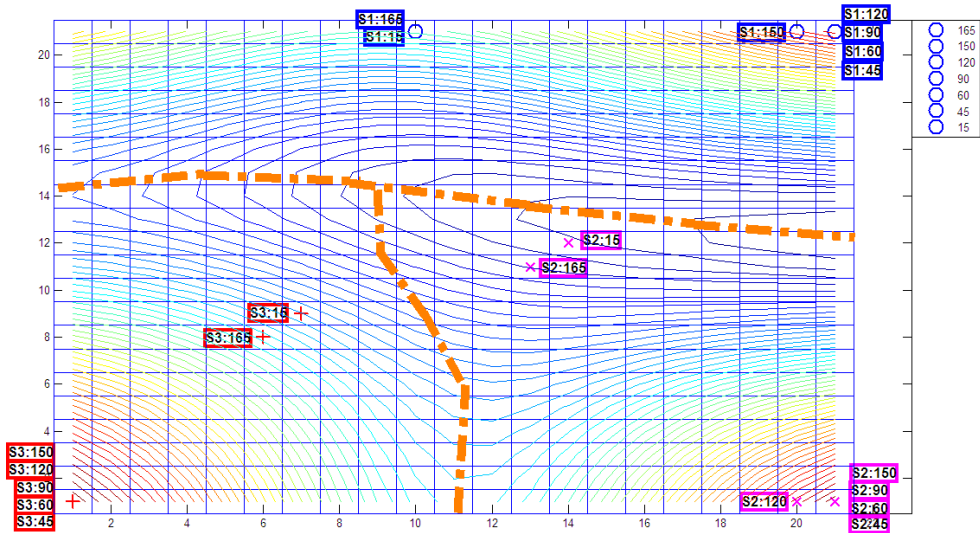


Figure 3.30 SOM Classifier #4 tested by noise-free feature vectors of spheres S1 (blue circles), S2 (magenta crosses) and S3 (red plus signs).

Then, the Classifier #4 is tested at by noisy feature vectors at 20 dB, 15 dB and 10 dB SNR levels at all aspects. Locations of the testing winning neurons are marked in Figure 3.31, Figure 3.32 and Figure 3.33 for the SNR levels of 20 dB, 15 dB and 10 dB, respectively. The correct classification rates computed at each testing SNR level are listed in Table 3.5 and these rates are also plotted in Figure 3.34. Table 3.5 reports the accuracy rates obtained over a restricted aspect range excluding the test cases for  $\theta = 5, 15, 165$  and  $179$  degree cases because most of the classification errors occur at those aspects which are close to the ends of the overall aspect range.

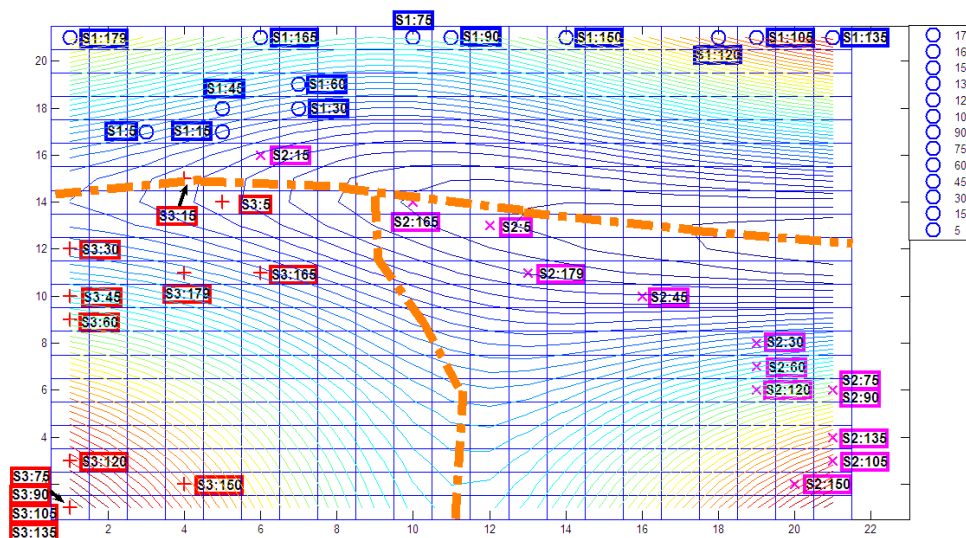


Figure 3.31 SOM Classifier #4 tested by noisy feature vectors of spheres S1 (blue circles), S2 (magenta crosses) and S3 (red plus signs) at 20 dB SNR level.

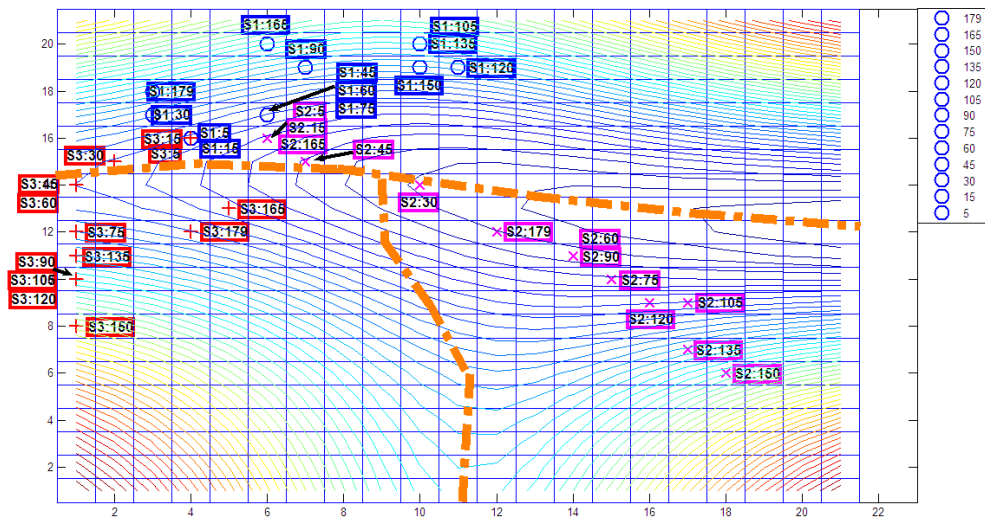


Figure 3.32 SOM Classifier #4 tested by noisy feature vectors of spheres S1 (blue circles), S2 (magenta crosses) and S3 (red plus signs) at 15 dB SNR level.

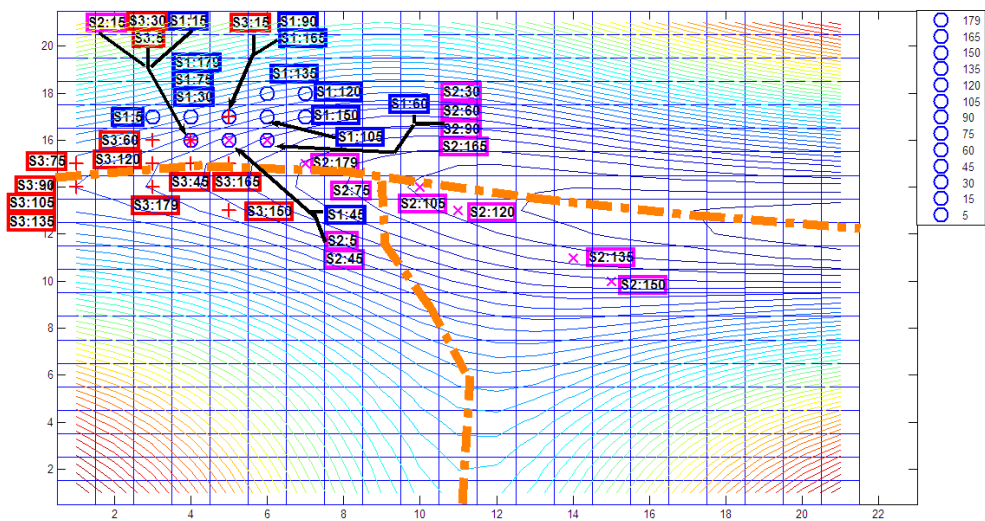


Figure 3.33 SOM Classifier #4 tested by noisy feature vectors of spheres S1 (blue circles), S2 (magenta crosses) and S3 (red plus signs) at 10 dB SNR level.

Table 3.5 Correct decision rates for the Classifier #4 at different testing SNR levels.

SNR	Type Of $\theta$ Range	
	For $5^\circ \leq \theta \leq 179^\circ$	For $15^\circ < \theta < 165^\circ$
Noise Free	100	100
20 dB	92	100
15 dB	80	89
10 dB	54	59

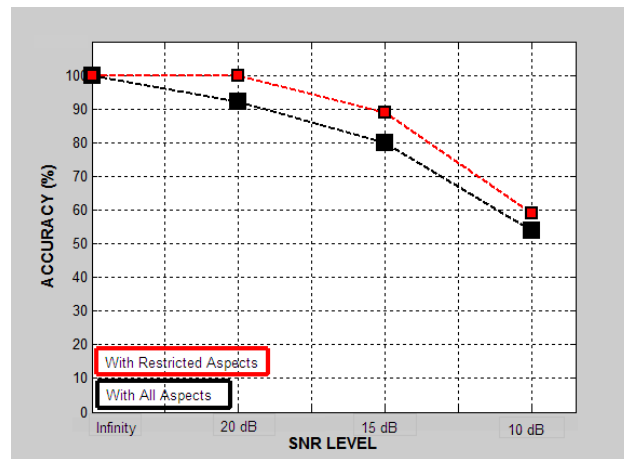


Figure 3.34 Correct classification rates computed for the Classifier #4 at various testing SNR levels.

As it seen clearly from Figure 3.34 and Table 3.5, the SOM based Classifier #4, which is designed by noise-free reference data, can successfully discriminate the spheres S1, S2 and S3 under low noise testing conditions but its performance degrades sharply as the testing SNR decreases, as also observed in the case of 2-Sphere Classifiers. In the next section, a new classifier will be designed for the same target library TL2 (of dielectric spheres S1, S2 and S3) by using slightly noisy reference data at 20 dB SNR level to improve the classification performance at lower testing SNR values.

### 3.3.2. Classifier Simulation #5: Design of a SOM Classifier Using Slightly Noisy (SNR Level of 20 dB) Reference Data for the Target Library TL2 of Spheres S1, S2 and S3

Classifier #5 is designed over the late-time interval [16.8-20.1] nsec using slightly noisy (SNR level of 20 dB) scattered data of spheres S1, S2 and S3 at the same reference aspects indicated in the previous simulations with default SOM design parameters. When the training phase is completed, the resulting SOM output with  $21 \times 21 = 441$  weight vectors (each having the length of 1024) is saved as the classifier design matrix of size  $441 \times 1024$ . Figure 3.35 shows the contour plot of the norms of the trained weight vectors over the SOM grid of size  $21 \times 21$ .

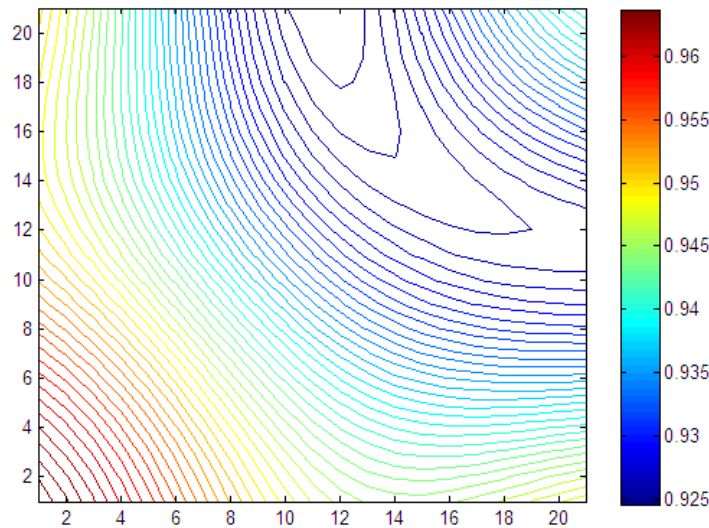


Figure 3.35 SOM output trained by slightly noisy (SNR Level of 20 dB) WD-based late time energy feature vectors of the dielectric spheres S1, S2 and S3.

The cluster boundary is constructed by using the midpoints of closest training winning neurons of different target clusters, as there is no natural cluster boundary implied in Figure 3.35. The winning neurons of all three spheres S1, S2, and S3 at

the training aspect of  $\theta = 5^\circ$  fall in the same lower left corner location. Therefore, that cell is chosen to be the intersection point of two cluster boundary curves drawn in Figure 3.36. The winning neuron locations of the reference features are also marked on this figure.

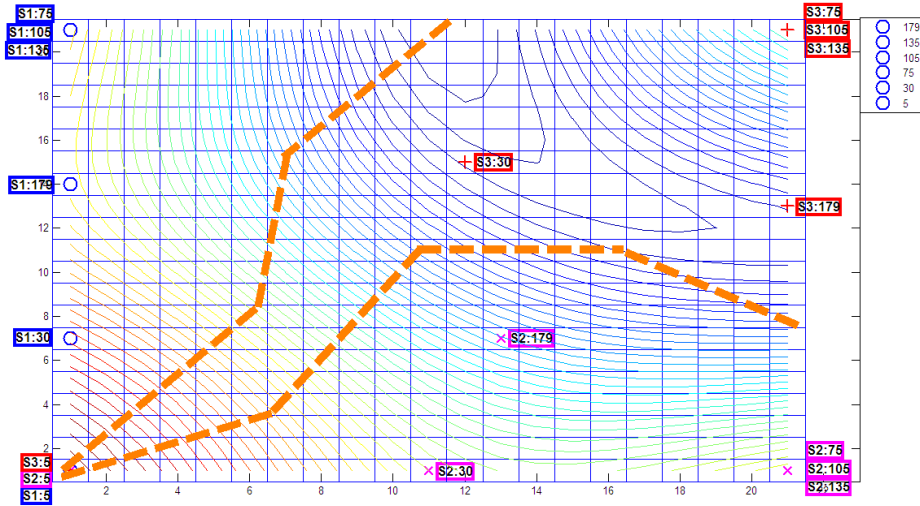


Figure 3.36 Winning neuron locations for the training features for spheres S1 (blue circles), S2 (magenta crosses) and S3 (red plus signs) over the SOM output grid for Classifier #5.

Next, Classifier #5 is tested with a total of 39 features (for three targets at 13 aspects) under noise free conditions and under noisy conditions with SNR levels of 15 dB and 10 dB. This classifier is also, tested with SNR level of 20 dB noisy target features at seven non-reference aspects. Locations of the testing winning neurons are marked in Figure 3.37, Figure 3.38, Figure 3.39 and Figure 3.40 for the testing SNR levels of infinity, 20 dB, 15 dB and 10 dB, respectively. The correct classification rates computed at each testing SNR level are listed in Table 3.6 and also plotted in Figure 3.41.

The correct classification rate of Classifier #5 is found to be 92 percent under noise-free testing. The test targets are discriminated clearly except the sphere S2 at  $\theta = 5^\circ$ ,  $15^\circ$  and  $165^\circ$  cases.

The winning test neurons of the sphere S1 are well localized on the upper left corner of the SOM grid. Most of the testing winning neurons for the sphere S2 are found on the lower right corner while most of the testing winning neurons of sphere S3 are localized on the upper right corner, as shown in Figure 3.37.

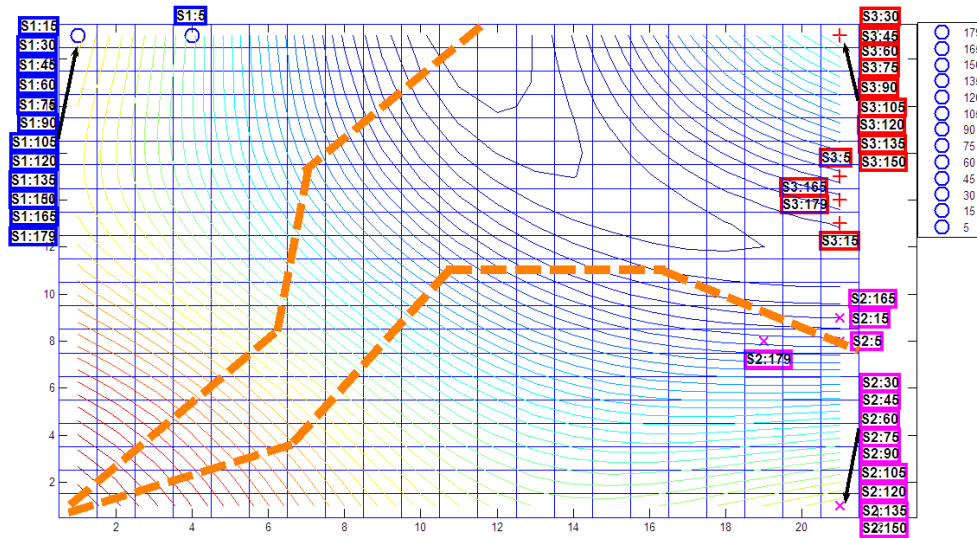


Figure 3.37 SOM Classifier #5 tested by noise-free feature vectors of spheres S1 (blue circles), S2 (magenta crosses) and S3 (red plus sign).

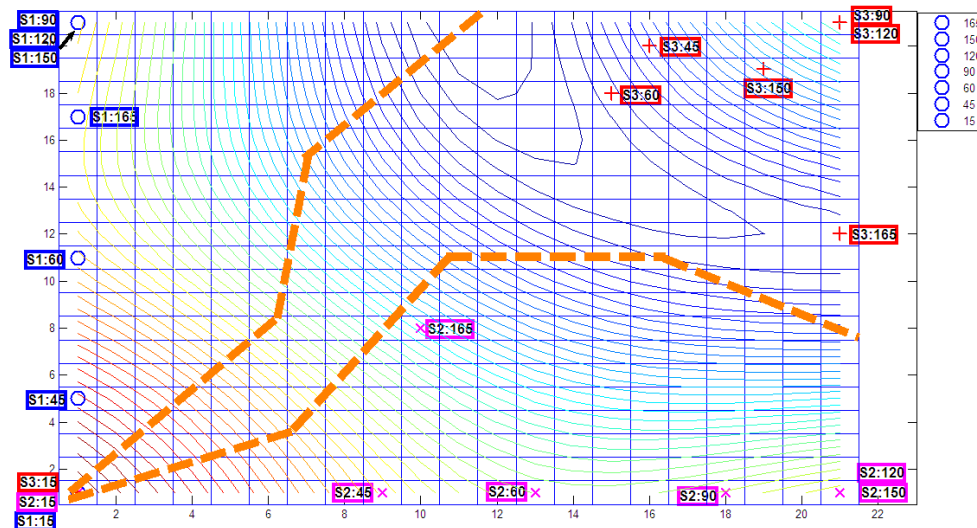


Figure 3.38 SOM Classifier #5 tested by noisy feature vectors of spheres S1 (blue circles), S2 (magenta crosses) and S3 (red plus sign) at 20 dB SNR level.

Accuracy rate of the Classifier #5 is found to be 86 percent at 20 dB testing SNR which is the same SNR level used for the design of this classifier. The only incorrect classification decisions are made for the spheres S1, S2 and S3 at 15 degrees aspect angle at this slightly noisy scenario as shown in Figure 3.38.

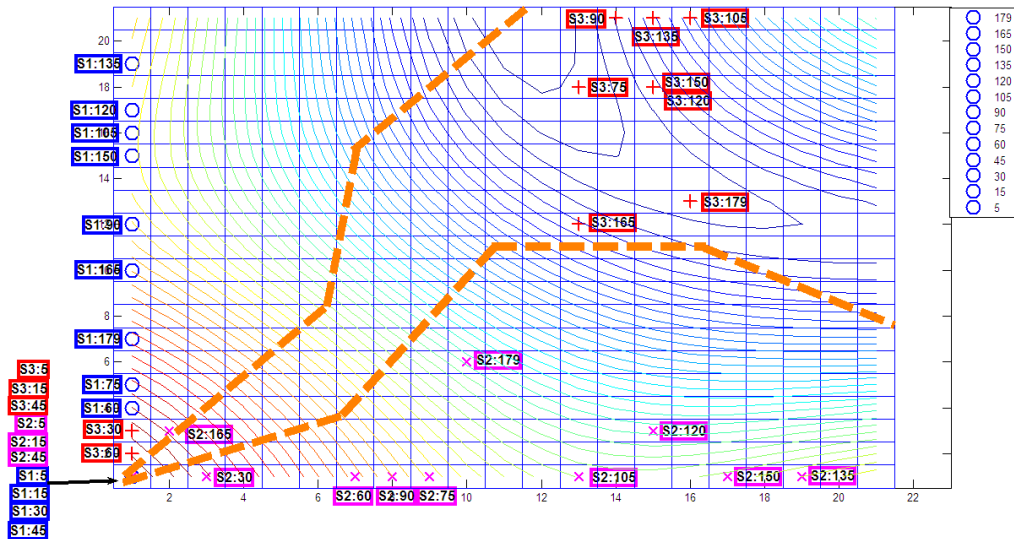


Figure 3.39 SOM Classifier #5 tested by noisy feature vectors of spheres S1 (blue circles), S2 (magenta crosses) and S3 (red plus signs) at 15 dB SNR level.

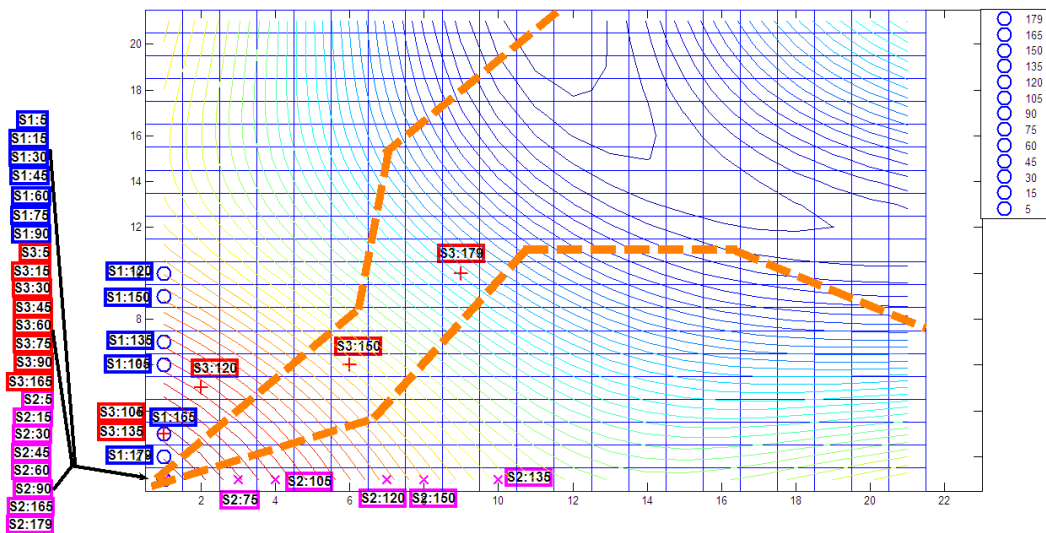


Figure 3.40 SOM Classifier #5 tested by noisy feature vectors of spheres S1 (blue circles), S2 (magenta crosses) and S3 (red plus signs) at 10 dB SNR level.



Table 3.6 Correct decision rates for Classifier #5 at different testing SNR levels.

SNR	Type Of $\theta$ Range	
	For $5^\circ \leq \theta \leq 179^\circ$	For $15^\circ < \theta < 165^\circ$
Noise Free	92	100
20 dB	86	100
15 dB	67	78
10 dB	33	37

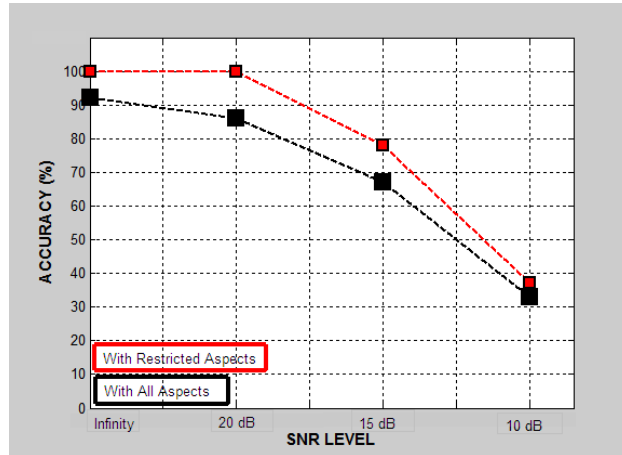


Figure 3.41 Correct classification rates computed for Classifier #5 at various testing SNR levels.

The accuracy rate of the classifier is found around 67 percent at 15 dB testing SNR and it becomes too low for 10 dB SNR testing level.

### 3.3.3. Classifier Simulation #6: Design of a SOM Classifier Using Moderately Noisy (SNR Level of 10 dB) Reference Data for the Target Library TL2 of Spheres S1, S2 and S3

Classifier #6 is designed over the late-time interval [9,8-13.0] nsec using SNR=10 dB scattered data of spheres S1, S2 and S3 at the reference aspects  $\theta = 5^\circ, 30^\circ, 75^\circ$ ,

105°, 135°, 179°. When the training phase is completed, the resulting SOM output with  $21 \times 21 = 144$  weight vectors (each having the length of 1024) is saved as the classifier design matrix of size  $441 \times 1024$ . Figure 3.42 shows the contour plot of the norms of the trained weight vectors over the SOM grid of size  $21 \times 21$ .

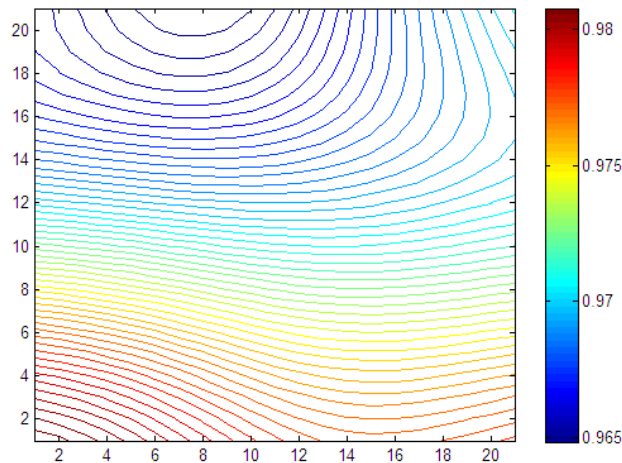


Figure 3.42. SOM output trained by noisy (SNR Level of 10 dB) WD-based late time energy feature vectors of the dielectric spheres S1,S2 and S3.

The winning neuron locations for the training target features belonging to each dielectric sphere are marked on SOM output in Figure 3.43. It is easily seen in this figure that, it is almost impossible to separate cluster regions in a dependable manner as 12 of 18 reference aspect winning neurons are located in the same neuron on the lower left corner of the SOM output map grid. The cluster boundary is roughly constructed however, using the remaining six winning neurons for training data as shown in Figure 3.43.

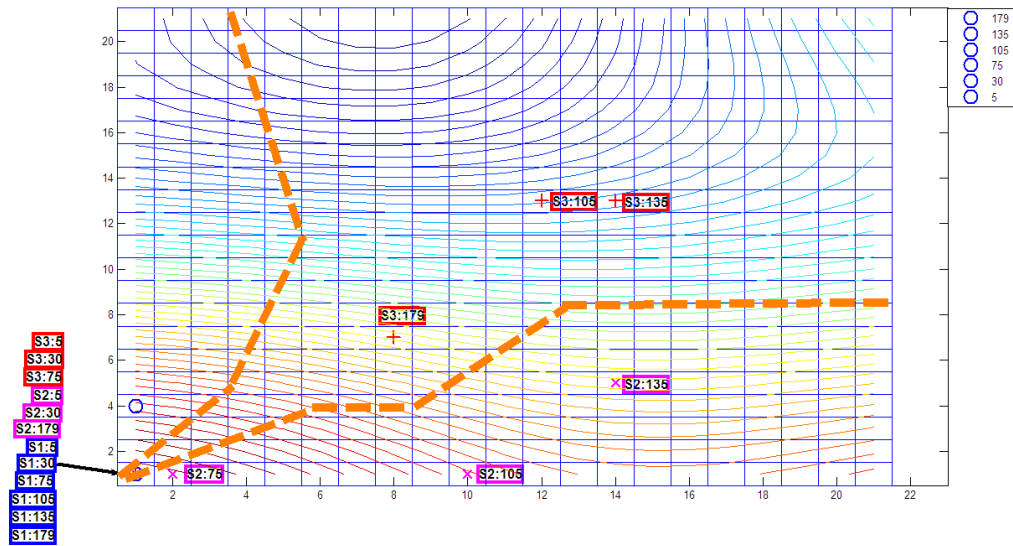


Figure 3.43 Winning neuron locations for the training features for S1, S2 and S3 over the SOM output grid for the Classifier #6.

As the Classifier #6 can not be successfully designed by using noisy reference data at 10 dB SNR, the accuracy rates obtained at various testing SNR levels stay around 20 percent. Details of these test results are not reported as they are not practically meaningful. The major conclusion that can be drawn out of Classifier Simulation #6 is that using too much noise in reference data leads to unsatisfactory design results especially as the number of spherical targets get larger.

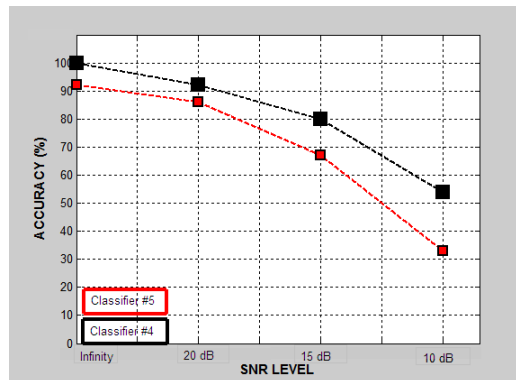


Figure 3.44 Correct classification rates computed for the Classifier #4 (noise-free design) and Classifier # 5 (design at 20 dB SNR at various testing SNR levels for aspect angles  $5^\circ \leq \theta \leq 179^\circ$ ).

Finally, before closing Section 3.3, the correct classification rates of Classifiers 4 and 5 are plotted in Figure 3.44 against decreasing SNR levels. As it seen clearly from this figure, the SOM based Classifier #4, which is designed by noise free reference data can successfully discriminate the spheres S1, S2 and S3 especially under low noise testing conditions although its performance degrades as the testing SNR decreases. Classifier #5 which is designed by slightly noisy ( SNR level of 20 dB ) reference data can also discriminate the spheres, but its performance of accuracy is poor as compared to Classier #4 at all testing noise levels. This difference in the performance of the Classier #4 and Classier #5 is probably due to the degenerate neuron location at the lower left corner of the SOM output map shown in Figure 3.36 which is found to be the winning neuron for the target features S1/5°, S2/5° and S3/5°.

### **3.4 Design of SOM Classifiers for the Target Library TL3 of Four Dielectric Spheres**

In this subsection, two different SOM classifiers will be designed for the target library TL4 of four dielectric spheres S1 ( $r=10$  cm,  $\epsilon=3$ ), S2 ( $r=10$  cm,  $\epsilon=4$ ), S3 ( $r=10$  cm,  $\epsilon=5$ ), S3 ( $r=10$  cm,  $\epsilon=6$ ). The first classifier will be designed by using noise-free reference data and it will be tested at SNR levels of infinity, 20 dB, 15 dB and 10 dB. Secondly, slightly noisy reference data at 20 dB SNR level will be used in SOM training. The resulting classifier will also be tested at the SNR levels of infinity, 20 dB, 15 dB, 10 dB. Classifier design with reference data at 10 dB SNR level will not be considered as the use of moderately noisy data in classifier design is demonstrated to be useless in Classifier Simulation #6 of Section 3.3.3

For the classifiers to be designed for the target library TL3, the optimal late-time design interval is found to be [16.8-20.1] nsec for both noise free design case and

for the slightly noisy (at SNR=20 dB) design case, based on the CCF versus  $q^*$  plots shown in Figure 3.45.

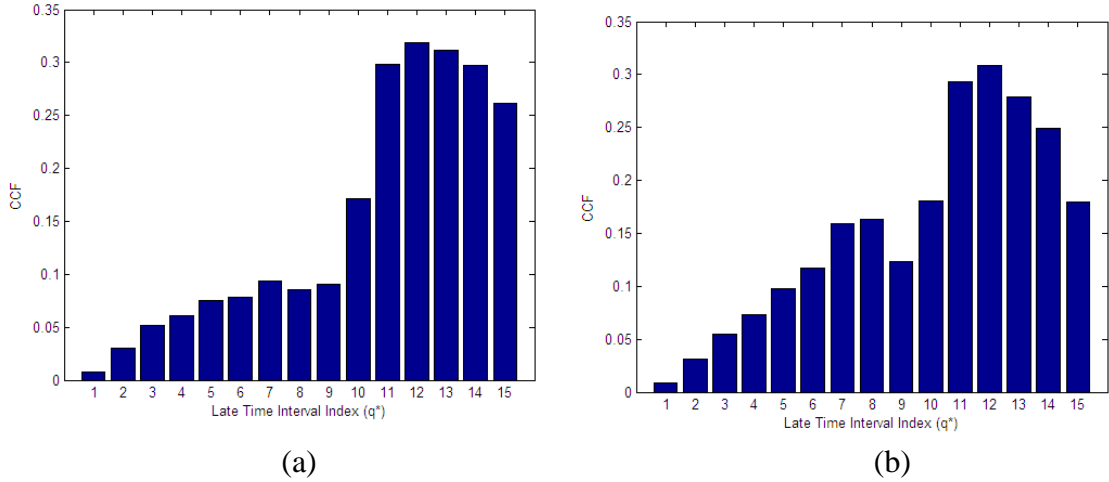


Figure 3.45 The CCF versus  $q^*$  plot generated to determine the optimal late-time design interval for the target library TL3 in the case of (a) noise-free and (b) slightly noisy (SNR level of 20 dB) classifier designs.

### 3.4.1. Classifier Simulation #7: Design of a SOM Classifier Using Noise-Free Reference Data for the Target Library TL3 with spheres S1, S2, S3 and S4

This classifier is designed over the late-time interval [16.8-20.1] nsec using noise-free scattered data of spheres S1, S2, S3 and S4 at the reference aspects  $\theta = 5^\circ, 30^\circ, 75^\circ, 105^\circ, 135^\circ, 179^\circ$ . The LTFV features extracted for all dielectric spheres at these aspects are used to train a SOM grid of size [30x30]. The SOM is initialized randomly at the beginning and the radius of the Gaussian neighborhood function is chosen to decrease from 15 to 11 during iterations. Sequential training of the SOM is completed after 500 epochs. During this training, a total of 24 training features

(for 4 targets at 6 reference aspects) are selected in random order to train the self organizing map. When the training phase is completed, the resulting SOM output with  $30 \times 30 = 900$  weight vectors (each having the length of 1024) is saved as the classifier design matrix of size  $900 \times 1024$ . Figure 3.46 shows the contour plot of the norms of the trained weight vectors over the SOM grid of size  $30 \times 30$ .

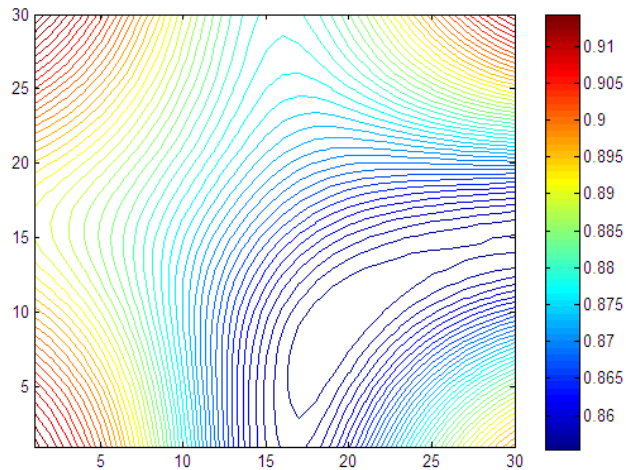


Figure 3.46 SOM output trained by the noise-free WD-based late time energy feature vectors of the dielectric spheres S1, S2, S3 and S4.

It is seen in this figure that four separate cluster regions are formed at the corners of the SOM output grid. The winning neuron locations for the training target features belonging to each dielectric spheres are marked on the SOM output map as shown in Figure 3.47. The cluster boundary is constructed by using the locus of minimum weight norms as well as using the midpoints of closest training winning neurons of different target clusters.

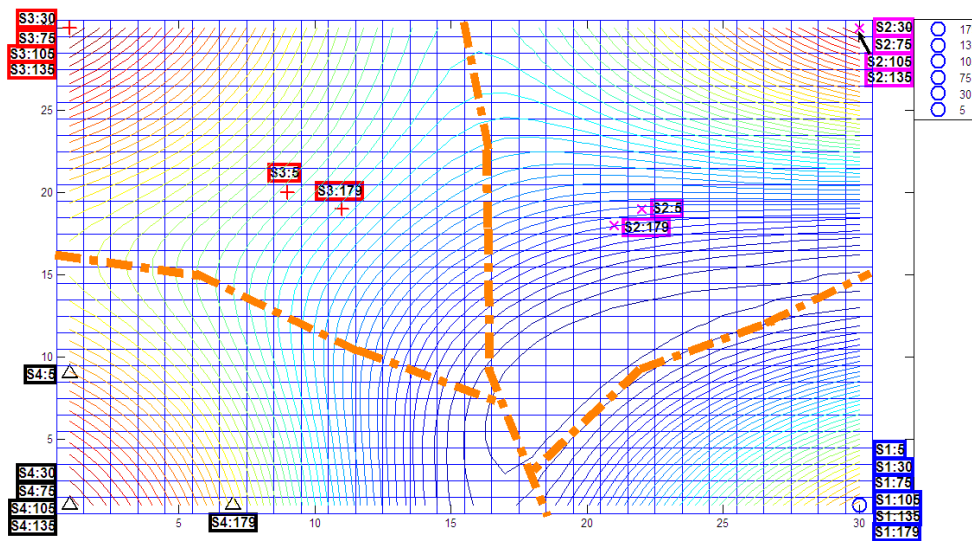


Figure 3.47 Cluster boundaries and winning neuron locations for the training features for S1 (blue circles), S2 (magenta crosses), S3 (red plus signs), S4 (black triangles) over the SOM output grid for Classifier #7.

Next, this SOM based Classifier #7 is tested first with noise-free target features at seven non-reference aspects. Locations of the winning neurons for these tests are marked in Figure 3.48 with a correct decision rate of 100 percent.

Then, the Classifier #7 is tested by noisy feature vectors at 20 dB, 15 dB and 10 dB SNR levels. Locations of the testing winning neurons are marked in Figure 3.49, Figure 3.50 and Figure 3.51 for the SNR levels of 20 dB, 15 dB and 10 dB, respectively. The correct classification rates computed at each testing SNR level are summarized Table 3.7 and also plotted in Figure 3.52. Table 3.7 also gives the accuracy rates obtained over a restricted aspect range where  $\theta = 5, 15, 165$  and  $179$  degree cases are excluded because most of the classification errors occur at those aspects close to the ends of the overall aspect range.

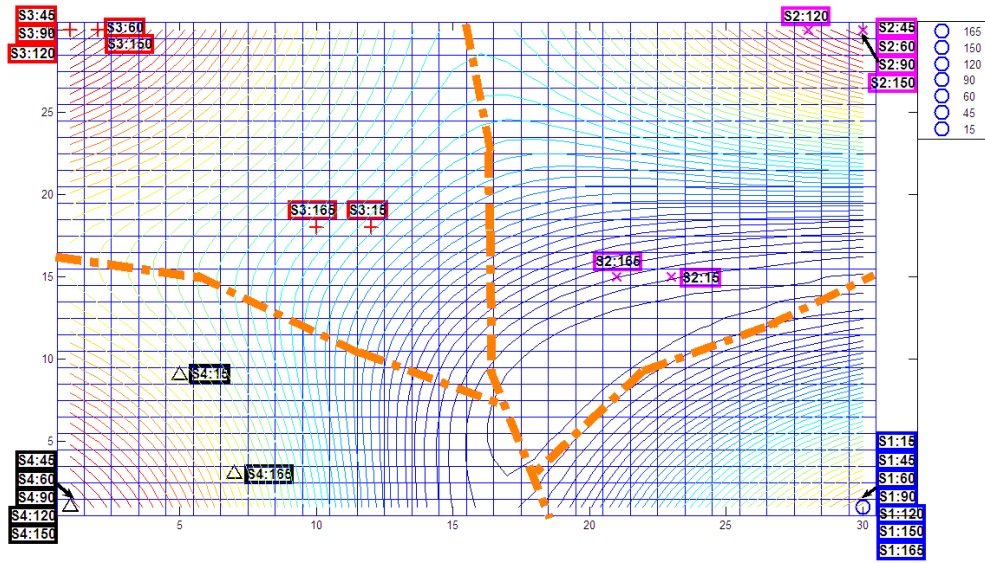


Figure 3.48 SOM Classifier #7 tested by noise-free feature vectors of the spheres S1 (blue circles), S2 (magenta crosses), S3 (red plus signs), S4 (black triangles).

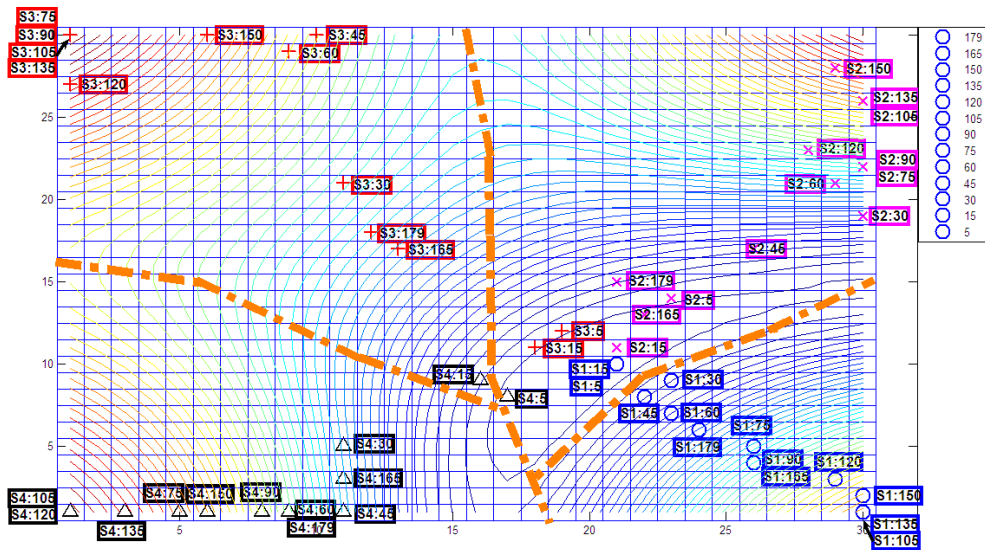


Figure 3.49 SOM Classifier #7 tested by noisy feature vectors of the spheres S1 (blue circles), S2 (magenta crosses), S3 (red plus signs), S4 (black triangles) at 20 dB SNR level.



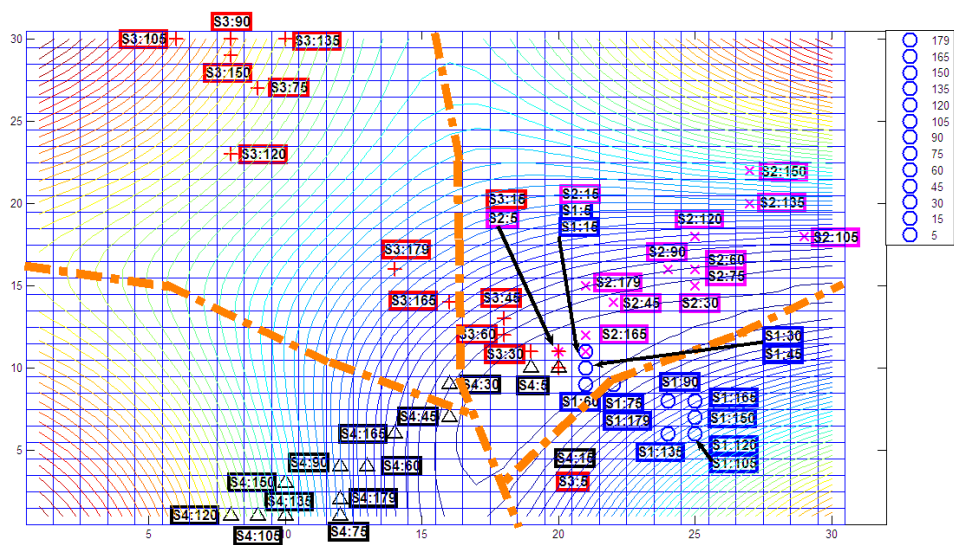


Figure 3.50 SOM Classifier #7 tested by noisy feature vectors of the spheres S1 (blue circles), S2 (magenta crosses), S3 (red plus signs), S4 (black triangles) at 15 dB SNR level.

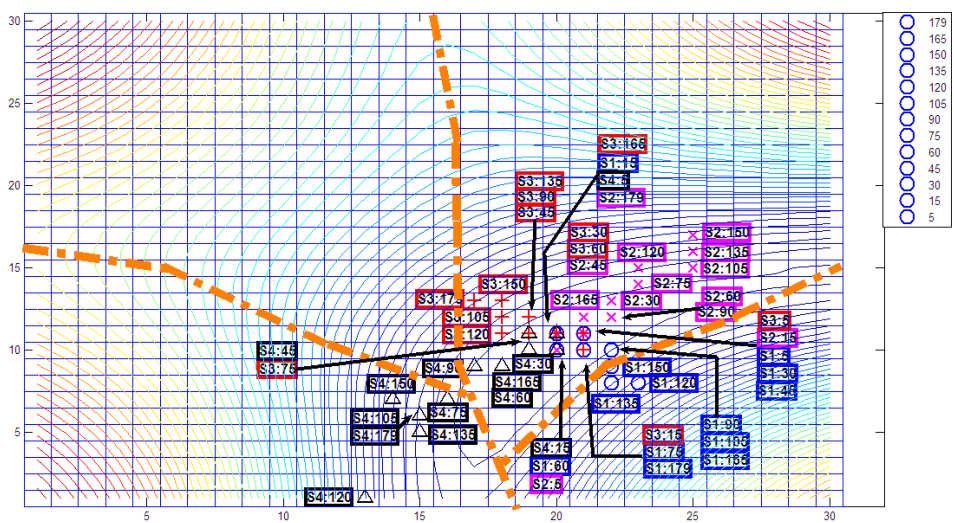


Figure 3.51 SOM Classifier #7 tested by noisy feature vectors of the spheres S1 (blue circles), S2 (magenta crosses), S3 (red plus signs), S4 (black triangles) at 10 dB SNR level.

Table 3.7 Correct decision rates for the Classifier #7 at different testing SNR levels.

SNR	Type of $\theta$ Range	
	For $5^\circ \leq \theta \leq 179^\circ$	For $15^\circ < \theta < 165^\circ$
Noise Free	100	100
20 dB	88	100
15 dB	75	81
10 dB	42	47

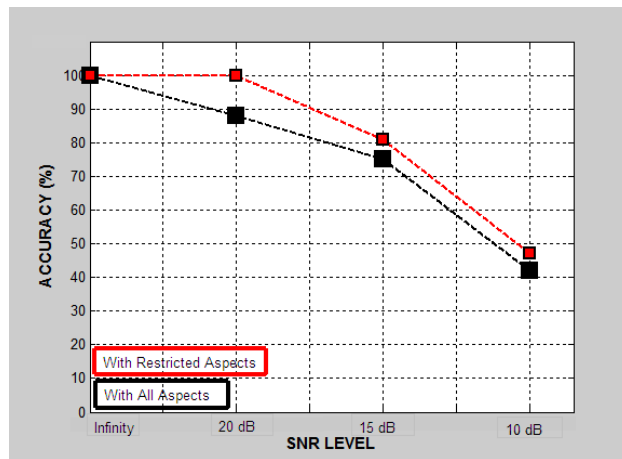


Figure 3.52 Correct classification rates computed for the Classifier #7 at various testing SNR levels.

As it seen clearly from Figure 3.52 and Table 3.7, the SOM based Classifier #7, which is designed by noise-free reference data, can successfully discriminate the spheres S1, S2, S3 and S4 under noise free and low noise testing conditions but its performance degrades as the testing SNR decreases. In the next section, a new classifier will be designed for the same target library TL3 (of dielectric spheres S1, S2, S3 and S4) by using slightly noisy reference data at 20 dB SNR level to see if the classification performance can be improved at lower testing SNR values.

### 3.4.2. Classifier Simulation #8: Design of a SOM Classifier Using Slightly Noisy (SNR Level of 20 dB) Reference Data for the Target Library TL3 with Spheres S1, S2, S3 and S4

Classifier #8 is designed over the late-time interval [16.8-20.1] nsec using slightly noisy (SNR level of 20 dB) scattered data of spheres S1, S2, S3 and S4 at the same reference aspects cited in the previous simulations. When the training phase is completed, the resulting SOM output with  $30 \times 30 = 900$  weight vectors (each having the length of 1024) is saved as the classifier design matrix of size  $900 \times 1024$ . Figure 3.53 shows the contour plot of the norms of the trained weight vectors over the SOM grid of size  $30 \times 30$ .

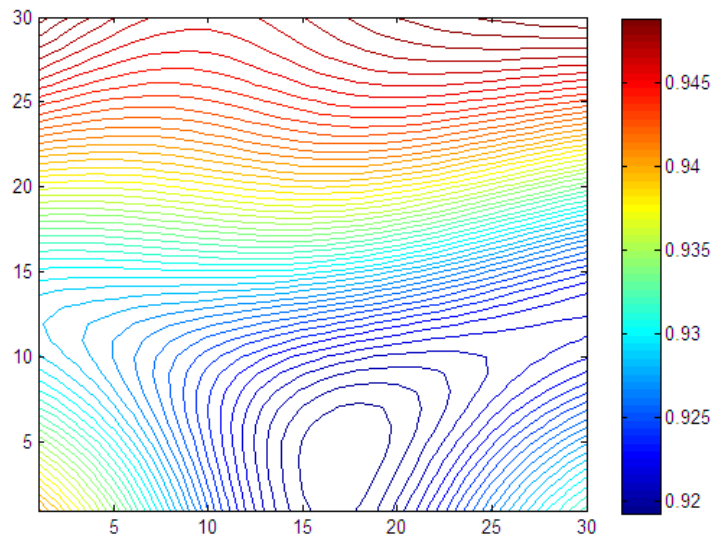


Figure 3.53 SOM output trained by slightly noisy (SNR Level of 20 dB) WD-based late time energy feature vectors of the dielectric spheres S1,S2,S3 and S4.

The cluster boundary is constructed by using the midpoints of closest training winning neurons of different target clusters, as shown in Figure 3.54.

The winning neuron locations for the training target features belonging to each dielectric sphere are also marked on this SOM output.

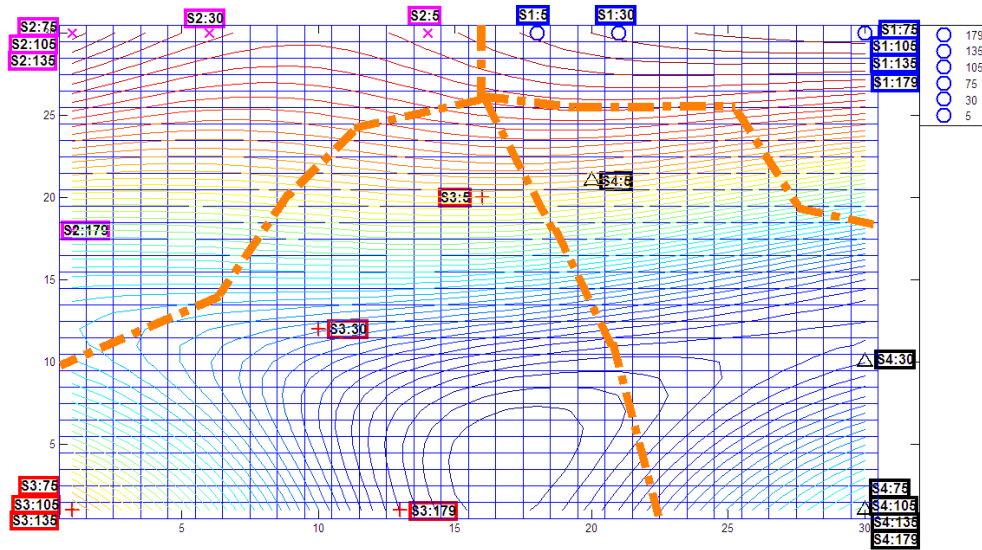


Figure 3.54 Winning neuron locations for the training features of the spheres S1 (blue circles), S2 (magenta crosses), S3 (red plus signs), S4 (black triangles) over the SOM output grid for the Classifier #8.

Next, the Classifier #8 is tested with a total of 52 features (for four targets at 13 aspects) under noise free and noisy conditions. Locations of the testing winning neurons are marked in Figure 3.55, Figure 3.56, Figure 3.57, and Figure 3.58 for the SNR levels of infinity, 20 dB, 15 dB and 10 dB, respectively. The correct classification rates computed at each testing SNR level are listed in Table 3.8 and also plotted in Figure 3.59.

The correct classification rate of Classifier #8 under noise free testing condition is 98 percent, all the targets at all test aspects are discriminated clearly except the sphere S2 at 5 degrees aspect angle.

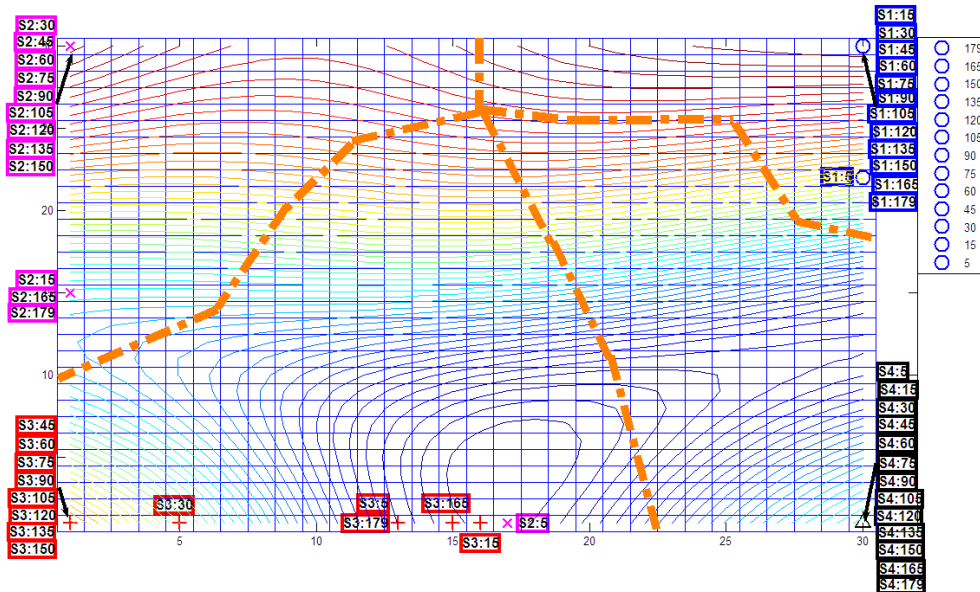


Figure 3.55 SOM Classifier #8 tested by noise-free feature vectors of the spheres S1 (blue circles), S2 (magenta crosses), S3 (red plus signs), S4 (black triangles).

Accuracy rate obtained for SNR=20 dB testing noise turned out to be 89 percent. The incorrect classification decisions are made for the spheres S2 and S4 at 15 degrees aspect angles; and for the sphere S2 at 165 degrees aspect angle.

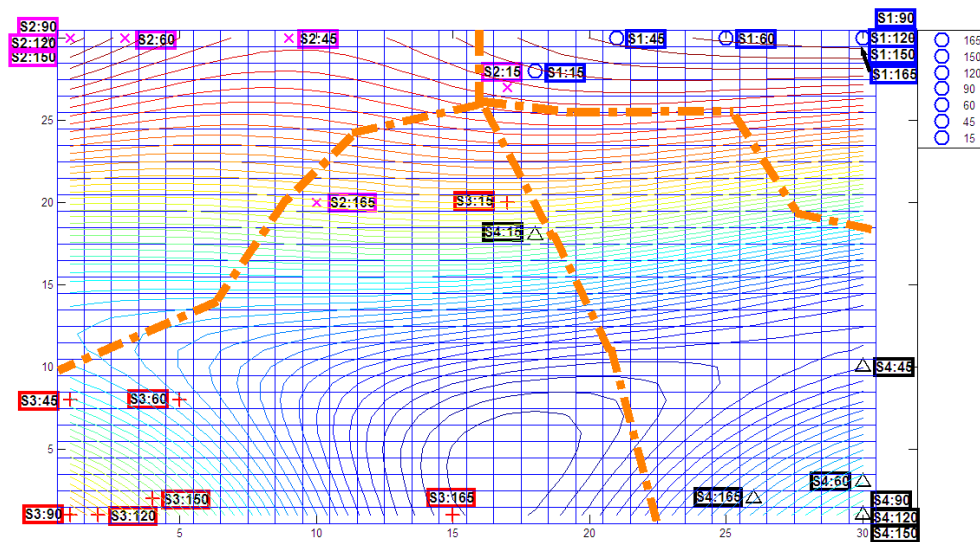


Figure 3.56 SOM Classifier #8 tested by noisy feature vectors of the spheres S1 (blue circles), S2 (magenta crosses), S3 (red plus signs), S4 (black triangles) at 20 dB SNR level.

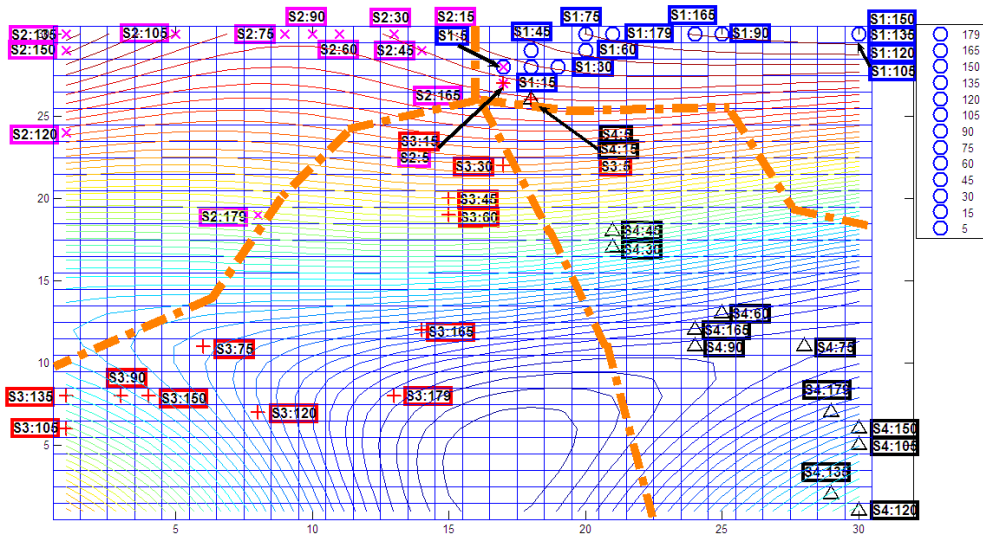


Figure 3.57 SOM Classifier #8 tested by noisy feature vectors of the spheres S1 (blue circles), S2 (magenta crosses), S3 (red plus signs), S4 (black triangles) at 15 dB SNR level.

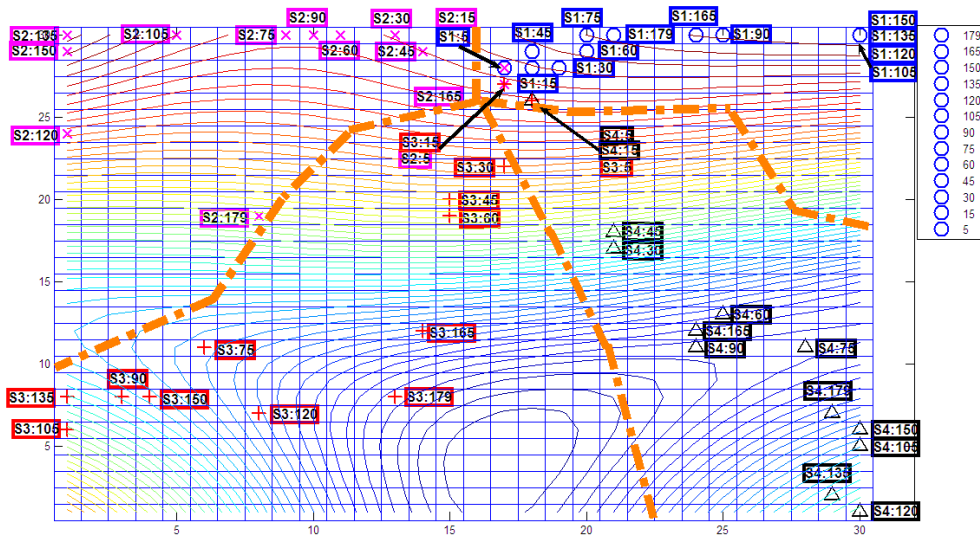


Figure 3.58 SOM Classifier #8 tested by noisy feature vectors of the spheres S1 (blue circles), S2 (magenta crosses), S3 (red plus signs), S4 (black triangles) at 10 dB SNR level.

Table 3.8 Correct decision rates for the Classifier #8 at different testing SNR levels.

SNR	Type Of $\theta$ Ranges	
	For $5^\circ \leq \theta \leq 179^\circ$	For $15^\circ < \theta < 165^\circ$
Noise Free	98	100
20 dB	89	100
15 dB	88	100
10 dB	67	75

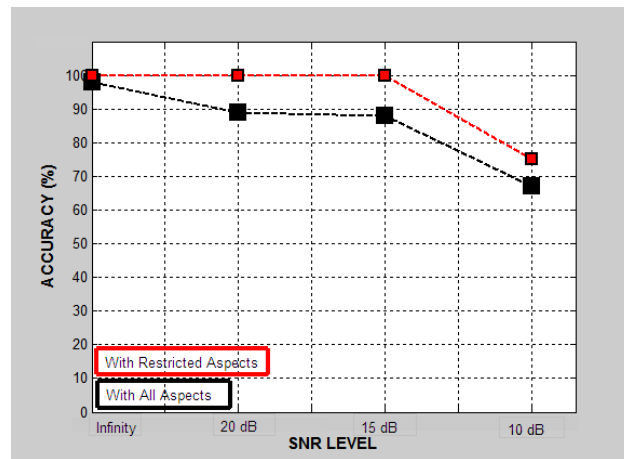


Figure 3.59 Correct classification rates computed for the Classifier #8 at various testing SNR levels.

The correct decision rate obtained with Classifier #8 for 15 dB SNR testing is still very high (88 percent) but the winning neurons for test features belonging to different spheres get very close to cluster boundaries in this case as seen in Figure 3.57. This situation gets even worse for the testing SNR level of 10 dB as shown in Figure 3.58. However the lowest correct classification rate obtained at this moderately noisy case is still acceptable especially when the aspects close to the ends of the  $\theta$  range are excluded.

Before closing this section, the correct classification rates obtained over all aspects for the Classifier #7 and Classifier #8 are plotted in Figure 3.60 against various testing SNR levels. Based on this figure, it can be concluded that use of slightly noisy reference data for the design of this 4-Sphere classifier helps improving the accuracy performance.

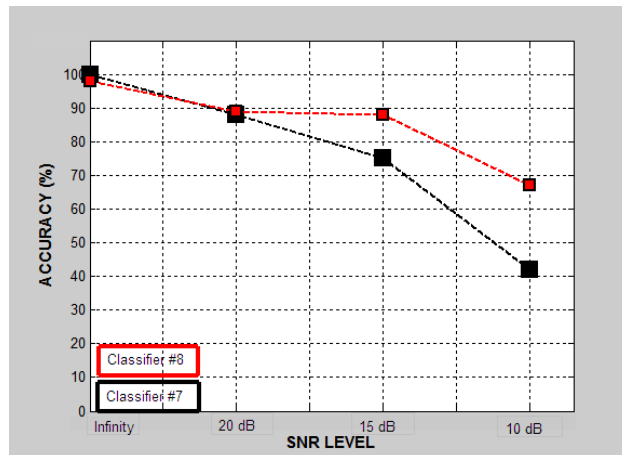


Figure 3.60 Correct classification rates computed for the Classifier #7, Classifier #8 at various testing SNR levels.



## CHAPTER 4

### DESIGN OF SOM CLASSIFIERS FOR SMALL-SCALE MODEL AIRCRAFT

In this chapter, SOM type electromagnetic target classifiers will be designed for three different target libraries TL4, TL5 and TL6 which contain two, three and four small scale model aircraft, respectively, as shown in Table 4.1. The library targets Airbus, Boeing 747, P-7 and Tu 154 are named as AC1, AC2, AC3 and AC4 in the rest of this chapter. These aircraft targets are modeled by perfectly conducting, straight, thin wires with length to radius ratio of 2000 for all wire structures. The wire lengths for body, wing and tail of each target are indicated in Table 4.2. These lengths are obtained by using a scale factor of 100 as compared to actual aircraft dimensions.

Table 4.1 Descriptions of target libraries containing small-scale aircraft targets.

Target Library	Targets
TL4	AC1 (Airbus), AC2 (Boeing 747)
TL5	AC1 (Airbus), AC2 (Boeing 747), AC4 (Tu 154)
TL6	AC1 (Airbus), AC2 (Boeing 747), AC3 (P-7), AC4 (Tu 154)

As discussed in Chapter 2, target classifiers will be designed by training self-organizing maps by means of Wigner Distribution (WD) based target feature vectors which are indirectly related to the aspect and polarization invariant system

poles of the library targets. The SOM Toolbox 2.0 developed by E. Alhoniemi et.al is utilized for sequential SOM training. Several MATLAB codes developed during this thesis study are used for classifier testing and for displaying the results in user friendly forms.

For any given target library, the SOM classifier will be first designed by using noise-free reference data at a chosen set of reference aspect angles. Then, the resulting classifier will be tested for its accuracy rate at the signal-to-noise ratio (SNR) levels of infinity (the noise-free testing database case), 20 dB, 15 dB, 10 dB and 5 dB to see if this classifier is robust under noisy testing conditions. If the noise performance of the SOM classifier is not found satisfactory, the design procedure will be repeated all over again by using slightly noisy (with SNR=20 dB) and moderately noisy (with SNR=10 dB) reference data. In each case, the resulting classifier will be tested against the same noisy feature database at the SNR levels of infinity, 20 dB, 15 dB, 10 dB and 5 dB to evaluate its noise performance. Usefulness of designing SOM classifiers by using noisy reference data will be evaluated based on the comparisons of resulting noise performances of these classifiers.

Table 4.2 Dimensions of the small-scale aircraft targets used in Chapter 4.

Substructures	AC1 (Airbus)	AC2 (Boeing 747)	AC3 (P-7)	AC4 (Tu 154)
Body length (m)	0.5408	0.7066	0.3435	0.4790
Wing length (m)	0.4484	0.5964	0.3250	0.3755
Tail length (m)	0.1626	0.2217	0.1573	0.1340

#### 4.1 Description of Electromagnetic Scattered Data of Small Scale Aircraft and Simulation Parameters Used in Classifier Design and Testing

Scattered responses of aircraft targets were obtained by using a simulation program FEKO, which is based on the Method of Moments, as described in [19] by Mehmet Okan Ersoy. The backscattered responses of the aircraft targets are obtained for  $\Phi$ -polarized uniform plane wave at a fixed elevation of  $\Theta = 60$  degrees over the frequency band from 4 MHz to 1024 MHz with frequency steps of 4 MHz at 12 different aspect angles  $\Phi = 5, 10, 15, 22.5, 30, 37.5, 45, 52.5, 60, 67.5, 75$  and  $82.5$  degrees. Five of them, which are equal to  $\Phi = 5, 15, 37.5, 60$  and  $82.5$  degrees, are chosen as the reference aspect angles to construct the feature databases of the classifiers using noise free, slightly noisy (with SNR=20 dB) and moderately noisy (with SNR=10 dB) reference data. The rest of the scattered database (at non-reference aspects) is used only for performance testing. The common time span of all these scattered responses is 250 nanoseconds with 512 time samples. The problem geometry used to synthesize the electromagnetic signals scattered from small-scale aircraft is described in Figure 4.1.

As discussed in Chapter 2, the first step of target classifier design is to extract the Wigner Distribution based target feature vectors (LTFVs) over a common optimal late-time interval for each target at each reference aspect.

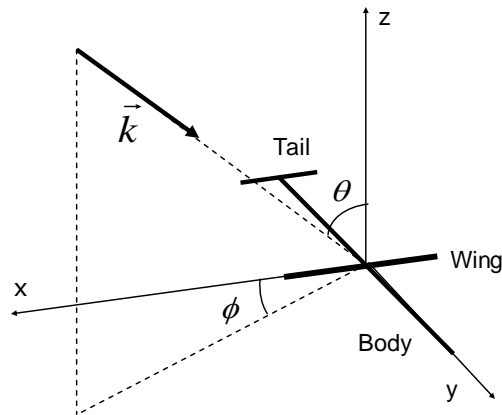


Figure 4.1 Problem geometry for aircraft library where the vector  $\vec{k}$  denotes the propagation direction of incident plane wave.

After the computation of discrete Wigner-Ville distributions and the corresponding energy density vectors for each reference scattered signal, an optimal late-time interval must be selected by using the optimization approach outlined in Chapter 2. This critical design interval depends on the SNR level of the signals in the reference database, so we have to choose the combination of the late-time bands (out of  $Q=16$  equally-wide non-overlapping time intervals) to determine the optimal design interval in all design cases for library targets TL4, TL5 and TL6 based on the correct classification factor (CCF) versus interval index ( $q^*$ ) plots. The CCF values of such plots are computed for each time interval index  $q^* = 1, \dots, Q-1$  by using Equation (2.11) as discussed in Chapter 2.

The SOM desing parameters described in Section 3.1 will also be used in this chapter. Size of the SOM grid and radius of the neighborhood function may change from one design simulation to another but the other SOM parameters will remain the same for all simulations to be reported in the following sections. Firstly, the SOM is initialized with randomly generated weight vectors assigned to each and every neuron over a planar square grid of size  $N$  by  $N$ . The length of each weight vector is equal to the length of the WD based feature vectors (LTFVs) of the feature database. In this thesis work, WD based target features have the length 512 for all small scale aircraft targets.

After the initialization, sequential SOM training will be accomplished in two steps; the target features at reference aspects  $\theta = 15^\circ, 37.5^\circ$  and,  $60^\circ$  will be used in the first step training, and then, those at reference aspects  $\theta = 5^\circ$  and  $82.5^\circ$  will be added to the training feature database in the second step. Based on experience, this two-step training is found useful to improve the performance of classifier at those aspects close to the ends of  $\theta$ -range  $0^\circ < \theta < 90^\circ$ .

The maximum number of training iterations will be 500 epochs, initial learning rate will be 0.5 and the Gaussian type neighborhood function will be used in all design simulations.

## 4.2 Design of SOM Classifiers for the Target Library TL4 of Two Small Scale Aircraft

In this subsection, three different SOM classifiers will be designed for the simplest target library of only two aircraft AC1 (Airbus) and AC2 (Boeing 747). The first classifier will be designed by using noise-free reference data and it will be tested at all non-reference aspects for the SNR levels of infinity, 20 dB, 15 dB, 10 dB and 5 dB. Secondly, slightly noisy reference data at 20 dB SNR level will be used in SOM training. The resulting classifier will also be tested at the SNR levels of infinity, 20 dB, 15 dB, 10 dB, and 5 dB. Finally, the similar classifier design and test simulations will be repeated while using the reference data at a moderate noise level of 10 dB for SOM training.

As the discrete Wigner-Ville distributions and the corresponding energy density vectors for each reference scattered signal were computed [6, 19, 28] earlier, the optimal late-time interval can be selected by computing the correct classification factor (CCF) versus interval index ( $q^*$ ) plot. Combination of the late-time bands 5 and 6 are chosen (out of  $Q=16$  equally-wide non-overlapping time intervals) to determine the optimal design interval [62.6-93.8] nsec in the noise-free classifier design case for the target library TL4 based on the correct classification factor (CCF) versus interval index ( $q^*$ ) plot shown in Figure 4.2. The CCF values of this plot are computed for each time interval index  $q^* = 1, \dots, Q-1$  by using Equation (2.11) as discussed in Chapter 2.

For the classifiers designed for the target library TL4 with noisy reference databases at the SNR levels of 20 dB and 10 dB, the optimal late-time design intervals are found to be [31.3-62.5] nsec and [15.6-46.9] nsec, respectively, based on the CCF versus  $q^*$  plots shown in parts (a) and (b) of Figure 4.3.

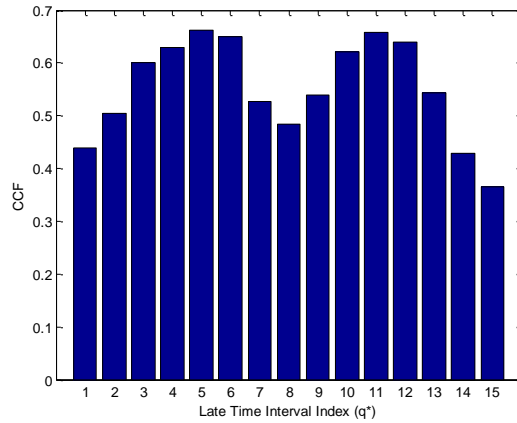


Figure 4.2 The CCF versus  $q^*$  plot generated to determine the optimal late-time design interval for the target library TL4 in the case of noise-free classifier design.

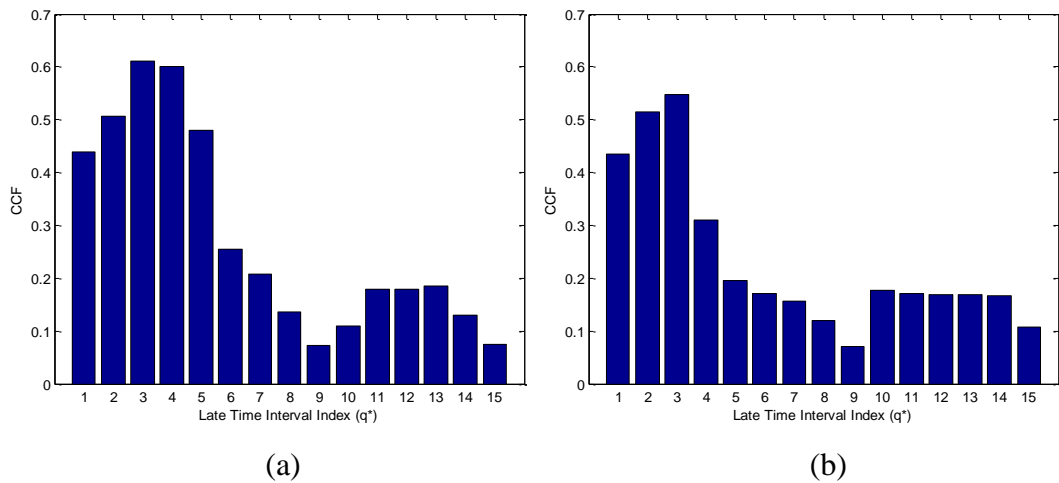


Figure 4.3 The CCF versus  $q^*$  plots generated to determine the optimal late-time design interval for the target library TL4 in the case of (a) SNR=20 dB and (b) SNR=10 dB noise levels.

#### 4.2.1. Classifier Simulation #9: Design of a SOM Classifier Using Noise-Free Reference Data for the Target Library TL4 with Two Aircraft

As indicated in Section 4.2 above, this classifier is designed over the late-time interval [62.6-93.8] nsec using noise-free scattered data of aircraft AC1 and AC2

at the reference aspects  $\theta = 5^\circ, 15^\circ, 37.5^\circ, 60^\circ, 82.5^\circ$ . The LTFV features extracted for both small scale aircraft at these aspects are used to train a SOM grid of size  $[12 \times 12]$ . The SOM is initialized randomly at the beginning and the radius of the Gaussian neighborhood function is chosen to decrease from 7 to 3 during iterations. Sequential training of the SOM is completed after 500 epochs. During this training, a total of 10 training features (for 2 targets at 5 reference aspects) are selected in random order to train the self organizing map. When the training phase is completed, the resulting SOM output with  $12 \times 12 = 144$  weight vectors (each having the length of 512) is saved as the classifier design matrix of size  $144 \times 512$ . Figure 4.4 shows the contour plot of the norms of the trained weight vectors over the SOM grid of size  $12 \times 12$ . It is seen in this figure that two separate cluster regions are formed at the right and the left side of the SOM output grid corresponding to the targets AC1 and AC2, respectively. As two different cluster regions can be clearly observed on this SOM output map, it is straightforward to draw the boundary curve separating these two regions over the map. The dot-dashed orange curve passes through the neuron locations with smallest norm values to define the cluster boundary for the SOM output as shown in Figure 4.5. The winning neurons for the training target features are also indicated on this figure.

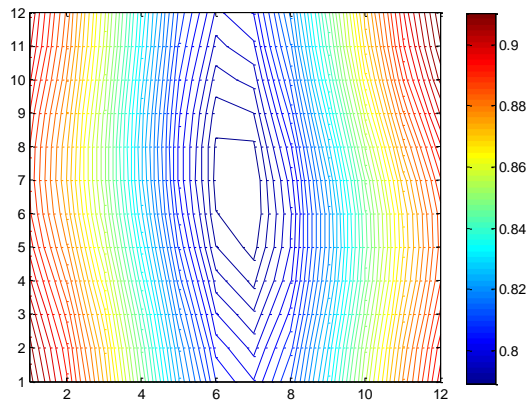


Figure 4.4 SOM output trained by the noise-free WD-based late time energy feature vectors of the small scale aircraft AC1 and AC2.

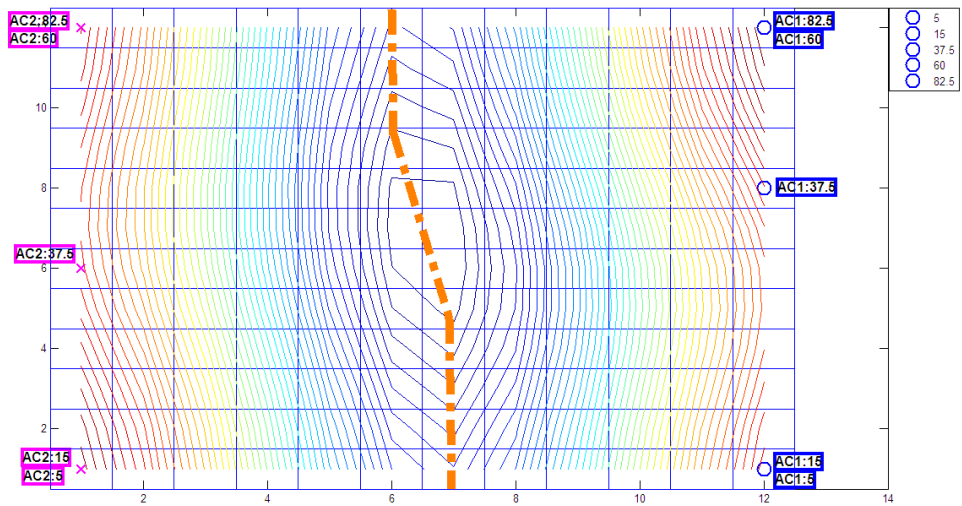


Figure 4.5 Winning neuron locations for the training features and the boundary curve to separate the cluster regions AC1 (blue circles) and AC2 (magenta crosses) over the SOM output grid for the Classifier #9.

This SOM based classifier is tested first with noise-free target features at seven non-reference aspects. Locations of the winning neurons for these tests are marked in Figure 4.6 with a correct decision rate of 100 percent.

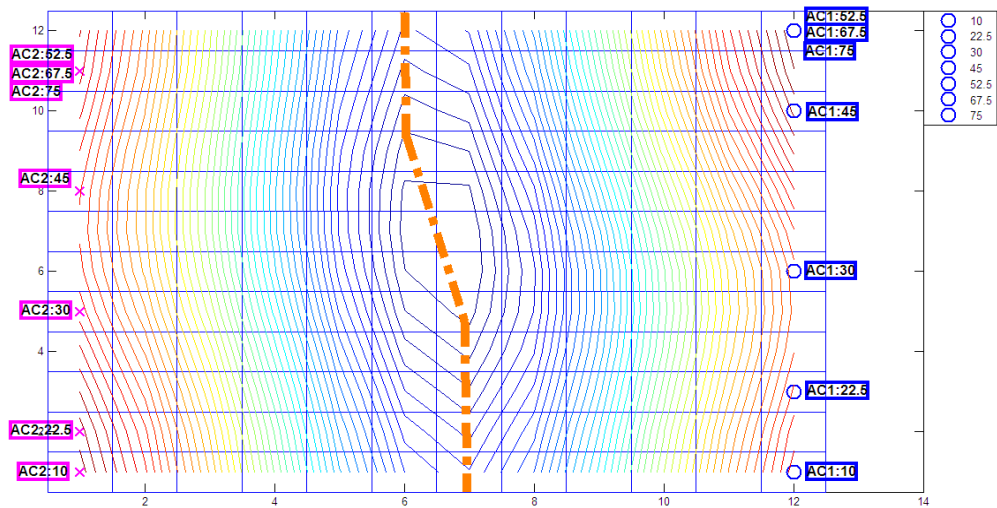


Figure 4.6 SOM Classifier #9 tested by noise-free feature vectors of aircraft AC1 (blue circles) and AC2 (magenta crosses).



Next, the Classifier #9 is tested by noisy feature vectors at 20 dB, 15 dB, 10 dB, 5 dB and 0 dB SNR levels. As the feature vectors at reference aspects are not the same as their noise-free counterparts anymore, Classifier #9 is tested with a total of 24 noisy features (for two targets at 12 aspects). Locations of the testing winning neurons are marked in Figure 4.7, through Figure 4.11 for the SNR levels of 20 dB, 15 dB and 10 dB 5 dB and 0 dB, respectively. The correct classification rates computed at each testing SNR level are listed in Table 4.3 and also plotted in Figure 4.12. Table 4.3 also gives the accuracy rates obtained over a restricted backscattered aspect range excluding  $\theta = 5, 10, 75$  and  $82.5$  degree cases because most of the classification errors are observed to occur at those aspects close to the ends of the overall aspect range. The accuracy rate of the classifier is observed to decrease sharply with decreasing SNR levels as the winning neurons of two different aircraft get closer to each other on the SOM output grid at lower testing SNR levels.

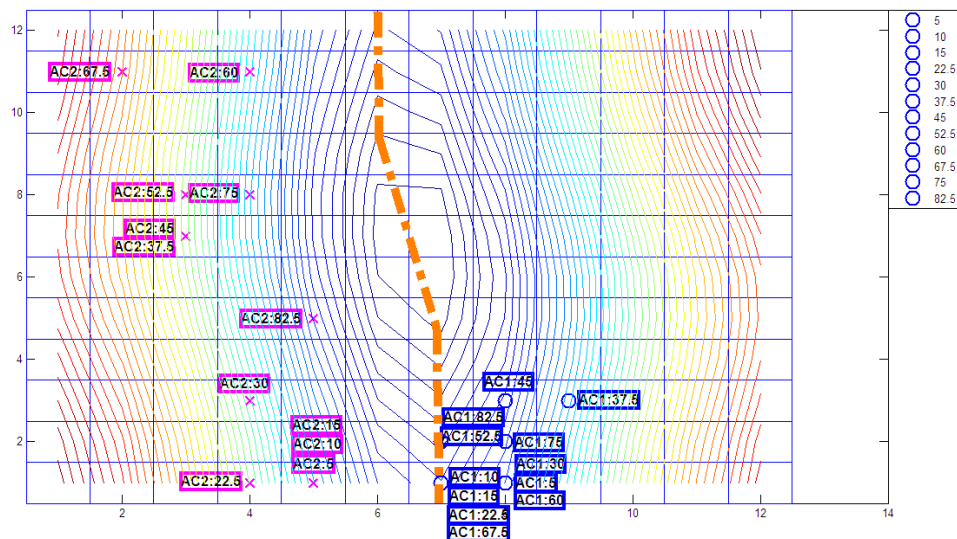


Figure 4.7 SOM Classifier #9 tested by noisy feature vectors of aircraft AC1 (blue circles) and AC2 (magenta crosses) at 20 dB SNR level.

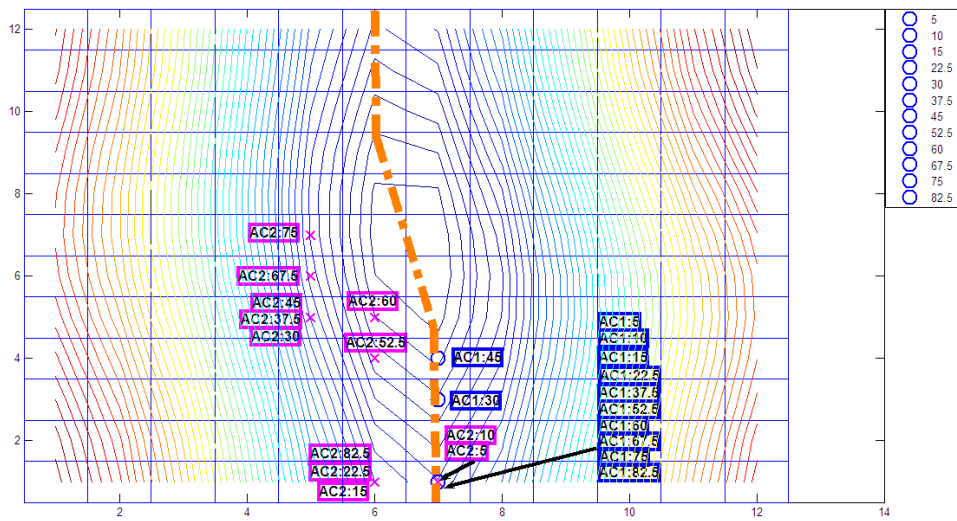


Figure 4.8 SOM Classifier #9 tested by noisy feature vectors of aircraft AC1 (blue circles) and AC2 (magenta crosses) at 15 dB SNR level.

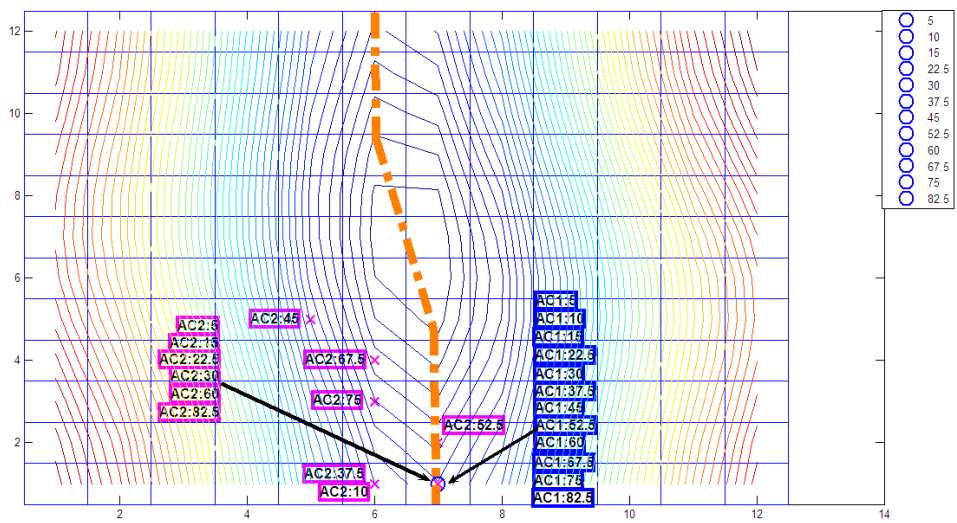


Figure 4.9 SOM Classifier #9 tested by noisy feature vectors of aircraft AC1 (blue circles) and AC2 (magenta crosses) at 10 dB SNR level.

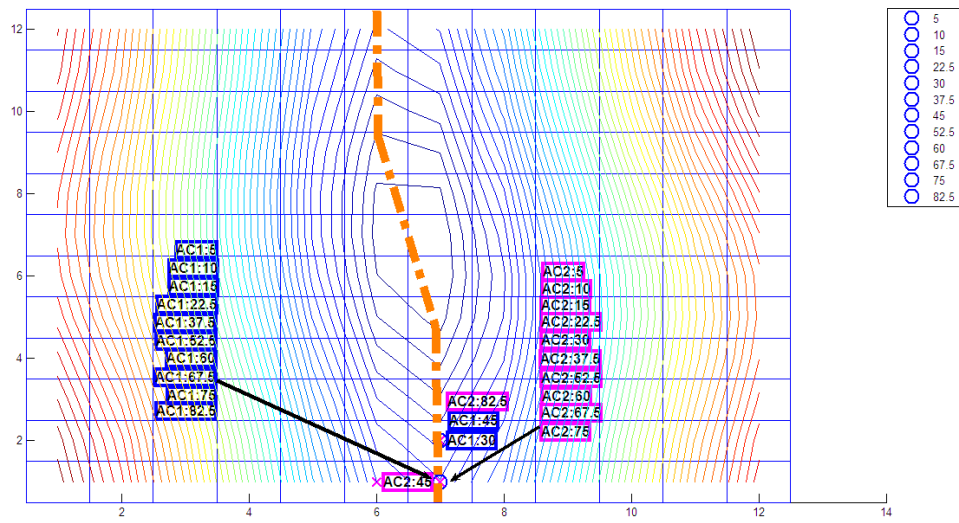


Figure 4.10 SOM Classifier #9 tested by noisy feature vectors of aircraft AC1 (blue circles) and AC2 (magenta crosses) at 5 dB SNR level.

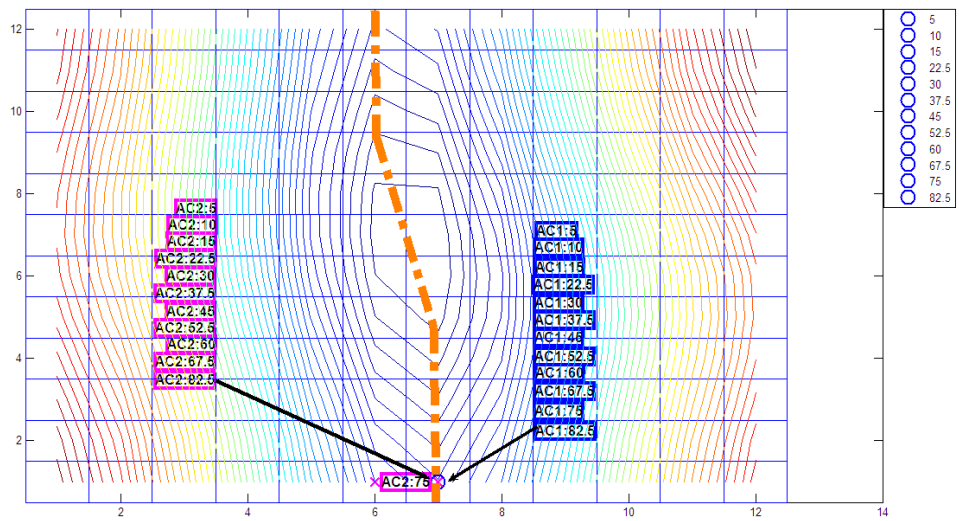


Figure 4.11 SOM Classifier #9 tested by noisy feature vectors of aircraft AC1 (blue circles) and AC2 (magenta crosses) at 0 dB SNR level.

Table 4.3 Correct decision rates for the Classifier #9 at different testing SNR levels for two different  $\theta$  range

SNR	Type Of Boundary	
	For $5^\circ \leq \theta \leq 82,5^\circ$	For $10^\circ < \theta < 75^\circ$
Noise Free	100	100
20 dB	75	75
15 dB	42	50
10 dB	21	19
5 dB	4	6
0 dB	4	0

As it seen clearly in Figure 4.12 and Table 4.3, the SOM based Classifier #9, which is designed by noise-free reference data, can successfully discriminate the small scale aircraft AC1 and AC2 under noise-free testing conditions but its performance degrades sharply as the testing SNR decreases, especially at SNR levels of 5 dB and 0 dB, winning neurons are gathered on the cluster boundary. In the next section, a new classifier will be designed for the same target library TL4 by using slightly noisy reference data at 20 dB SNR level to improve the classification performance at lower testing SNR values.

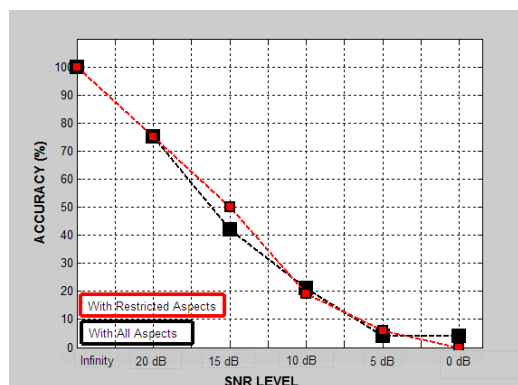


Figure 4.12 Correct classification rates computed for the Classifier #9 at various testing SNR levels for two different  $\theta$  range.

#### 4.2.2. Classifier Simulation #10: Design of a SOM Classifier Using Slightly Noisy (SNR Level of 20 dB) Reference Data for the Target Library TL4 with Two Aircraft

Classifier Simulation #10 is designed over the late-time interval [31.3-62.5] nsec using slightly noisy scattered data of small scale aircraft AC1 and AC2 at the reference aspects  $\theta = 5^\circ, 15^\circ, 37.5^\circ, 60^\circ, 82.5^\circ$ . When the training phase is completed, the resulting SOM output with  $12 \times 12 = 144$  weight vectors (each having the length of 512) is saved as the classifier design matrix of size  $144 \times 512$ . Figure 4.13 shows the contour plot of the norms of the trained weight vectors over the SOM grid of size. The cluster boundary drawn as a curve passing through the neuron locations with smallest norm values. The winning neuron locations for the training target features belonging to each small scale aircraft are also marked on this SOM output.

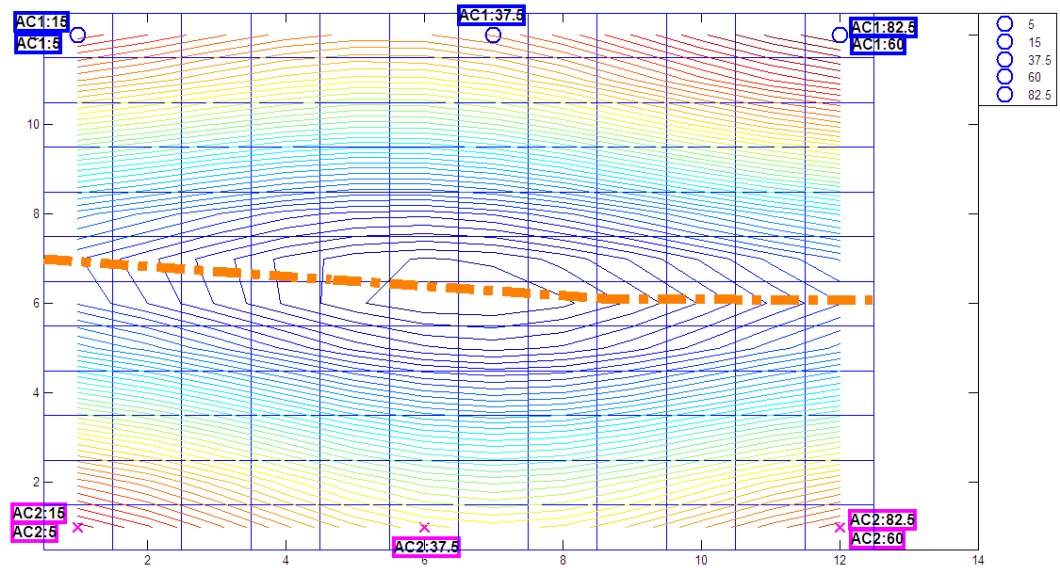


Figure 4.13 Winning neuron locations for the training features and the boundary curve to separate the cluster regions AC1 (blue circles) and AC2 (magenta crosses) over the SOM output grid for the Classifier #10.

Then, the Classifier #10 is tested by noise-free and noisy feature vectors at 20 dB, 15 dB, 10 dB, 5 dB and 0 dB SNR levels. Locations of the testing winning neurons are marked in Figure 4.14, Figure 4.15, Figure 4.16, Figure 4.17, Figure 4.18 and Figure 4.19 for the SNR levels of infinity, 20 dB, 15 dB, 10 dB, 5 dB and 0 dB, respectively. The correct classification rates computed at each testing SNR level turn out to be 100 percent as listed in Table 4.4 and plotted in Figure 4.20. Therefore, we can safely come to the conclusions that training the SOM with slightly noisy reference data leads to a prominent improvement in classifier accuracy at lower SNR testing levels. The correct classification rate of the Classifier #9 was only 21 percent at 10 dB testing SNR, but that of Classifier #10 is now found to be 100 percent.

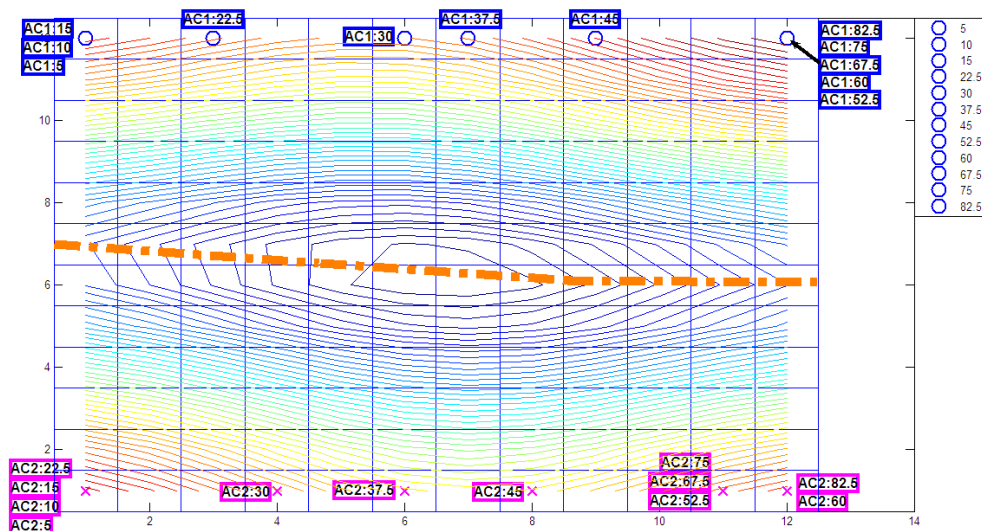


Figure 4.14 SOM Classifier #10 tested by noise-free feature vectors of aircraft AC1 (blue circles) and AC2 (magenta crosses).

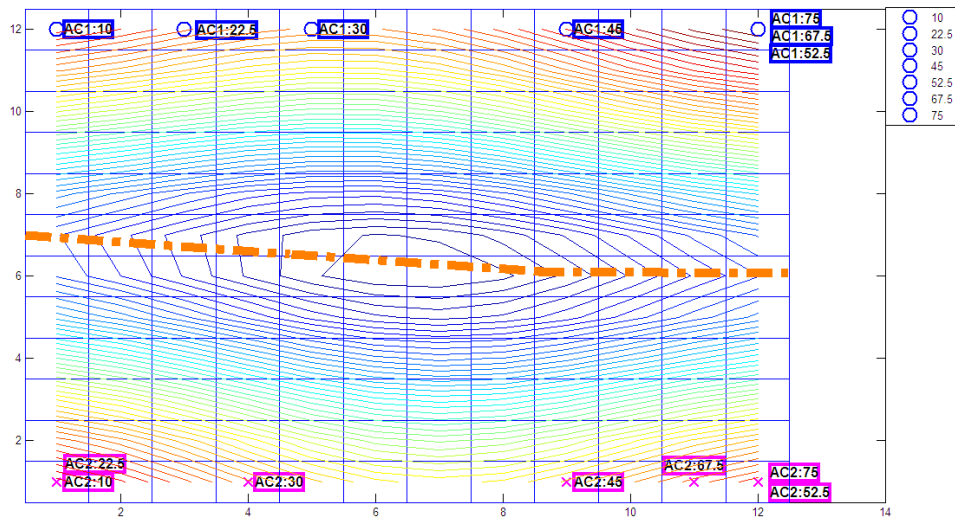


Figure 4.15 SOM Classifier #10 tested by noisy feature vectors of aircraft AC1 (blue circles) and AC2 (magenta crosses) at 20 dB SNR level.

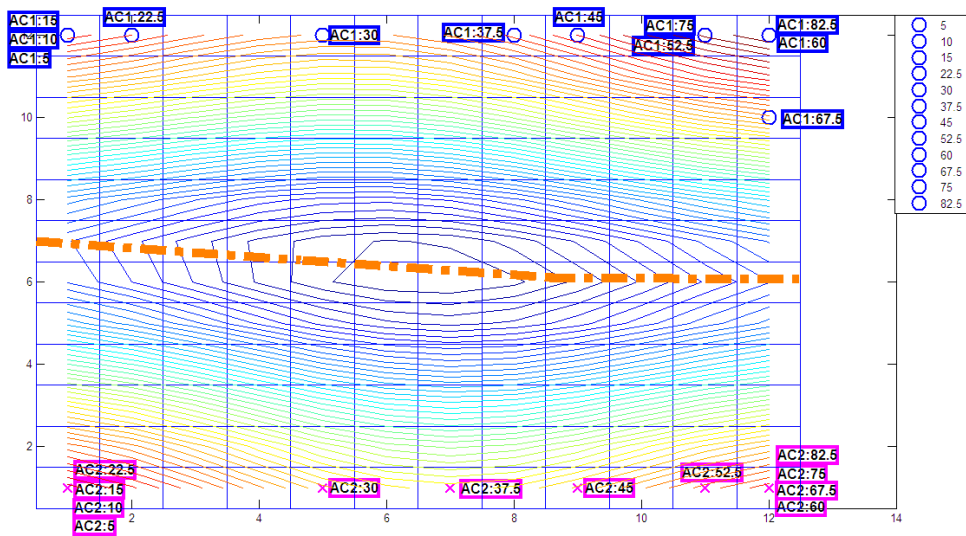


Figure 4.16 SOM Classifier #10 tested by noisy feature vectors of aircraft AC1 (blue circles) and AC2 (magenta crosses) at 15 dB SNR level.

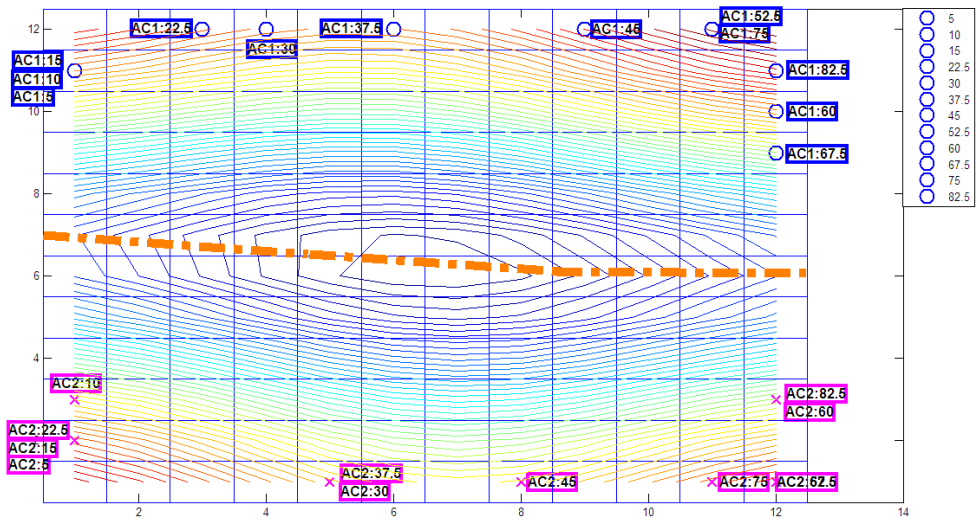


Figure 4.17 SOM Classifier #10 tested by noisy feature vectors of aircraft AC1 (blue circles) and AC2 (magenta crosses) at 10 dB SNR level.

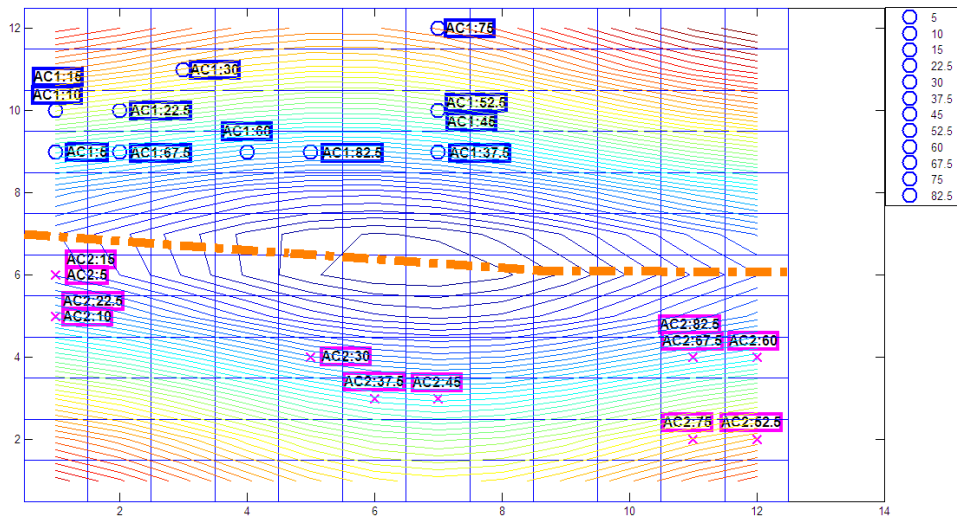


Figure 4.18 SOM Classifier #10 tested by noisy feature vectors of aircraft AC1 (blue circles) and AC2 (magenta crosses) at 5 dB SNR level.



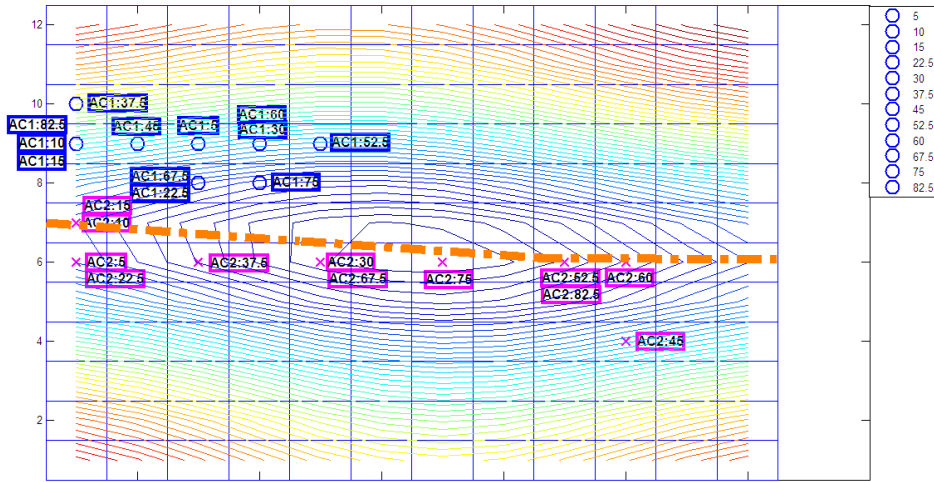


Figure 4.19 SOM Classifier #10 tested by noisy feature vectors of aircraft AC1 (blue circles) and AC2 (magenta crosses) at 0 dB SNR level.

Table 4.4 Correct decision rates for the Classifier #10 at different testing SNR levels for two different  $\theta$  range.

SNR	Type Of Boundary	
	For $5^\circ \leq \theta \leq 82,5^\circ$	For $10^\circ < \theta < 75^\circ$
Noise Free	100	100
20 dB	100	100
15 dB	100	100
10 dB	100	100
5 dB	100	100
0 dB	79	81

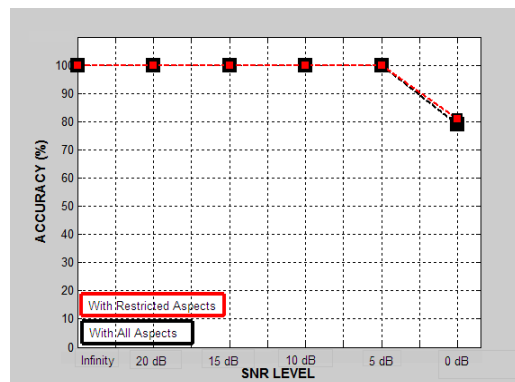


Figure 4.20 Correct classification rates computed for the Classifier #10 at various testing SNR levels for two different  $\theta$  range.

#### 4.2.3. Classifier Simulation #11: Design of a SOM Classifier Using Moderately Noisy (SNR Level of 10 dB) Reference Data for the Target Library TL4 with Two Aircraft

Classifier #11 is designed over the late-time interval [15.6-46.9] nsec using moderately noisy (at 10 dB SNR) scattered data of small scale aircraft AC1 and AC2 at the reference aspects  $\theta = 5^\circ, 15^\circ, 37.5^\circ, 60^\circ, 82.5^\circ$ . The resulting SOM output with  $12 \times 12 = 144$  weight vectors (each having the length of 512) is saved as the classifier design matrix of size  $144 \times 512$ . Figure 4.21 shows the contour plot of the norms of the trained weight vectors over the SOM grid of size  $12 \times 12$ .

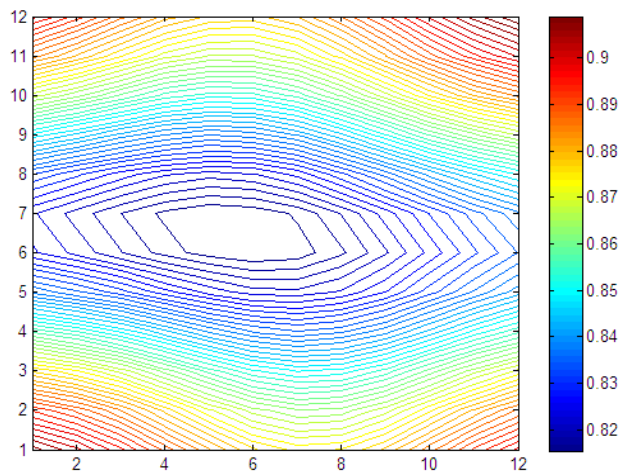


Figure 4.21 SOM output trained by noisy (SNR Level of 10 dB) WD-based late time energy feature vectors of the small scale aircraft AC1 and AC2.

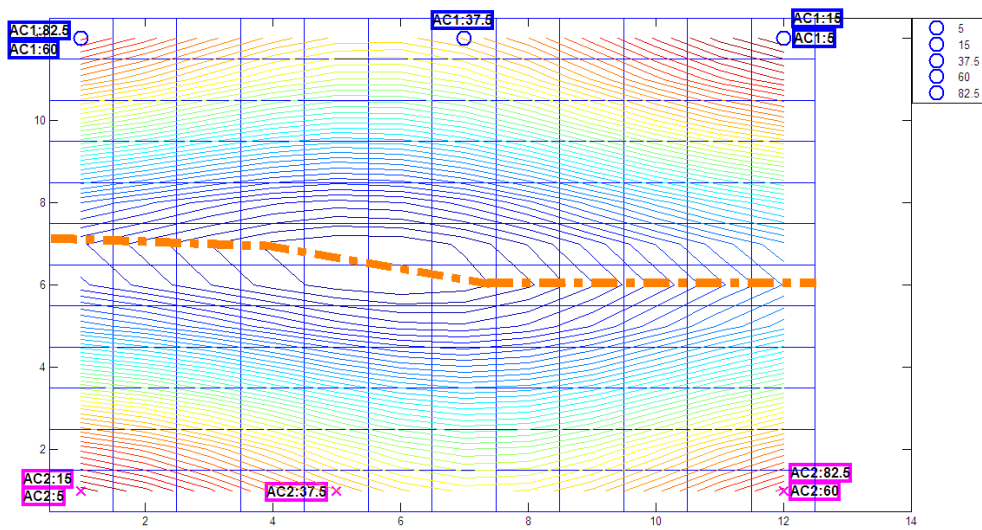


Figure 4.22 Winning neuron locations for the training features and the boundary curve to separate the cluster regions AC1 and AC2 over the SOM output grid for the Classifier #11.

The winning neuron locations for the training target features belonging to each small scale aircraft are marked on this SOM output in Figure 4.22. Also the cluster boundary is drawn as a curve passing through the neuron locations with smallest norm values on the same figure. Then, the Classifier #11 is tested by noise-free and noisy feature vectors at 20 dB, 15 dB, 10 dB, 5 dB and 0 dB SNR levels. Locations of the testing winning neurons are marked in Figure 4.23, Figure 4.24, Figure 4.25, Figure 4.26, Figure 4.27 and Figure 4.28 for the SNR levels of infinity, 20 dB, 15 dB, 10 dB, 5 dB and 0 dB, respectively. The correct classification rates computed at each testing SNR level are listed in Table 4.5.

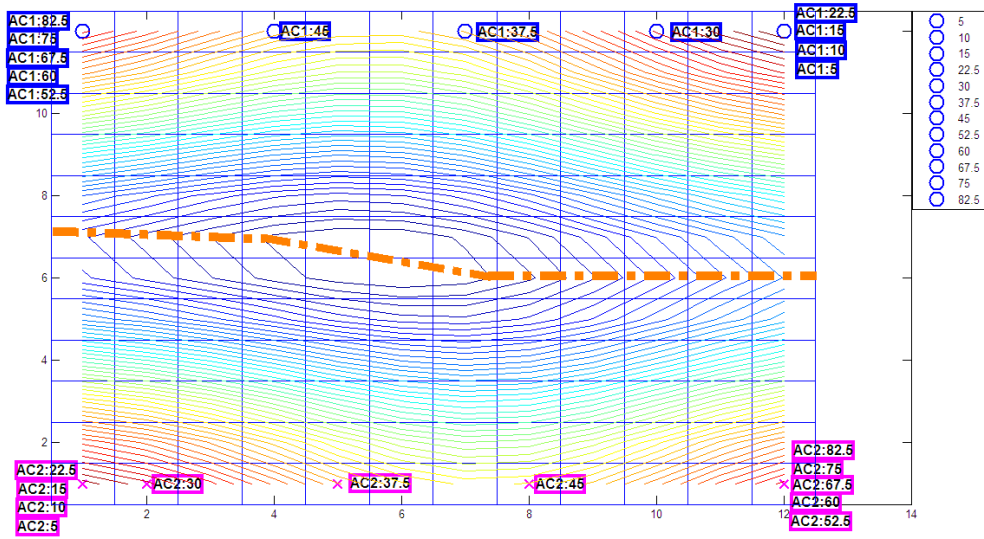


Figure 4.23 SOM Classifier #11 tested by noise-free feature vectors of aircraft AC1 (blue circles) and AC2 (magenta crosses).

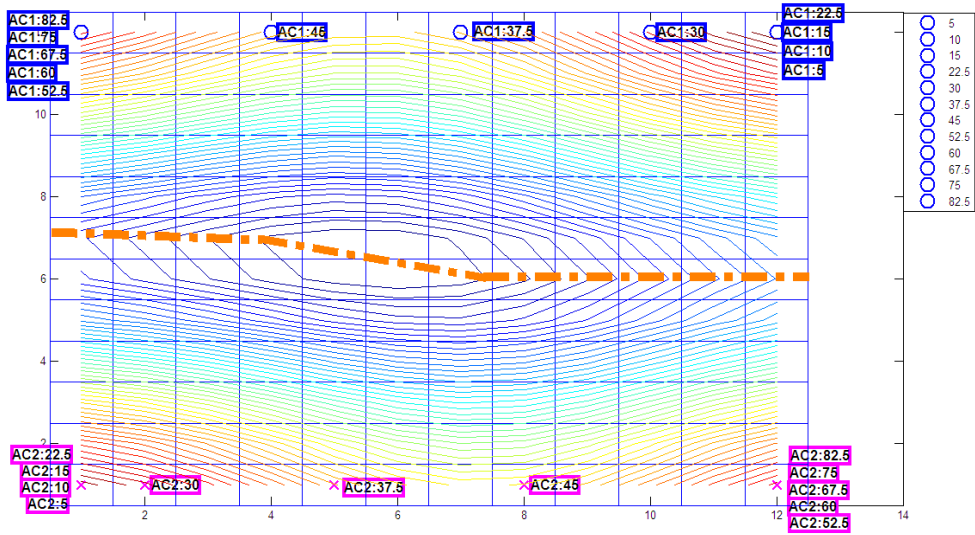


Figure 4.24 SOM Classifier #11 tested by noisy feature vectors of aircraft AC1 (blue circles) and AC2 (magenta crosses) at 20 dB SNR level.

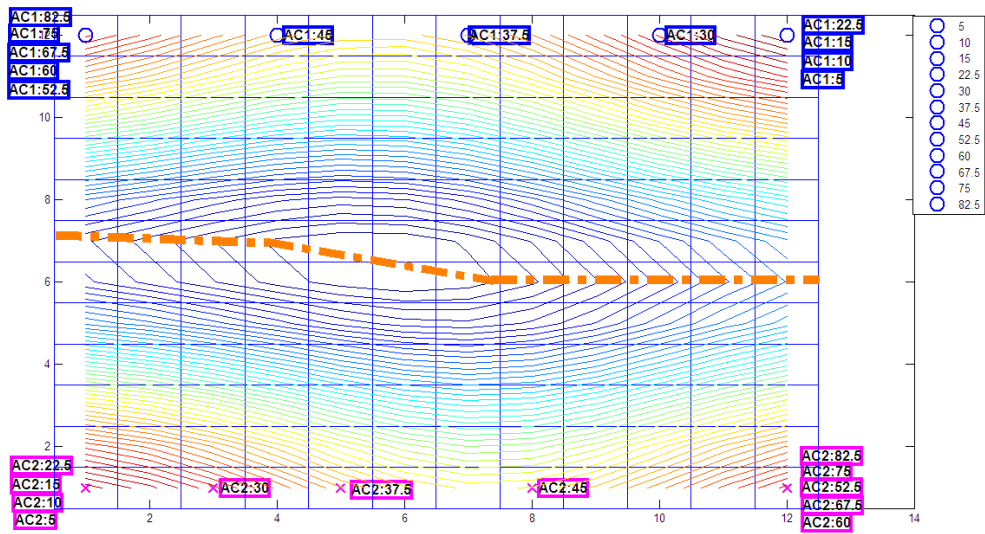


Figure 4.25 SOM Classifier #11 tested by noisy feature vectors of aircraft AC1 (blue circles) and AC2 (magenta crosses) at 15 dB SNR level.

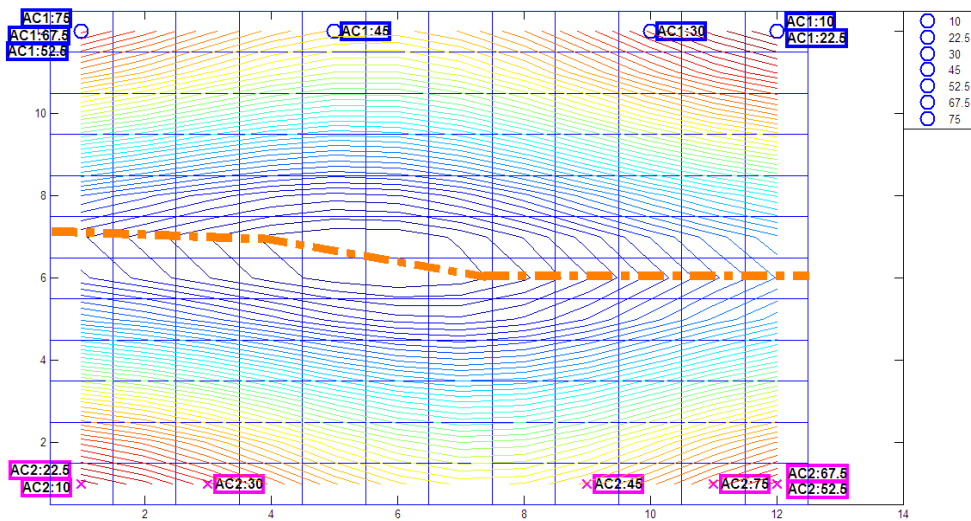


Figure 4.26 SOM Classifier #11 tested by noisy feature vectors of aircraft AC1 (blue circles) and AC2 (magenta crosses) at 10 dB SNR level.

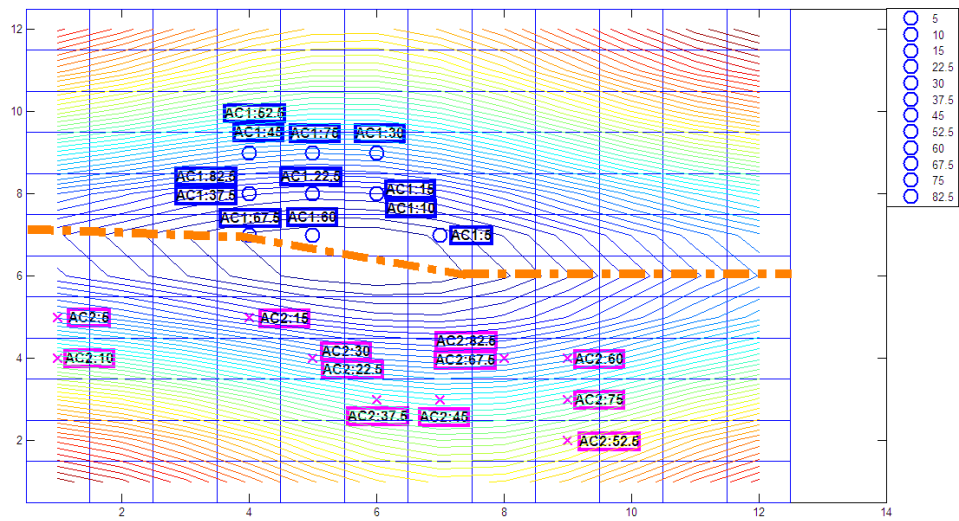


Figure 4.27 SOM Classifier #11 tested by noisy feature vectors of aircraft AC1 (blue circles) and AC2 (magenta crosses) at 5 dB SNR level.

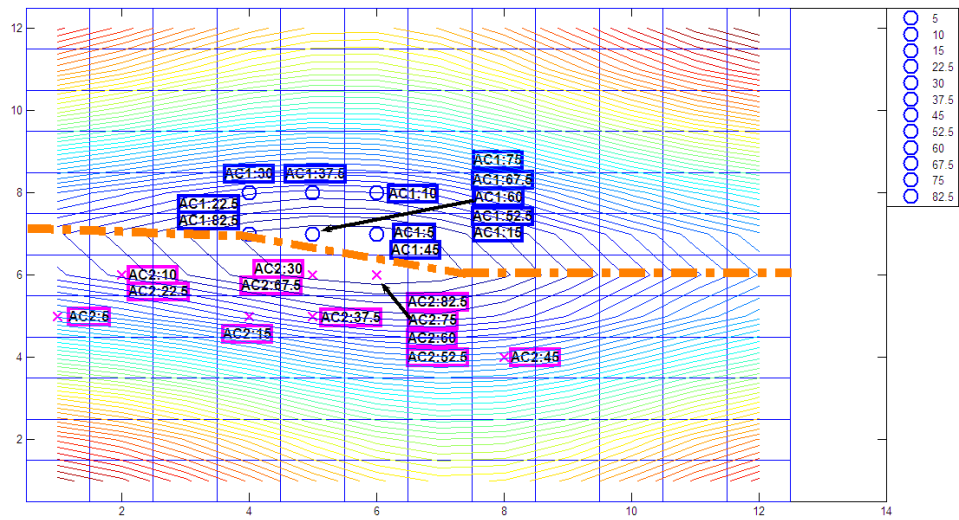


Figure 4.28 SOM Classifier #11 tested by noisy feature vectors of aircraft AC1 (blue circles) and AC2 (magenta crosses) at 0 dB SNR level.

Table 4.5 Correct decision rates for the Classifier #11 at different testing SNR levels for two different  $\theta$  range

SNR	Type Of Boundary	
	For $5^\circ \leq \theta \leq 82,5^\circ$	For $10^\circ < \theta < 75^\circ$
Noise Free	100	100
20 dB	100	100
15 dB	100	100
10 dB	100	100
5 dB	96	94
0 dB	92	94

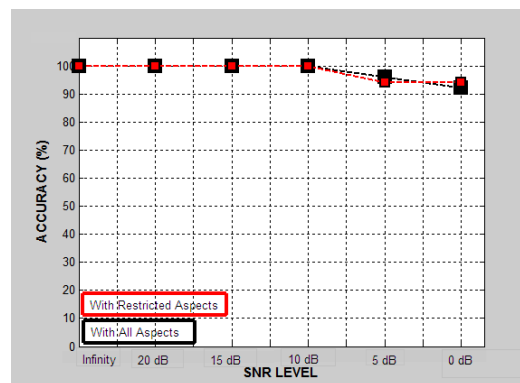


Figure 4.29 Correct classification rates computed for the Classifier #11 at various testing SNR levels for two different  $\theta$  range

Accuracy levels of the Classifier #9, Classifier #10 and Classifier #11 are plotted in Figure 4.30 against decreasing SNR levels. As it seen clearly in Figure 4.30, the SOM based Classifier #9, which is designed by noise-free reference data, can successfully discriminate the aircraft AC1 and AC2 under noise free testing conditions but its performance degrades as the testing SNR decreases. On the other hand, performances of the Classifier #10 and Classifier #11 are perfect, at least for the SNR level considered. This results demonstrate the usefulness of using slightly / moderately noisy reference data in classifier design problems.

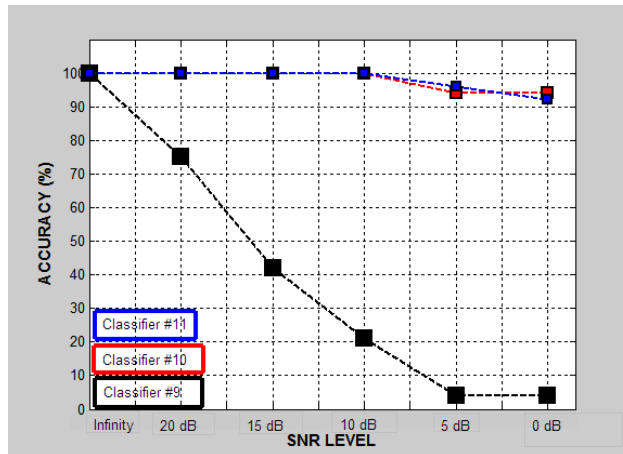


Figure 4.30 Correct classification rates computed for the Classifier #9, Classifier #10 and Classifier #11 at various testing SNR levels.

### 4.3 Design of SOM Classifiers for the Target Library TL5 of Three Small-Scale Aircraft

In this subsection, three different SOM classifiers will be designed for the target library TL5 of three aircraft AC1 (Airbus), AC2 (Boeing 747) and AC4 (Tu 154). The first classifier will be designed by using noise-free reference data and it will be tested at all non-reference aspects for the SNR levels of infinity, 20 dB, 15 dB, 10 dB, 5 dB and 0 dB. Secondly, slightly noisy reference data at 20 dB SNR level will be used in SOM training. The resulting classifier will also be tested at the SNR levels of infinity, 20 dB, 15 dB, 10 dB, 5 dB and 0 dB. Finally, the similar classifier design and test simulations will be repeated while using the reference data at a moderate noise level of 10 dB for SOM training.

The optimal late-time interval for the classifier designed by noise-free reference database is found to be [31.3-62.5] nsec from the CCF versus  $q^*$  plot shown in Figure 4.31. Similarly, for the classifiers designed for the target library TL5 with noisy reference databases at the SNR levels of 20 dB and 10 dB, the same optimal



late-time design interval is found to be [15.6-46,9] nsec, based on the CCF versus  $q^*$  plots shown in parts (a) and (b) of Figure 4.32.

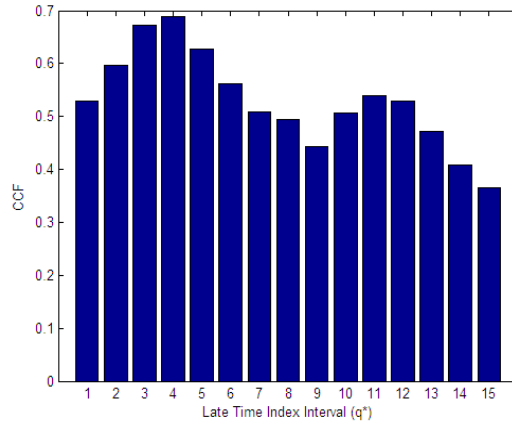


Figure 4.31 The CCF versus  $q^*$  plot generated to determine the optimal late-time design interval for the target library TL5 in the case of noise-free classifier design.

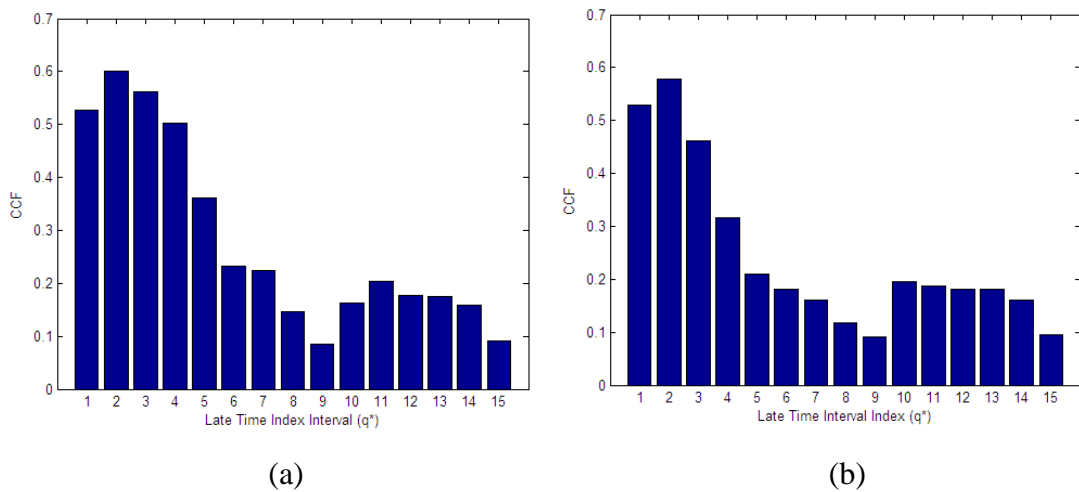


Figure 4.32 The CCF versus  $q^*$  plot generated to determine the optimal late-time design interval for the target library TL5 in the case of (a) SNR level of 20 dB and (b) SNR level of 10 dB designs.

#### 4.3.1. Classifier Simulation #12: Design of a SOM Classifier Using Noise-Free Reference Data for the Target Library TL5 with Three Aircraft

This classifier is designed over the late-time interval [31.3-62.5] nsec using noise-free scattered data of aircraft AC1, AC2 and AC4 at the reference aspects  $\theta = 5^\circ, 15^\circ, 37.5^\circ, 60^\circ, 82.5^\circ$ . The LTFV features extracted for all three small scale aircraft at these backscattered aspects are used to train a SOM grid of size [21x21]. The SOM is initialized randomly at the beginning and the radius of the Gaussian neighborhood function is chosen to decrease from 10 to 7 during iterations. Sequential training of the SOM is completed after 500 epochs. During this training, a total of 15 training features (for 3 targets at 5 reference aspects) are selected in random order to train the self organizing map. When the training phase is completed, the resulting SOM output with  $21 \times 21 = 441$  weight vectors (each having the length of 512) is saved as the classifier design matrix of size  $441 \times 512$ . Figure 4.33 shows the contour plot of the norms of the trained weight vectors over the SOM grid of size  $21 \times 21$ .

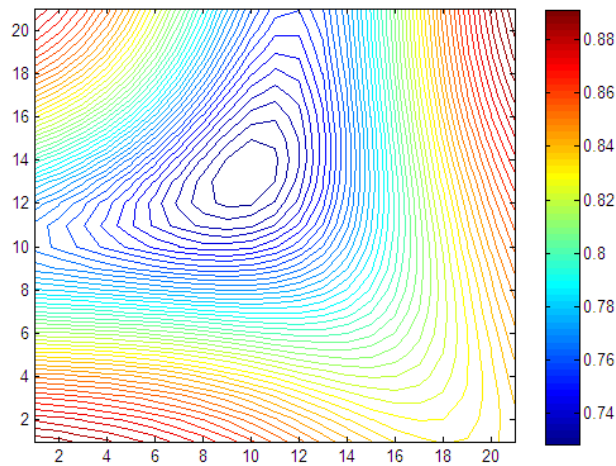


Figure 4.33 SOM output trained by noise-free WD-based late time energy feature vectors of the small scale aircraft AC1, AC2 and AC4.

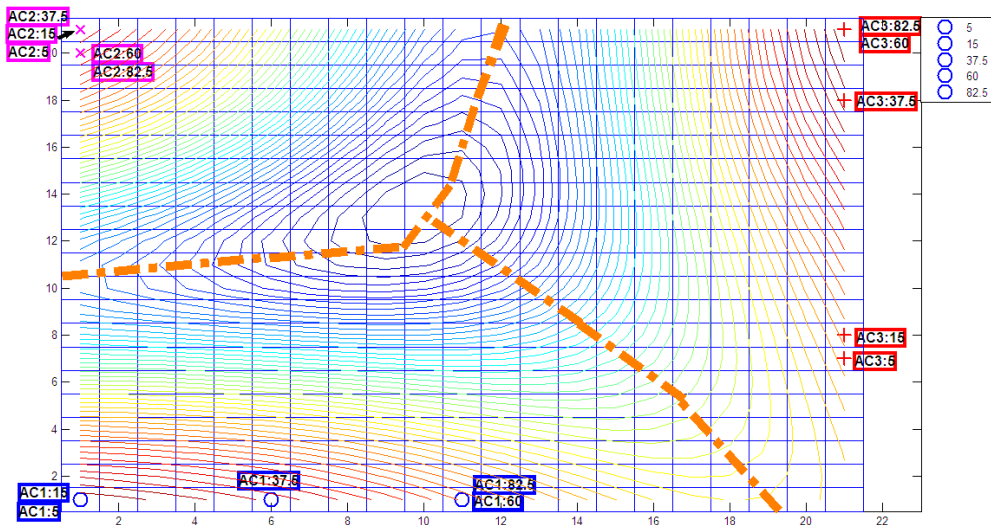


Figure 4.34 Winning neuron locations for the training features and the boundary curve to separate the cluster regions AC1 (blue circles), AC2 (magenta crosses) and AC4 (red plus signs) over the SOM output grid for the Classifier #12.

Three separate cluster regions are formed at the lower left, upper left and the upper right corners of the SOM output grid corresponding to the targets AC1, AC2 and AC4, respectively. The dot-dashed orange curve passing through the neuron locations with smallest norm values to define the cluster boundary for the SOM output is shown in Figure 4.34. Then, the Classifier #12 is tested by noise-free and noisy feature vectors at 20 dB, 15 dB, 10 dB, 5 dB and 0 dB SNR levels. Locations of the testing winning neurons are marked in Figure 4.35, Figure 4.36, Figure 4.37, Figure 4.38, Figure 4.39 and Figure 4.40 for the SNR levels of infinity, 20 dB, 15 dB, 10 dB, 5 dB and 0 dB, respectively. The correct classification rates computed at each testing SNR level are listed in Table 4.6 and also plotted in Figure 4.41.

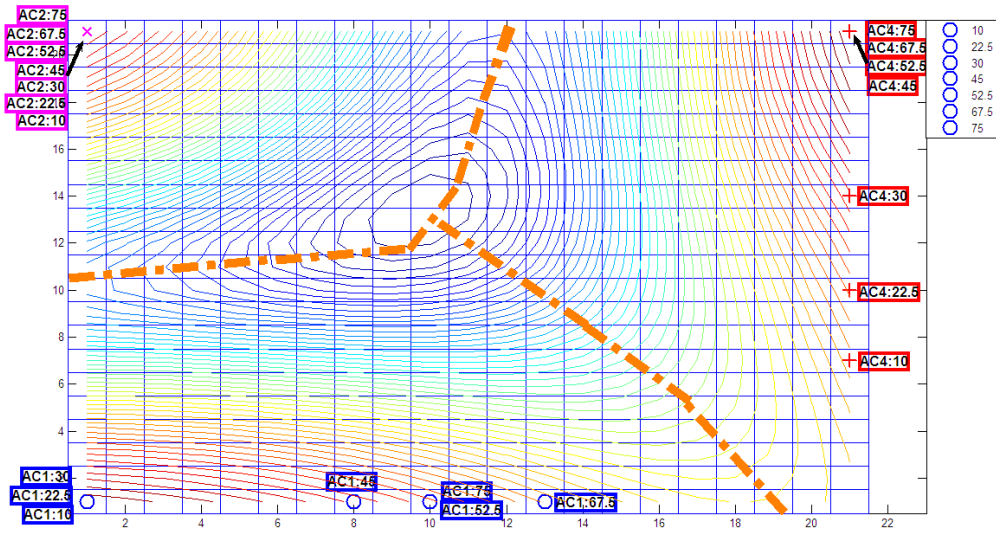


Figure 4.35 SOM Classifier #12 tested by noise-free feature vectors of the aircraft AC1 (blue circles), AC2 (magenta crosses) and AC4 (red plus signs).

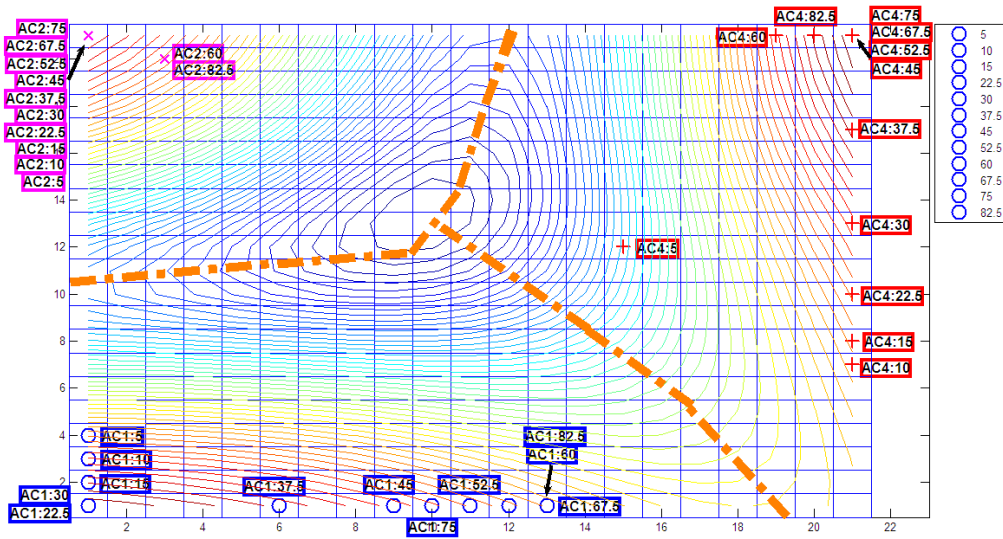


Figure 4.36 SOM Classifier #12 tested by noisy feature vectors of the aircraft AC1 (blue circles), AC2 (magenta crosses) and AC4 (red plus signs) at 20 dB SNR level.

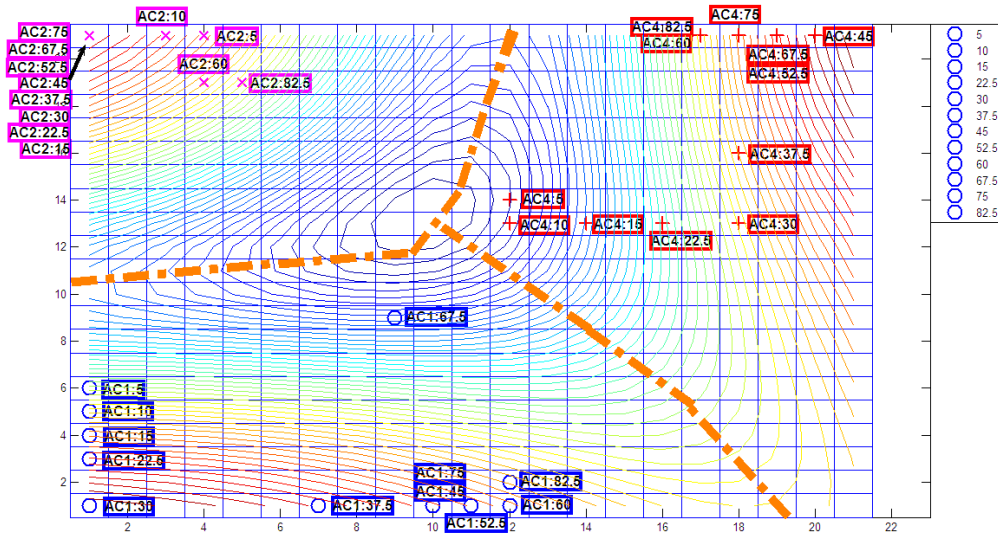


Figure 4.37 SOM Classifier #12 tested by noisy feature vectors of the aircraft AC1 (blue circles), AC2 (magenta crosses) and AC4 (red plus signs) at 15 dB SNR level.

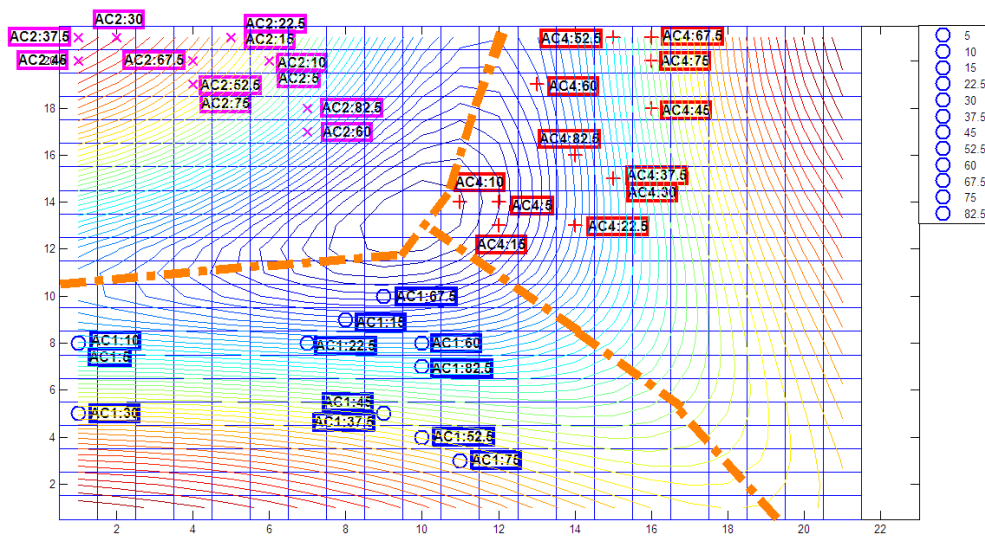


Figure 4.38 SOM Classifier #12 tested by noisy feature vectors of the aircraft AC1 (blue circles), AC2 (magenta crosses) and AC4 (red plus signs) at 10 dB SNR level.

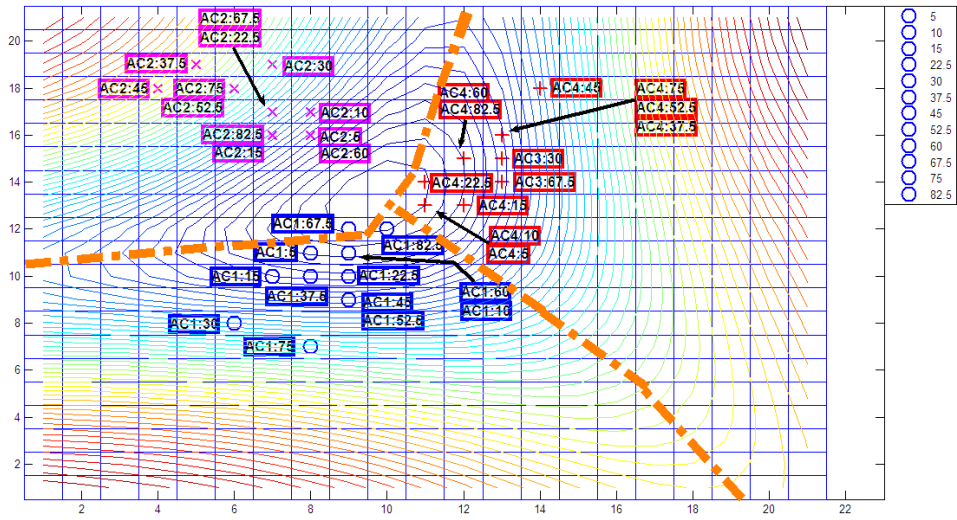


Figure 4.39 SOM Classifier #12 tested by noisy feature vectors of the aircraft AC1 (blue circles), AC2 (magenta crosses) and AC4 (red plus signs) at 5 dB SNR level.

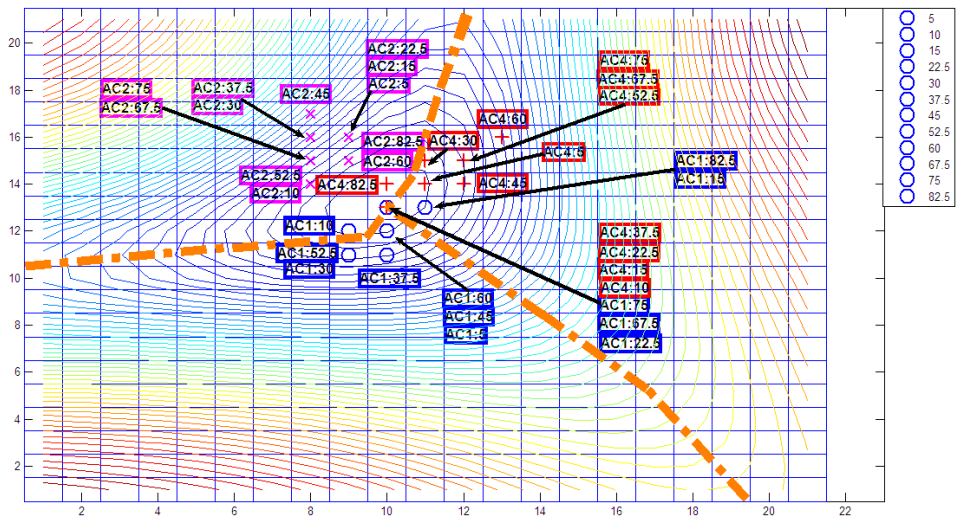


Figure 4.40 SOM Classifier #12 tested by noisy feature vectors of the aircraft AC1 (blue circles), AC2 (magenta crosses) and AC4 (red plus signs) at 0 dB SNR level.

Table 4.6 Correct decision rates for the Classifier #12 at different testing SNR levels for two different  $\theta$  range

SNR	Type Of Boundary	
	For $5^\circ \leq \theta \leq 82,5^\circ$	For $10^\circ < \theta < 75^\circ$
Noise Free	100	100
20 dB	100	100
15 dB	100	100
10 dB	100	100
5 dB	96	94
0 dB	92	94

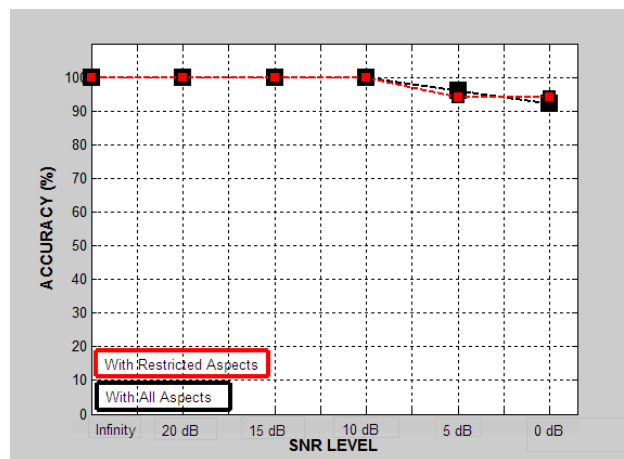


Figure 4.41 Correct classification rates computed for the Classifier #12 at various testing SNR levels for two different  $\theta$  range

Accuracy level of the Classifier #12 becomes less than 100 percent only at 5 dB and 0 dB testing SNR levels. Although, a perfect accuracy figure of 100 percent is obtained at other SNR levels, the winning neurons of tested target features get closer to each other in the center of the SOM grid as the SNR levels gets smaller. In other words, not the accuracy figure itself but the safety margin of classification degrades by decreasing SNR.

#### 4.3.2. Classifier Simulation #13: Design of a SOM Classifier Using Slightly Noisy (SNR Level of 20 dB) Reference Data for the Target Library TL5 with Three Aircraft

Classifier #13 is designed over the late-time interval [15.6-46.9] nsec using slightly noisy scattered data of small scale aircraft AC1, AC2 and AC4 at the reference aspects  $\theta = 5^\circ, 15^\circ, 37.5^\circ, 60^\circ, 82.5^\circ$ . The resulting SOM output with  $21 \times 21 = 441$  weight vectors (each having the length of 512) is saved as the classifier design matrix of size  $21 \times 512$ . Figure 4.42 shows the contour plot of the norms of the trained weight vectors over the SOM grid of size  $21 \times 21$ . The boundary curve separating the target clusters is shown in Figure 4.43 together with the winning neuron locations for the training target features belonging to each small scale aircraft. Two branches of the cluster boundary pass through the neuron locations with minimum norm values. The third branch of the boundary curve, however, is passed through the midpoints of closest winning neurons belonging to aircraft AC2 and AC3.

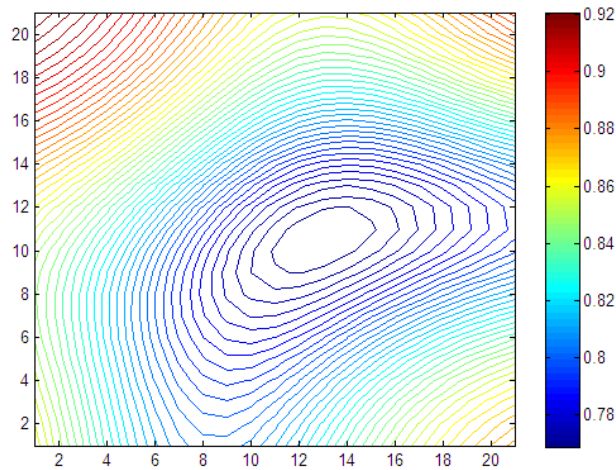


Figure 4.42 SOM output trained by slightly noisy (SNR Level of 20 dB) WD-based late time energy feature vectors of the small scale aircraft AC1, AC2 and AC4.



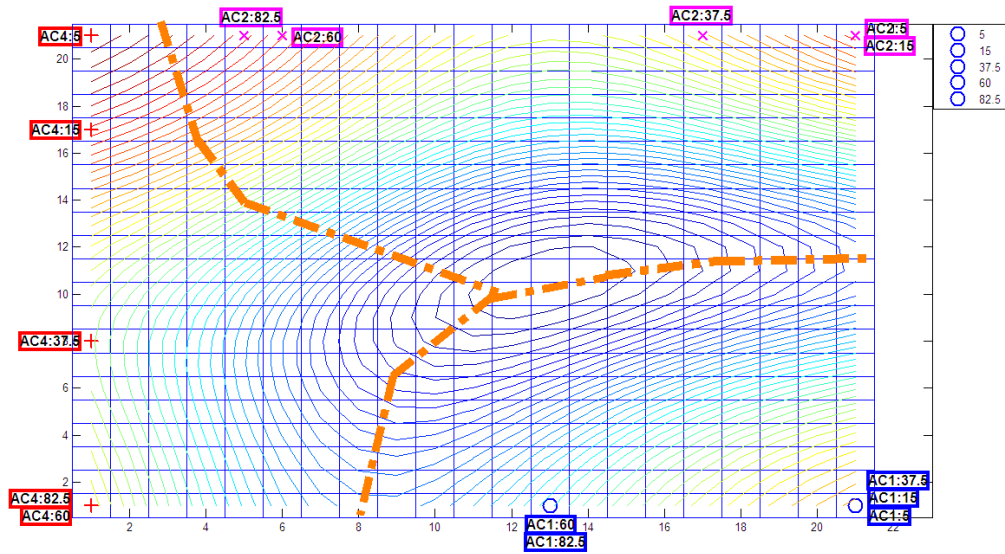


Figure 4.43 Winning neuron locations for the training features of the aircraft AC1 (blue circles), AC2 (magenta crosses) and AC4 (red plus signs) over the SOM output grid for the Classifier #13.

Next, the Classifier #13 is tested by noise-free and noisy feature vectors at 20 dB, 15 dB, 10 dB, 5 dB and 0 dB SNR levels. Locations of the testing winning neurons are marked in Figure 4.44, Figure 4.45, Figure 4.46, Figure 4.47, Figure 4.48 and Figure 4.49 for the SNR levels of infinity, 20 dB, 15 dB, 10 dB, 5 dB and 0 dB, respectively. The correct classification rates computed at each testing SNR level are listed in Table 4.7 and also plotted in Figure 4.50.

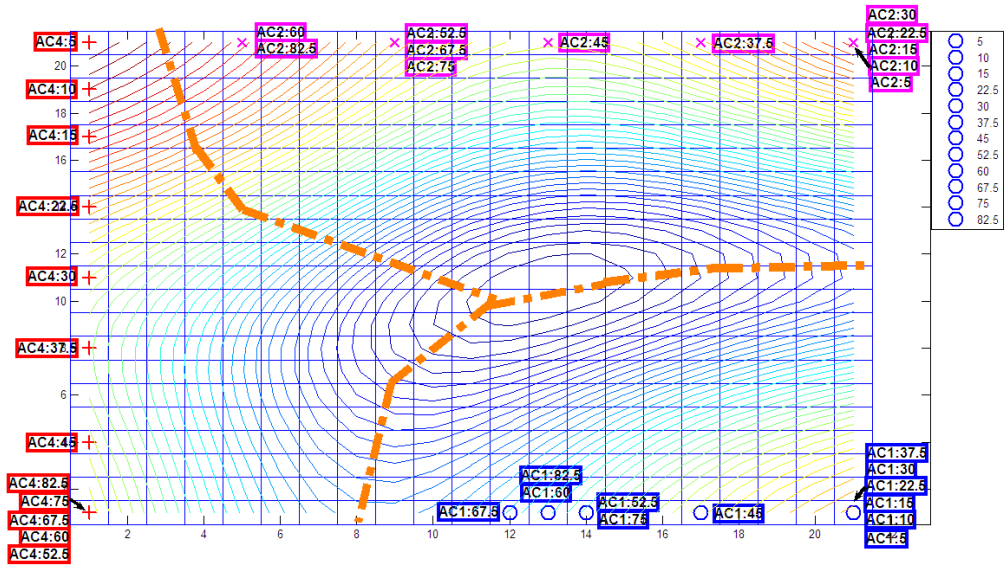


Figure 4.44 SOM Classifier #13 tested by noise-free feature vectors of the aircraft AC1 (blue circles), AC2 (magenta crosses) and AC4 (red plus signs).

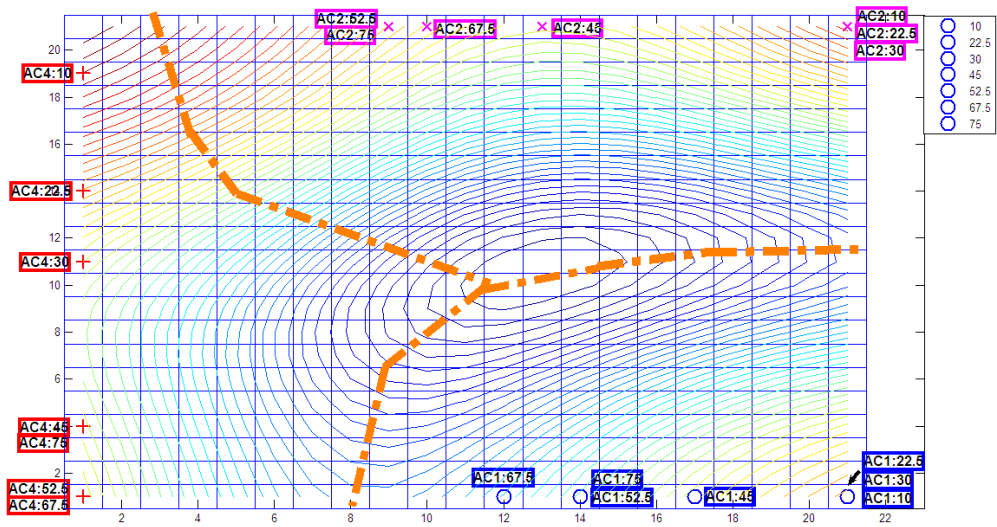


Figure 4.45 SOM Classifier #13 tested by noisy feature vectors of the aircraft AC1 (blue circles), AC2 (magenta crosses) and AC4 (red plus signs) at 20 dB SNR level.

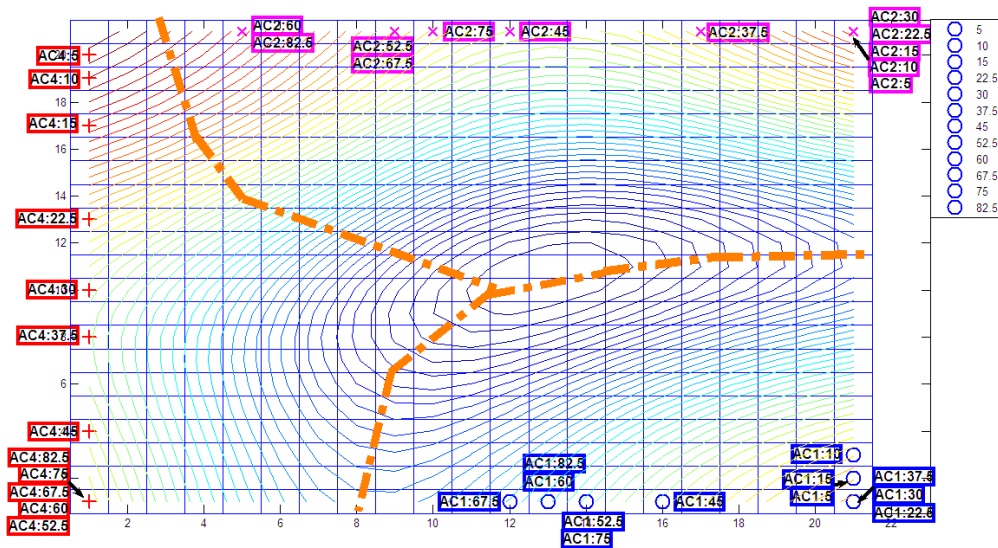


Figure 4.46 SOM Classifier #13 tested by noisy feature vectors of the aircraft AC1 (blue circles), AC2 (magenta crosses) and AC4 (red plus signs) at 15 dB SNR level.

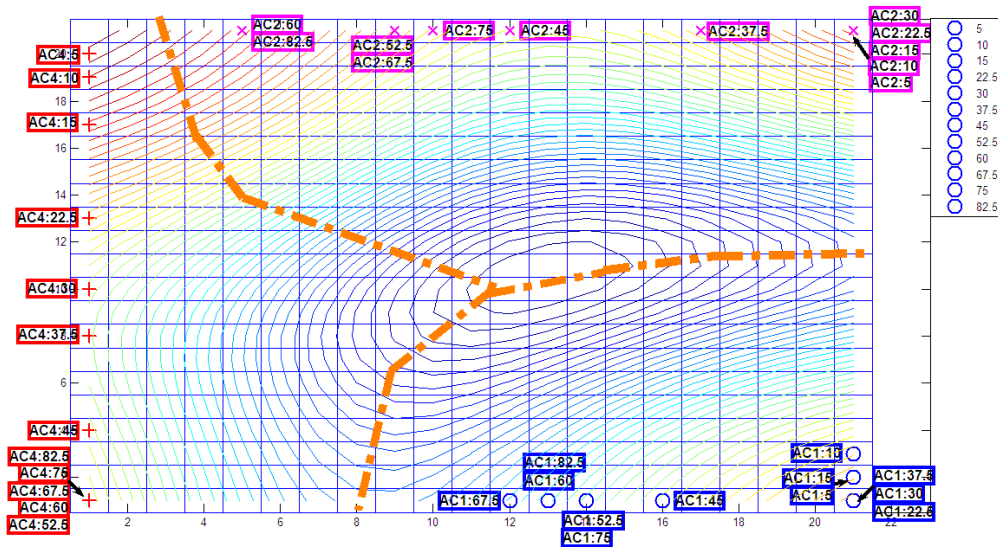


Figure 4.47 SOM Classifier #13 tested by noisy feature vectors of the aircraft AC1 (blue circles), AC2 (magenta crosses) and AC4 (red plus signs) at 10 dB SNR level.

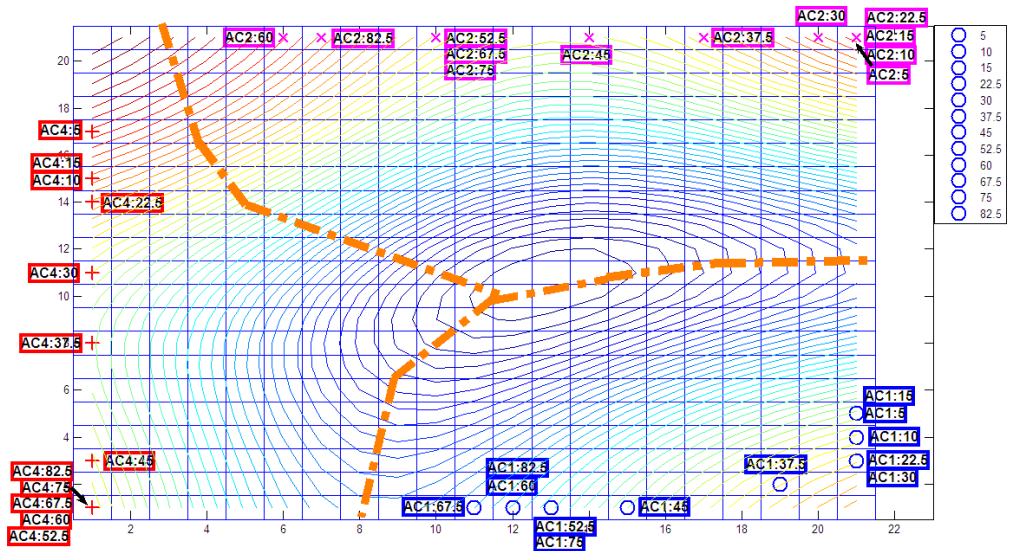


Figure 4.48 SOM Classifier #13 tested by noisy feature vectors of the aircraft AC1 (blue circles), AC2 (magenta crosses) and AC4 (red plus signs) at 5 dB SNR level.

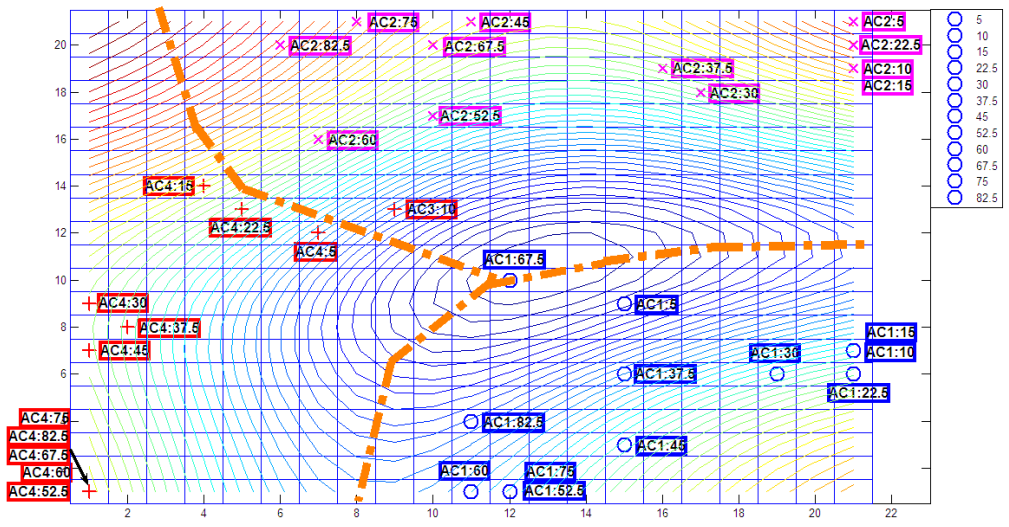


Figure 4.49 SOM Classifier #13 tested by noisy feature vectors of the aircraft AC1 (blue circles), AC2 (magenta crosses) and AC4 (red plus signs) at 0 dB SNR level.

Table 4.7 Correct decision rates for the Classifier #13 at different testing SNR levels for two different  $\theta$  range.

SNR	Type Of Boundary	
	For $5^\circ \leq \theta \leq 82,5^\circ$	For $10^\circ < \theta < 75^\circ$
Noise Free	100	100
20 dB	100	100
15 dB	100	100
10 dB	100	100
5 dB	100	100
0 dB	94	96

Accuracy level of Classifier #13 is found to be 100 percent at all testing SNR levels except the SNR level of 0 dB as can be seen in Table 4.7 and Figure 4.50.

In other words, the SOM based Classifier #13, which is designed by using slightly noisy reference data, can perfectly discriminate the aircraft targets AC1, AC2 and AC4 under all these testing cases. Locations of winning neurons show little changes with decreasing SNR level, as opposed to the case that observed for the Classifier #12.

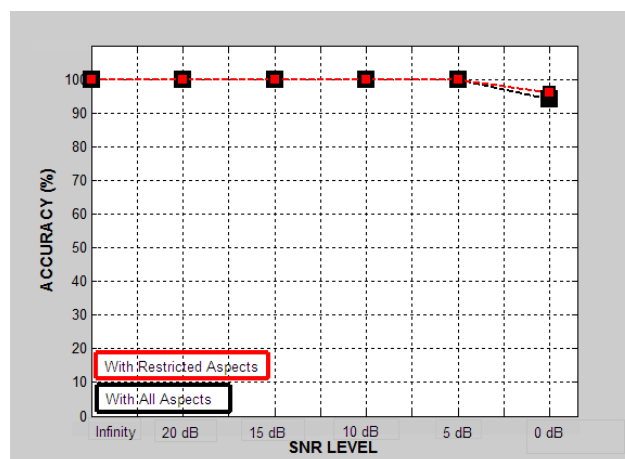


Figure 4.50 Correct classification rates computed for the Classifier #13 at various testing SNR levels for two different  $\theta$  range.

### 4.3.3. Classifier Simulation #14: Design of a SOM Classifier Using Moderately Noisy (SNR Level of 10 dB) Reference Data for the Target Library TL5 with Three Aircraft

Classifier Simulation #14 is designed over the late-time interval [15.6-46.9] nsec using noise-free scattered data of small scale aircraft AC1, AC2 and AC4 at the reference aspects  $\theta = 5^\circ, 15^\circ, 37.5^\circ, 60^\circ, 82.5^\circ$ . The resulting SOM output with  $21 \times 21 = 441$  weight vectors (each having the length of 512) is saved as the classifier design matrix of size  $441 \times 512$ . Figure 4.51 shows the contour plot of the norms of the trained weight vectors over the SOM grid of size  $21 \times 21$ .

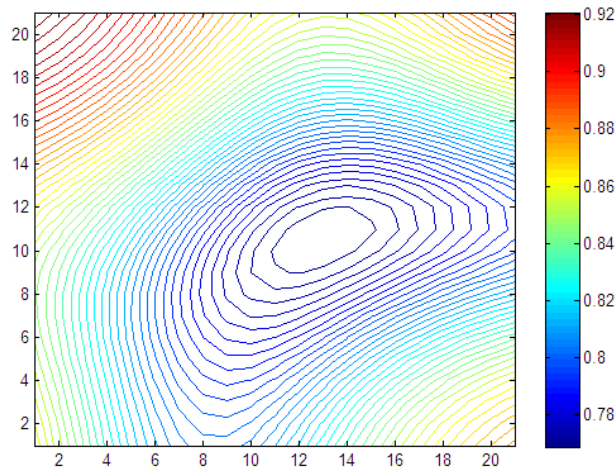


Figure 4.51 SOM output trained by noisy (SNR Level of 10 dB) WD-based late time energy feature vectors of the small scale aircraft AC1, AC2 and AC4.

Figure 4.52 shows the boundary curve separating the target clusters as well as the winning neuron locations for the training target features belonging to each small scale aircraft.

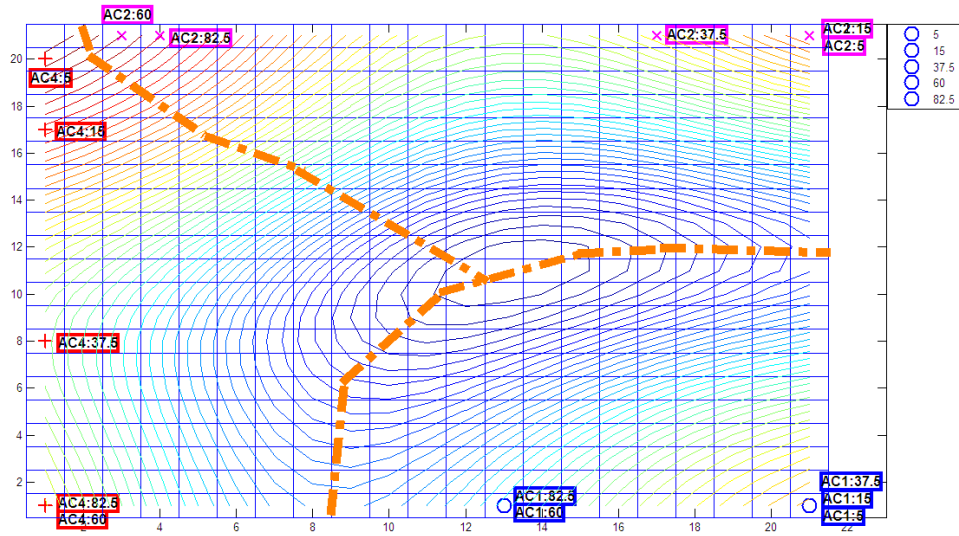


Figure 4.52 Winning neuron locations for the training features of the aircraft AC1 (blue circles), AC2 (magenta crosses) and AC4 (red plus signs) over the SOM output grid for the Classifier #14.

Then, the Classifier #14 is tested by noise-free and noisy feature vectors at 20 dB, 15 dB, 10 dB, 5 dB and 0 dB SNR levels. Locations of the testing winning neurons are marked in Figure 4.53, Figure 4.54, Figure 4.55, Figure 4.56, Figure 4.57 and Figure 4.58 for the SNR levels of infinity, 20 dB, 15 dB, 10 dB, 5 dB and 0 dB, respectively. The correct classification rates computed at each testing SNR levels are listed in Table 4.8 and plotted in Figure 4.59.

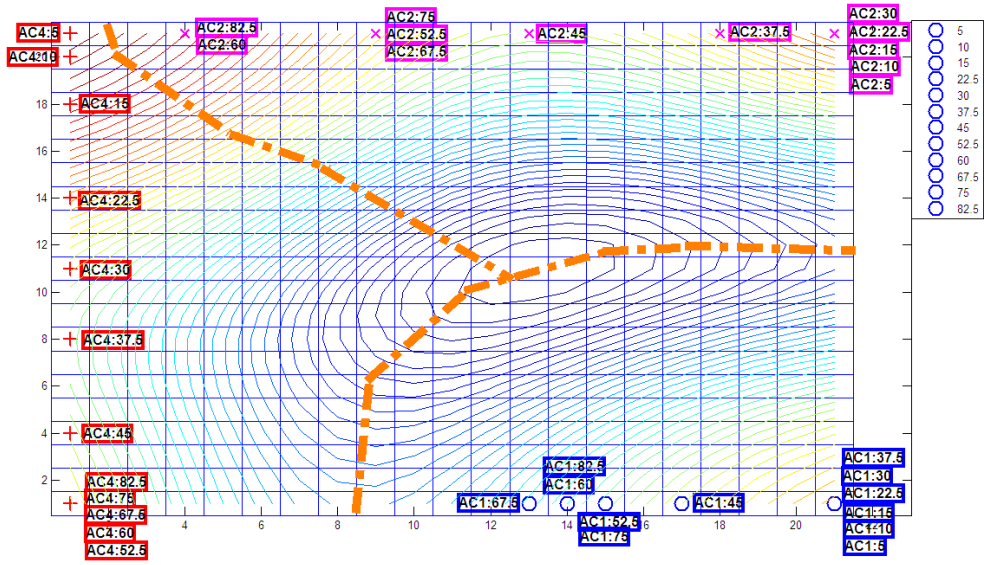


Figure 4.53 SOM Classifier #14 tested by noise-free feature vectors of the aircraft AC1 (blue circles), AC2 (magenta crosses) and AC4 (red plus signs).

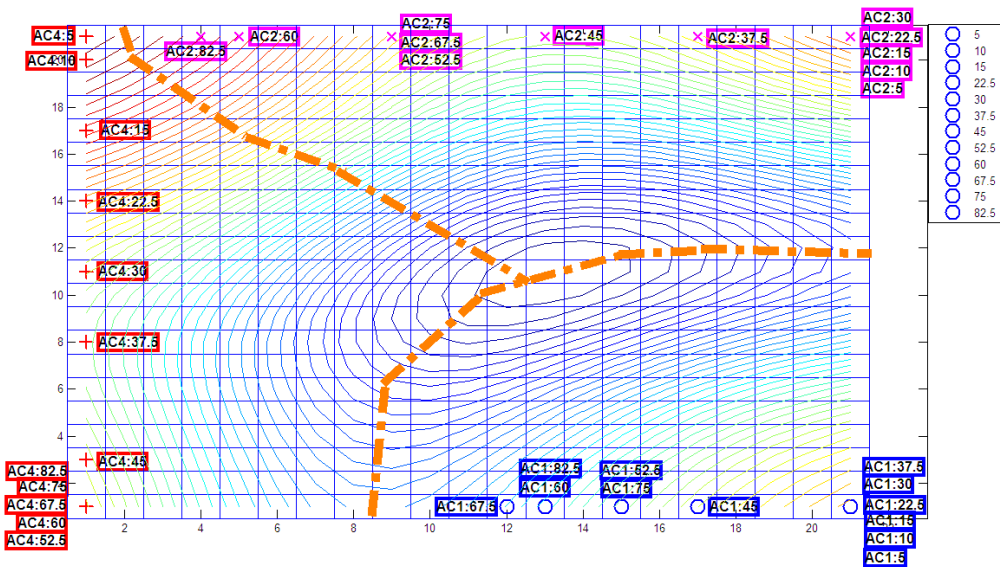


Figure 4.54 SOM Classifier #14 tested by noisy feature vectors of the aircraft AC1 (blue circles), AC2 (magenta crosses) and AC4 (red plus signs) at 20 dB SNR level.



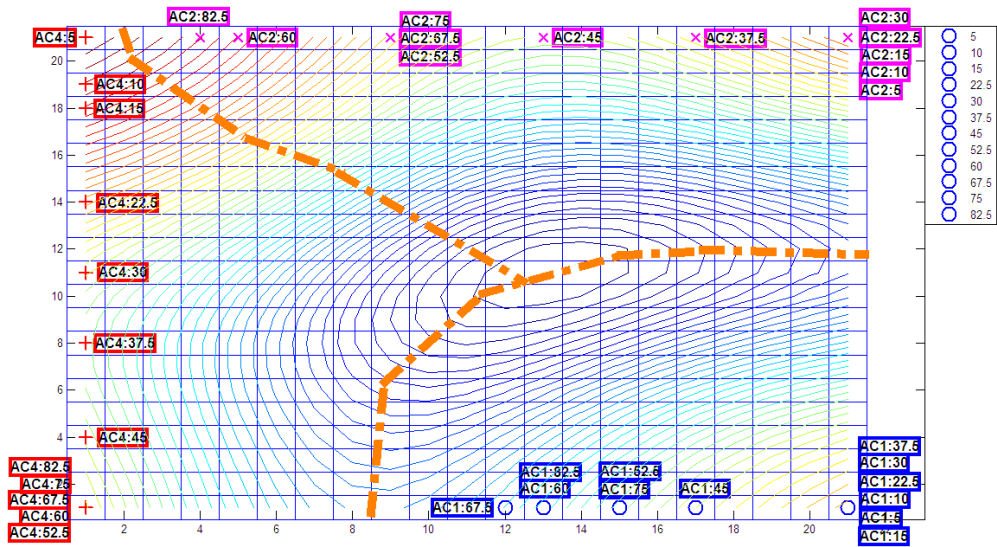


Figure 4.55 SOM Classifier #14 tested by noisy feature vectors of the aircraft AC1 (blue circles), AC2 (magenta crosses) and AC4 (red plus signs) at 15 dB SNR level.

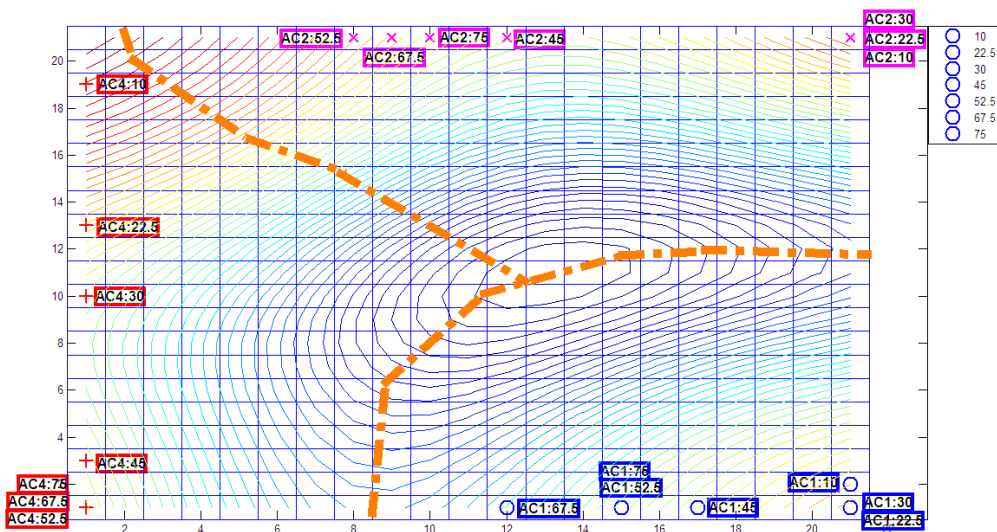


Figure 4.56 SOM Classifier #14 tested by noisy feature vectors of the aircraft AC1 (blue circles), AC2 (magenta crosses) and AC4 (red plus signs) at 10 dB SNR level.

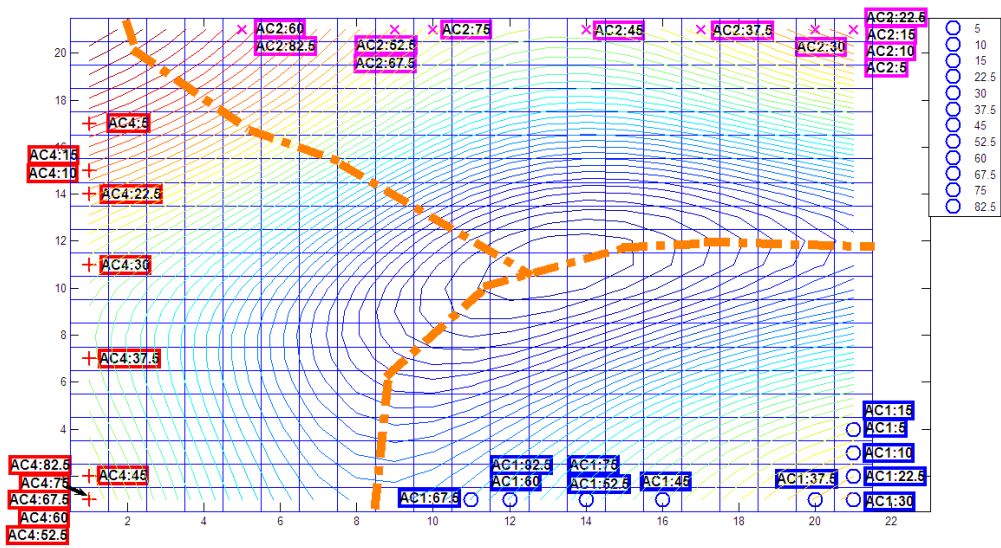


Figure 4.57 SOM Classifier #14 tested by noisy feature vectors of the aircraft AC1 (blue circles), AC2 (magenta crosses) and AC4 (red plus signs) at 5 dB SNR level.

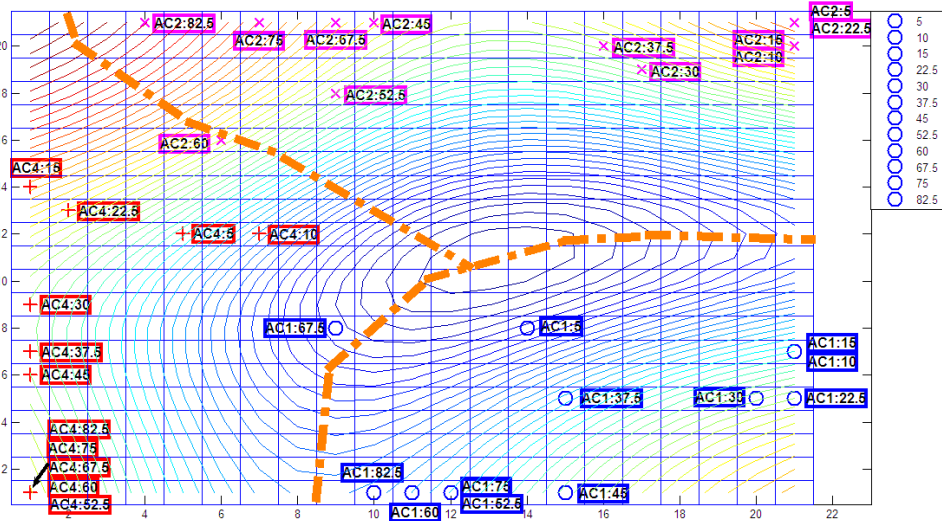


Figure 4.58 SOM Classifier #14 tested by noisy feature vectors of the aircraft AC1 (blue circles), AC2 (magenta crosses) and AC4 (red plus signs) at 0 dB SNR level.

Table 4.8 Correct decision rates for the Classifier #14 at different testing SNR levels for two different  $\theta$  range.

SNR	Type Of Boundary	
	For $5^\circ \leq \theta \leq 82,5^\circ$	For $10^\circ < \theta < 75^\circ$
Noise Free	100	100
20 dB	100	100
15 dB	100	100
10 dB	100	100
5 dB	100	100
0 dB	94	92

Likewise Classifier #13, Classifier #14 also perfectly discriminates the aircraft targets AC1, AC2 and AC4 under all testing SNR levels except the 0 dB SNR case, with wide safety margins.

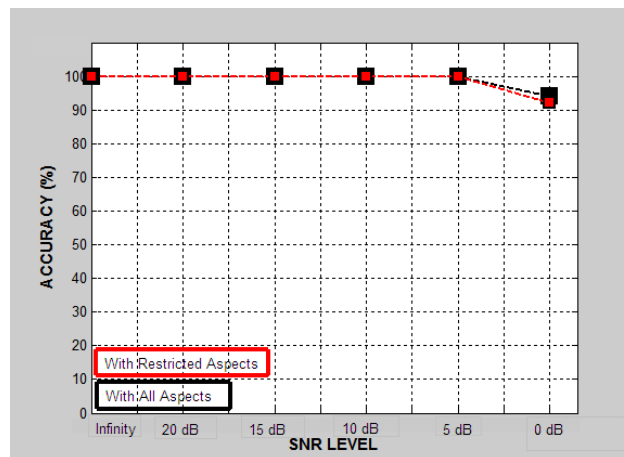


Figure 4.59 Correct classification rates computed for the Classifier #14 at various testing SNR levels for two different  $\theta$  range.

#### 4.4 Design of SOM Classifiers for the Target Library TL6 of Four Small Scale Aircraft

In this subsection, three different SOM classifiers will be designed for target library TL6 which contains four aircraft targets AC1 (Airbus), AC2 (Boeing 747), AC3 (P-7) and AC4 (Tu 154). The first classifier will be designed by using noise-free reference data. Secondly, slightly noisy reference data at 20 dB SNR level will be used in SOM training. Finally, the similar classifier design will be repeated while using the reference data at a moderate noise level of 10 dB for SOM training. All three classifiers will be tested at the SNR levels of infinity, 20 dB, 15 dB, 10 dB, 5 dB and 0 dB.

The correct classification factor (CCF) versus interval index ( $q^*$ ) for the target library TL6 with noise free reference database is shown in Figure 4.60. The optimal late-time design interval of [31.3-62.5] nsec is selected based on this figure. Similarly, the optimal design intervals of the classifiers designed at 20 dB and 10 dB reference SNR levels are found to be the same [15.6-46,9] nsec by the help of CCF versus  $q^*$  plots shown in parts (a) and (b) of Figure 4.61.

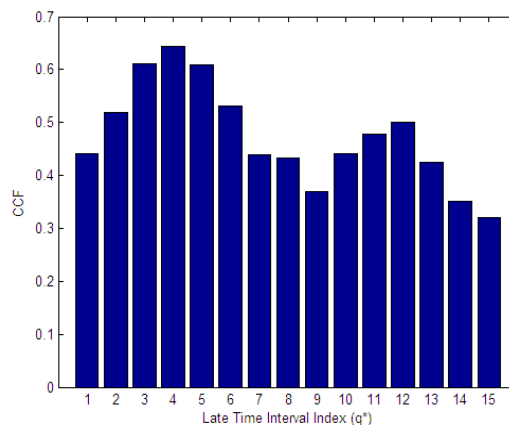


Figure 4.60 The CCF versus  $q^*$  plot generated to determine the optimal late-time design interval for the target library TL6 in the case of noise-free classifier design.

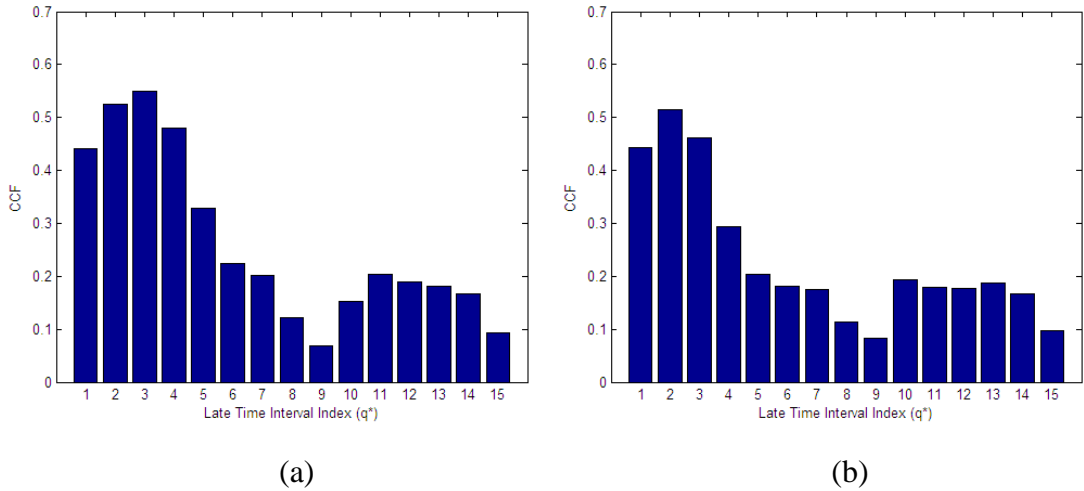


Figure 4.61 The CCF versus  $q^*$  plot generated to determine the optimal late-time design interval for the target library TL6 in the case of (a) SNR=20 dB and (b) SNR=10 dB classifier design simulations.

#### 4.4.1. Classifier Simulation #15: Design of a SOM Classifier Using Noise-Free Reference Data for the Target Library TL6 with Four Aircraft

This classifier is designed over the late-time interval [31.3-62.5] nsec by using noise-free scattered data of aircraft AC1, AC2, AC3 and AC4 at the reference aspects  $\theta = 5^\circ, 15^\circ, 37.5^\circ, 60^\circ, 82.5^\circ$ . The LTFV features extracted for all four small scale aircrafts at these backscattered (monostatic) aspects are used to train a SOM grid of size [30x30]. The SOM is initialized randomly at the beginning and the radius of the Gaussian neighborhood function is chosen to decrease from 15 to 11 during iterations. Sequential training of the SOM is completed after 500 epochs. During this training, a total of 20 training features (for 4 targets at 5 reference aspects) are selected in random order to train the self organizing map. When the training phase is completed, the resulting SOM output with 30x30=900 weight vectors (each having the length of 512) is saved as the classifier design

matrix of size 900x512. Figure 4.52 shows the contour plot of the norms of the trained weight vectors over the SOM grid of size 30x30.

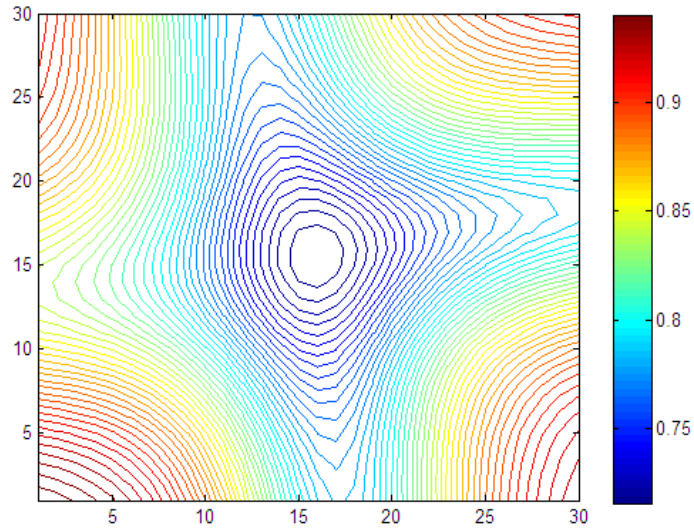


Figure 4.62 SOM output trained by noise-free WD-based late time energy feature vectors of the small scale aircraft AC1, AC2, AC3 and AC4.

Four separate cluster regions are formed at the corners of the SOM output grid. The dot-dashed orange curves passing through the neuron locations with smallest norm values to define the cluster boundary for the SOM output is shown in Figure 4.63. Then, the Classifier #15 is tested by noise-free and noisy feature vectors at 20 dB, 15 dB, 10 dB, 5 dB and 0 dB SNR levels. Locations of the testing winning neurons are marked in Figure 4.64, Figure 4.65, Figure 4.66, Figure 4.67, Figure 4.68 and Figure 4.69 for the SNR levels of infinity, 20 dB, 15 dB, 10 dB, 5 dB and 0 dB, respectively. Correct classification rates computed at each testing SNR level are listed in Table 4.9 and also plotted in Figure 4.70.

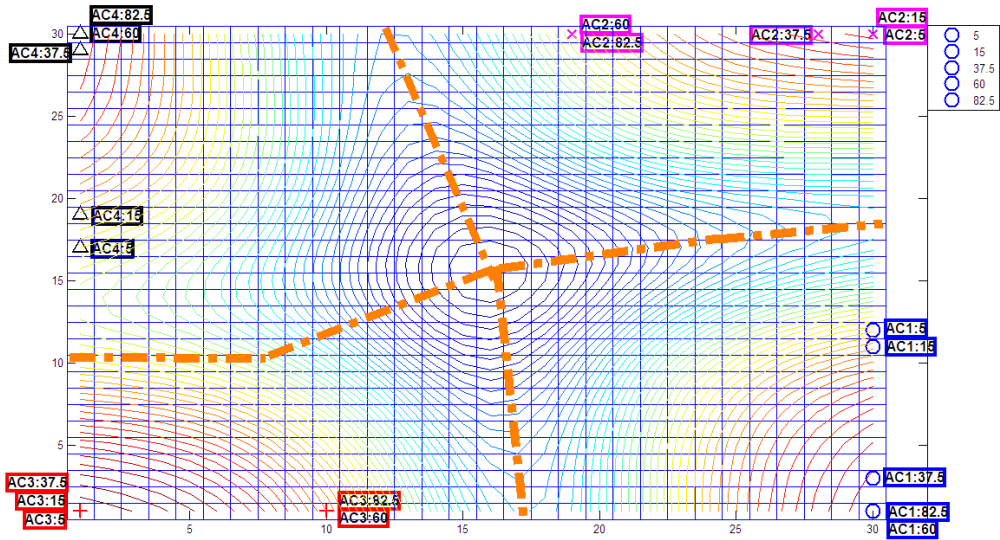


Figure 4.63 Winning neuron locations for the training features and the boundary curve to separate the cluster regions for the aircraft AC1 (blue circles), AC2 (magenta crosses), AC3 (red plus signs) and AC4 (black triangles) over the SOM output grid for the Classifier #15.

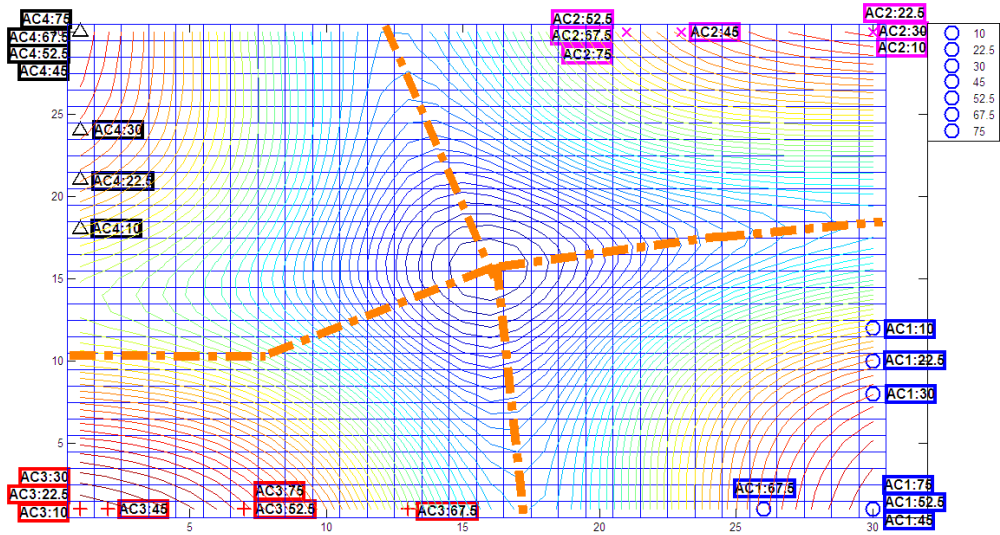


Figure 4.64 SOM Classifier #15 tested by noise-free feature vectors of the aircraft AC1 (blue circles), AC2 (magenta crosses), AC3 (red plus signs) and AC4 (black triangles).

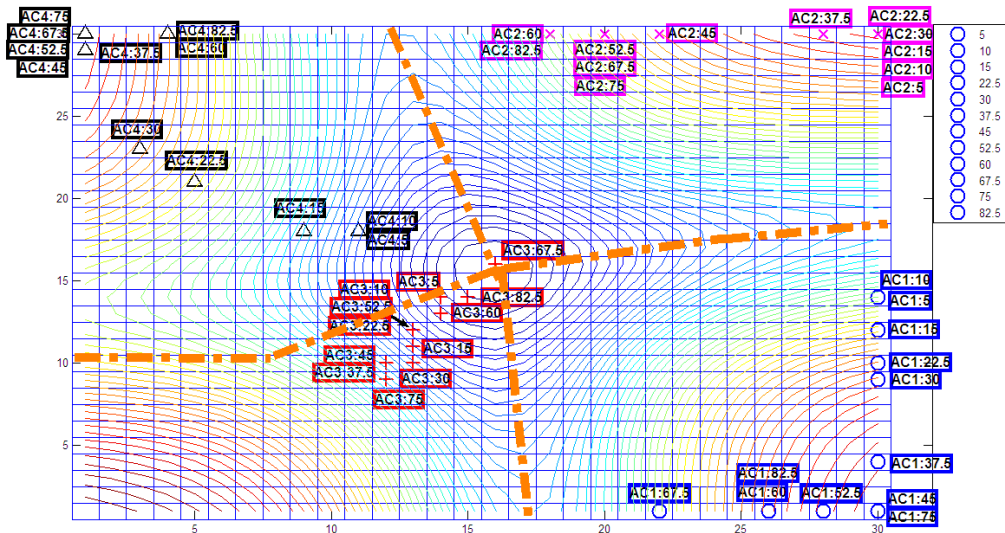


Figure 4.65 SOM Classifier #15 tested by noisy feature vectors of the aircraft AC1 (blue circles), AC2 (magenta crosses), AC3 (red plus signs) and AC4 (black triangles) at 20 dB SNR level.

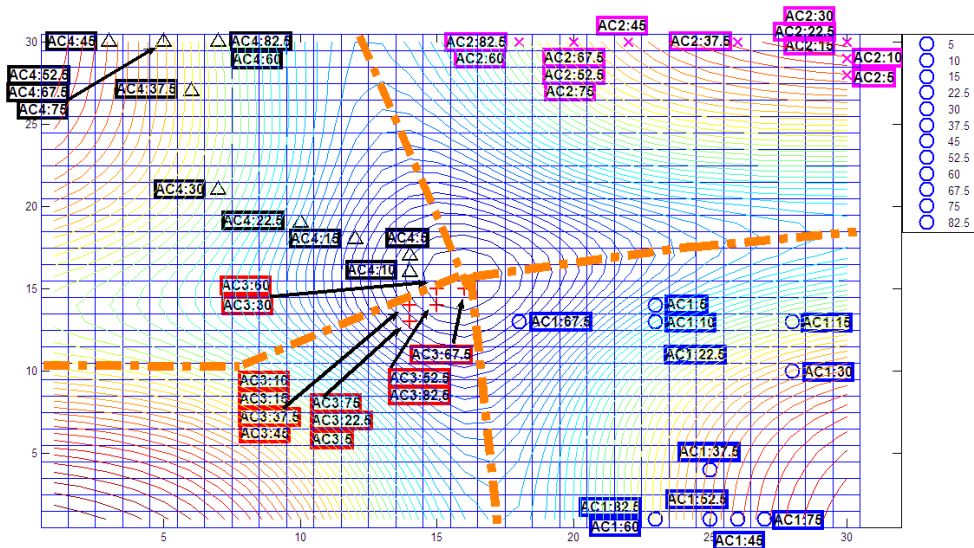


Figure 4.66 SOM Classifier #15 tested by noisy feature vectors of the aircraft AC1 (blue circles), AC2 (magenta crosses), AC3 (red plus signs) and AC4 (black triangles) at 15 dB SNR level.



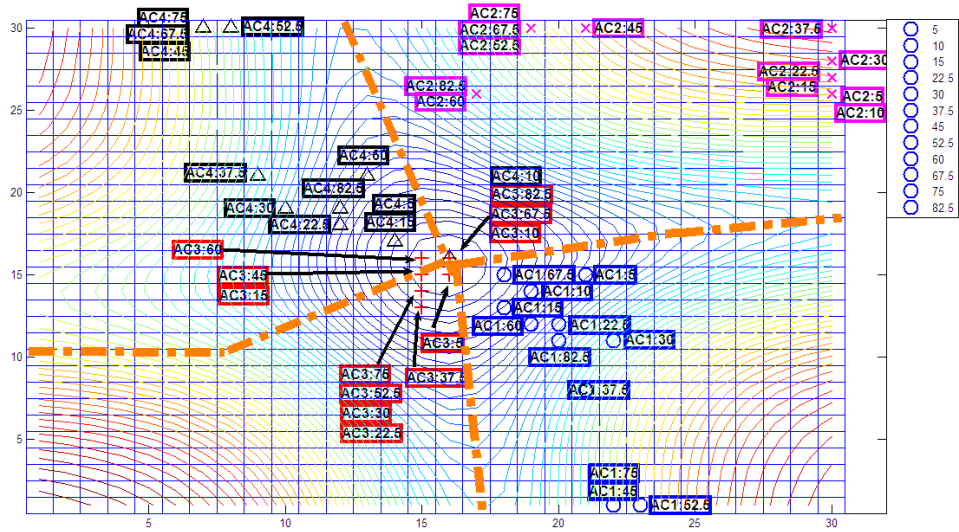


Figure 4.67 SOM Classifier #15 tested by noisy feature vectors of the aircraft AC1 (blue circles), AC2 (magenta crosses), AC3 (red plus signs) and AC4 (black triangles) at 10 dB SNR level.

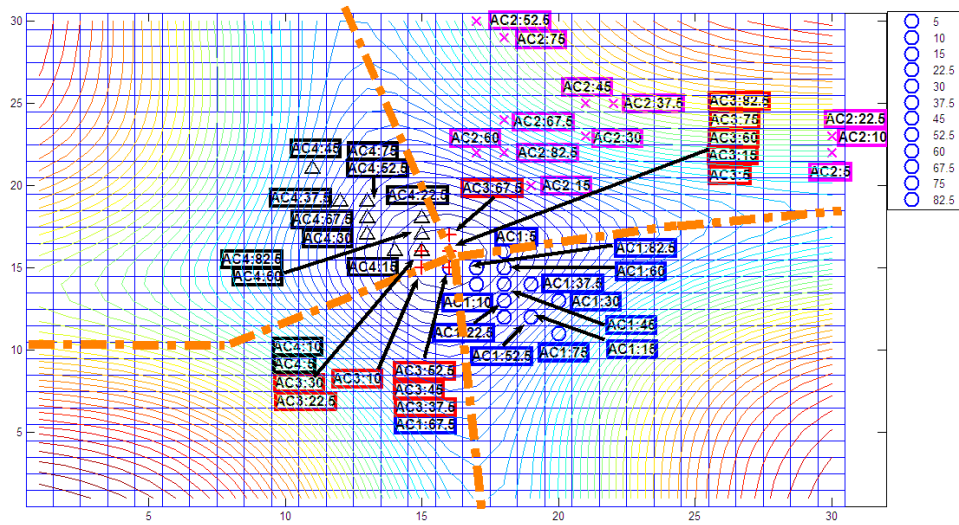


Figure 4.68 SOM Classifier #15 tested by noisy feature vectors of the aircraft AC1 (blue circles), AC2 (magenta crosses), AC3 (red plus signs) and AC4 (black triangles) at 5 dB SNR level.

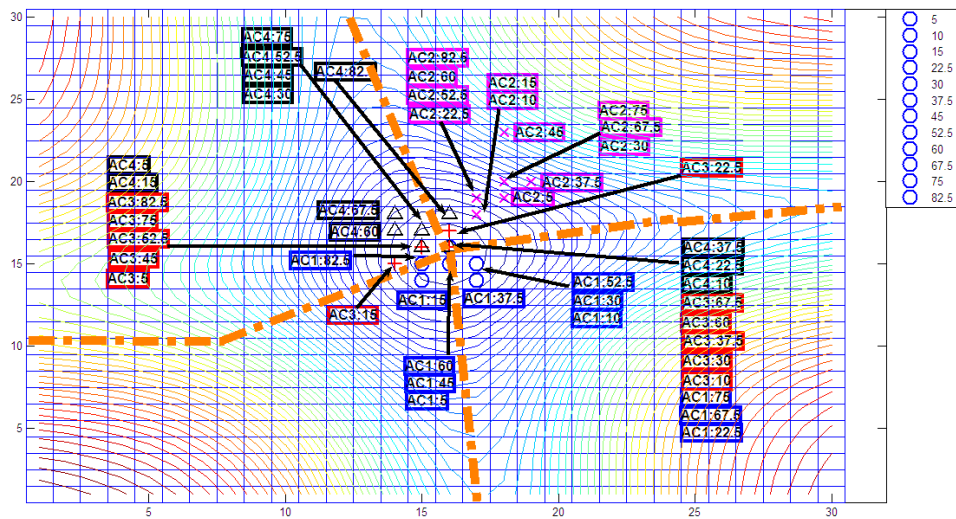


Figure 4.69 SOM Classifier #15 tested by noisy feature vectors of the aircraft AC1 (blue circles), AC2 (magenta crosses), AC3 (red plus signs) and AC4 (black triangles) at 0 dB SNR level.

Table 4.9 Correct decision rates for the Classifier #15 at different testing SNR levels for two different  $\theta$  range

SNR	Type Of Boundary	
	For $5^\circ \leq \theta \leq 82,5^\circ$	For $10^\circ < \theta < 75^\circ$
Noise Free	100	100
20 dB	98	97
15 dB	96	94
10 dB	85	88
5 dB	77	81
0 dB	50	50

As it seen clearly from Figure 4.70 and Table 4.9, the SOM based Classifier #15, which is designed by noise-free reference data, can successfully discriminate the small scale aircraft targets AC1, AC2, AC3 and AC4 under noise-free testing conditions but its performance degrades slowly as the testing SNR decreases. More importantly, the safety margins of classification seriously degrades as the

testing SNR levels gets lower. In the next simulation, a new classifier will be designed for the same target library TL6 (of small scale aircraft AC1, AC2, AC3 and AC4) by using slightly noisy reference data at 20 dB SNR level to improve the classification performance at lower SNR values.

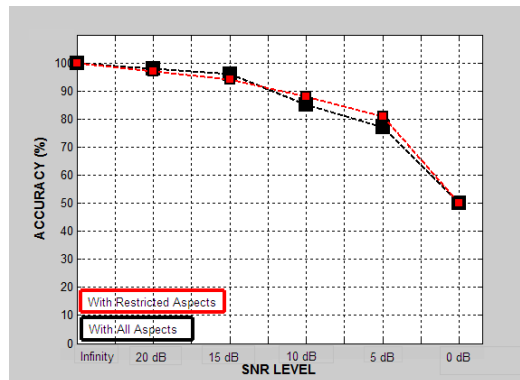


Figure 4.70 Correct classification rates computed for the Classifier #15 at various testing SNR levels for different  $\theta$  range.

#### 4.4.2. Classifier Simulation #16: Design of a SOM Classifier Using Slightly Noisy (SNR Level of 20 dB) Reference Data for the Target Library TL6 with Four Aircraft

Classifier Simulation #16 is designed over the late-time interval [15.6-46.9] nsec using slightly noisy (with SNR=20 dB) scattered data of small scale aircraft AC1, AC2, AC3 and AC4 at the reference aspects  $\theta = 5^\circ, 15^\circ, 37.5^\circ, 60^\circ, 82.5^\circ$ . The resulting SOM output with  $30 \times 30 = 900$  weight vectors (each having the length of 512) is saved as the classifier design matrix of size  $900 \times 512$ . Figure 4.71 shows the contour plot of the norms of the trained weight vectors over the SOM grid of size. Two of the branches of the cluster boundary passing through the neuron locations with smallest norm values. The other two branches pass through the midpoints of the closest training winning neurons of different target clusters. The

cluster boundary is shown in Figure 4.72 where the winning neuron locations for the training target features belonging to each small scale aircraft are also marked on this SOM output.

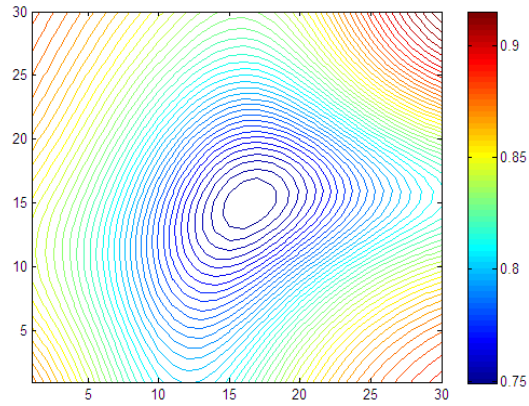


Figure 4.71 SOM output trained by slightly noisy (SNR Level of 20 dB) WD-based late time energy feature vectors of the small scale aircraft AC1, AC2, AC3 and AC4.

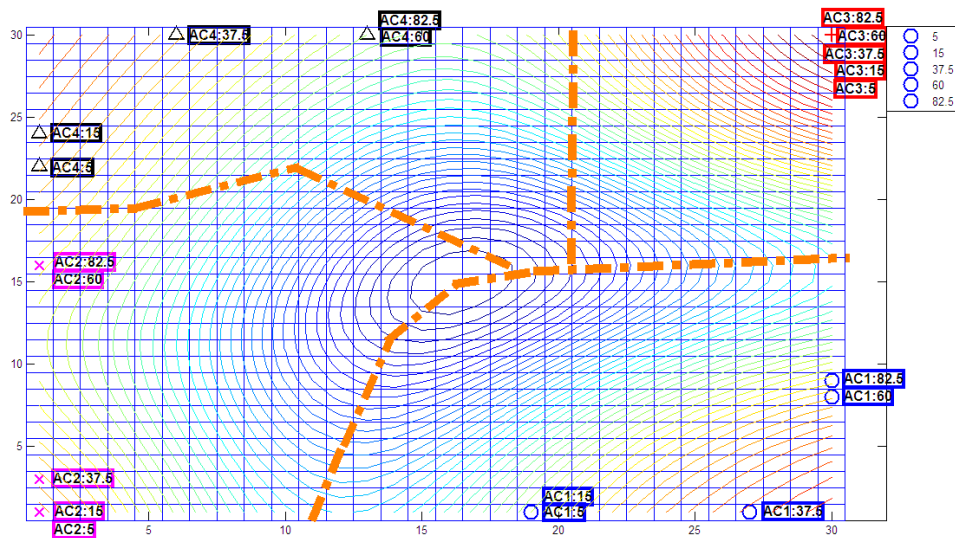


Figure 4.72 Winning neuron locations for the training features of the aircraft AC1 (blue circles), AC2 (magenta crosses), AC3 (red plus signs) and AC4 (black triangles) over the SOM output grid for the Classifier #16.

As usual, the Classifier #16 is tested by noise-free and noisy feature vectors at 20 dB, 15 dB, 10 dB, 5 dB and 0 dB SNR levels. Locations of the testing winning neurons are marked in Figure 4.73, Figure 4.74, Figure 4.75, Figure 4.76, Figure 4.77 and Figure 4.78 for the SNR levels of infinity, 20 dB, 15 dB, 10 dB, 5 dB and 0 dB, respectively. The correct classification rates computed at each testing SNR level are listed in Table 4.10 and plotted in Figure 4.79.

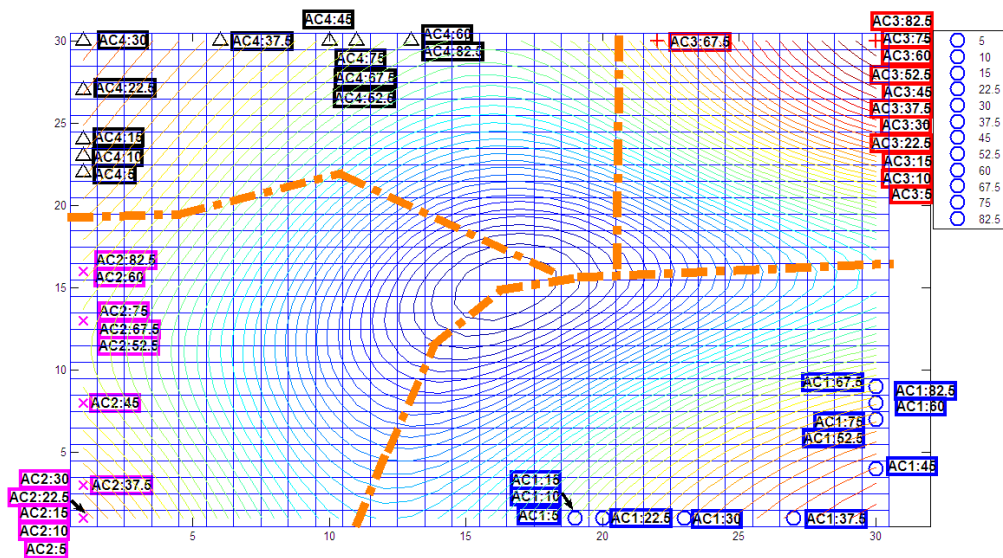


Figure 4.73 SOM Classifier #16 tested by noise-free feature vectors of the aircraft AC1 (blue circles), AC2 (magenta crosses), AC3 (red plus signs) and AC4 (black triangles).

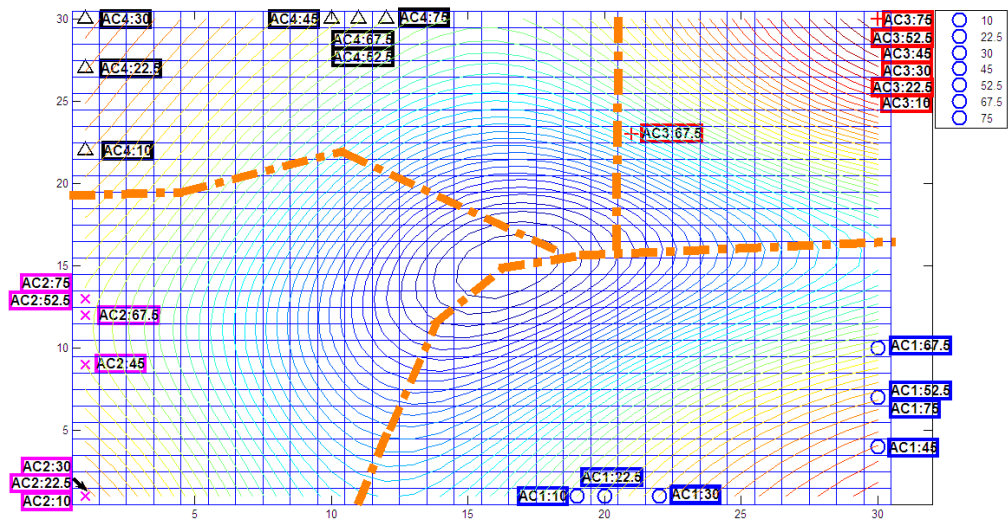


Figure 4.74 SOM Classifier #16 tested by noisy feature vectors of the aircraft AC1 (blue circles), AC2 (magenta crosses), AC3 (red plus signs) and AC4 (black triangles) at 20 dB SNR level.

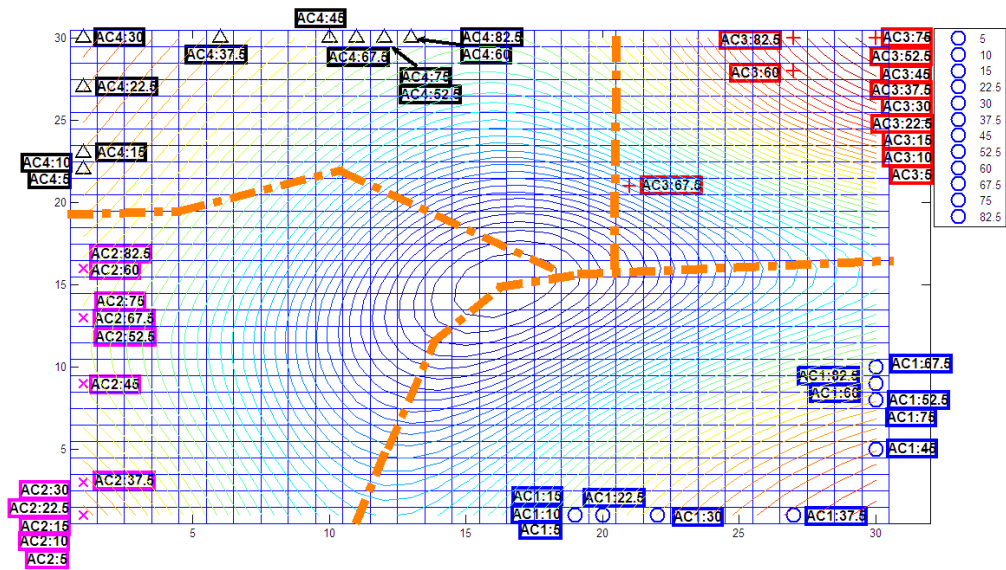


Figure 4.75 SOM Classifier #16 tested by noisy feature vectors of the aircraft AC1 (blue circles), AC2 (magenta crosses), AC3 (red plus signs) and AC4 (black triangles) at 15 dB SNR level.

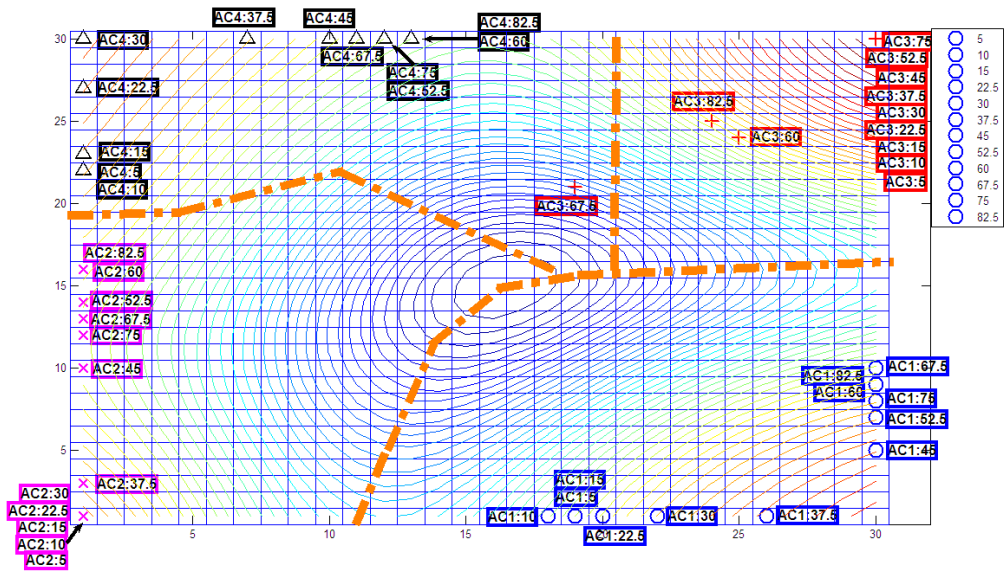


Figure 4.76 SOM Classifier #16 tested by noisy feature vectors of the aircraft AC1 (blue circles), AC2 (magenta crosses), AC3 (red plus signs) and AC4 (black triangles) at 10 dB SNR level.

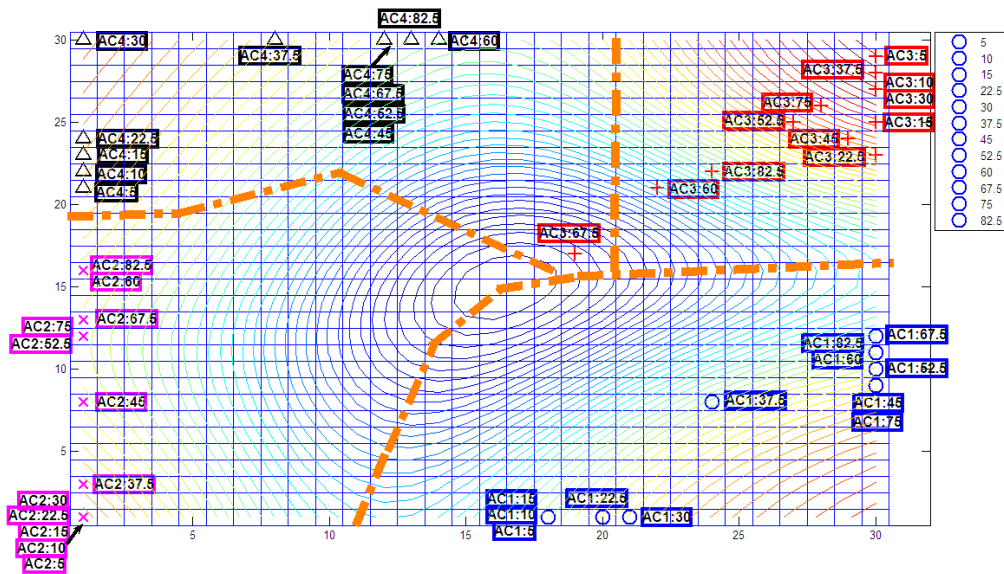


Figure 4.77 SOM Classifier #16 tested by noisy feature vectors of the aircraft AC1 (blue circles), AC2 (magenta crosses), AC3 (red plus signs) and AC4 (black triangles) at 5 dB SNR level.

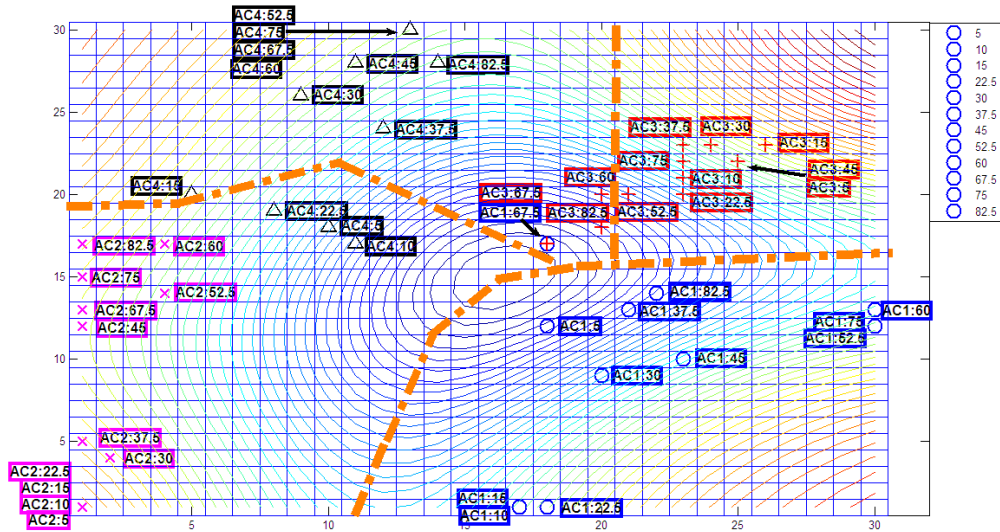


Figure 4.78 SOM Classifier #16 tested by noisy feature vectors of the aircraft AC1 (blue circles), AC2 (magenta crosses), AC3 (red plus signs) and AC4 (black triangles) at 0 dB SNR level.

Table 4.10 Correct decision rates for the Classifier #16 at different testing SNR levels for two different  $\theta$  range.

SNR	Type Of Boundary	
	For $5^\circ \leq \theta \leq 82,5^\circ$	For $10^\circ < \theta < 75^\circ$
Noise Free	100	100
20 dB	100	100
15 dB	100	100
10 dB	98	97
5 dB	98	97
0 dB	92	97

Variations of the accuracy level of Classifier #16 against decreasing SNR level is plotted in Figure 4.79. This classifier, which is designed by slightly noisy reference data, can successfully discriminate the aircraft AC1, AC2, AC3 and AC4



at all aspects and SNR levels except the target AC3 at 67.5 degree aspect angle for SNR=10 dB and SNR=5 dB testing conditions.

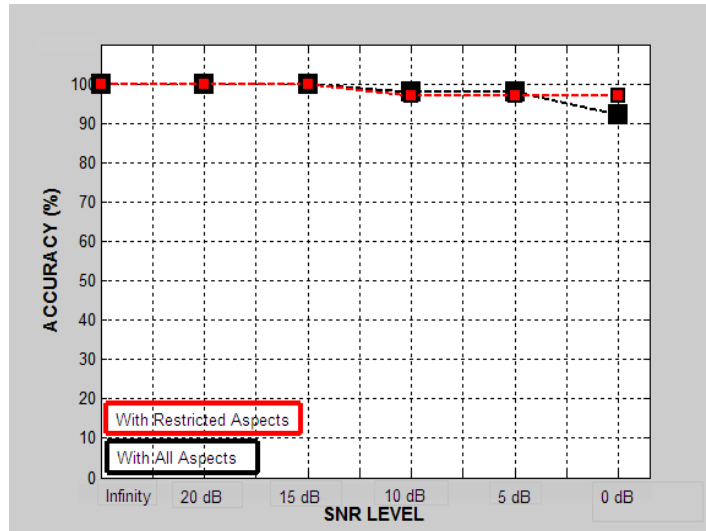


Figure 4.79 Correct classification rates computed for the Classifier #16 at various testing SNR levels for different  $\theta$  range.

#### 4.4.3. Classifier Simulation #17: Design of a SOM Classifier Using Moderately Noisy (SNR Level of 10 dB) Reference Data for the Target Library TL6 with Four Aircraft

Finally, the Classifier #17 is designed over the late-time interval [15.6-46.9] nsec using noise-free scattered data of small scale aircraft AC1, AC2, AC3 and AC4 at the reference aspects  $\theta = 5^\circ, 15^\circ, 37.5^\circ, 60^\circ, 82.5^\circ$ . The resulting SOM output with  $30 \times 30 = 900$  weight vectors (each having the length of 512) is saved as the classifier design matrix of size  $900 \times 512$ . Figure 4.80 shows the contour plot of the norms of the trained weight vectors over the SOM grid of size  $30 \times 30$ .

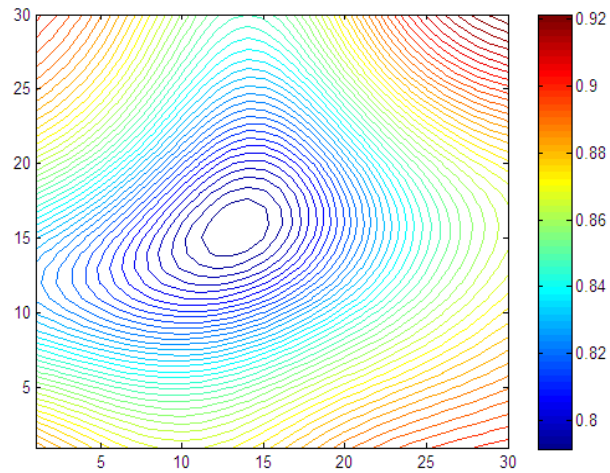


Figure 4.80 SOM output trained by noisy (SNR Level of 10 dB) WD-based late time energy feature vectors of the small scale aircraft AC1, AC2, AC3 and AC4.

The cluster boundaries as well as the winning neuron locations for the training target features are marked on this SOM output, as shown in Figure 4.81.

Next, the Classifier #17 is tested by noise-free and noisy feature vectors at 20 dB, 15 dB, 10 dB, 5 dB and 0 dB SNR levels. Locations of the testing winning neurons are marked in Figure 4.82, Figure 4.83, Figure 4.84, Figure 4.85, Figure 4.86 and Figure 4.87 for the SNR levels of infinity, 20 dB, 15 dB, 10 dB, 5 dB and 0 dB, respectively. The correct classification rates computed at each testing SNR level for each type of cluster boundary are listed in Table 4.11 and shown in Figure 4.88.

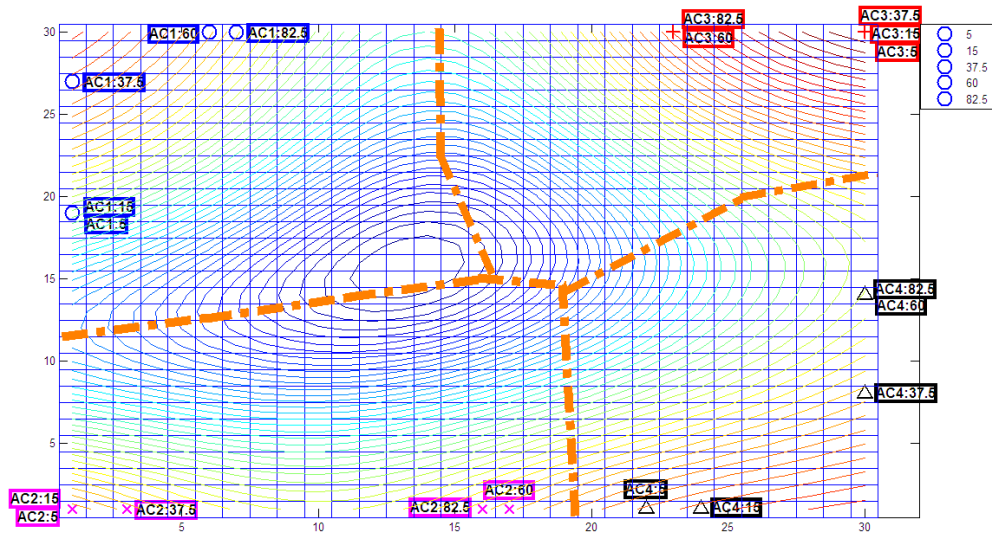


Figure 4.81 Cluster boundaries and the winning neuron locations for the training features of the aircraft AC1 (blue circles), AC2 (magenta crosses), AC3 (red plus signs) and AC4 (black triangles) over the SOM output grid for the Classifier #17.

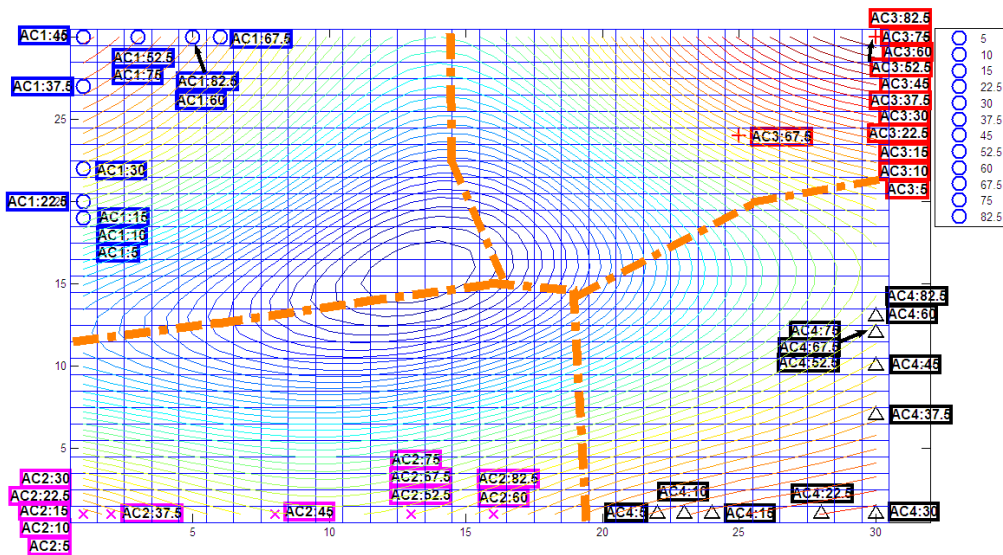


Figure 4.82 SOM Classifier #17 tested by noise-free feature vectors of the aircraft AC1 (blue circles), AC2 (magenta crosses), AC3 (red plus signs) and AC4 (black triangles).

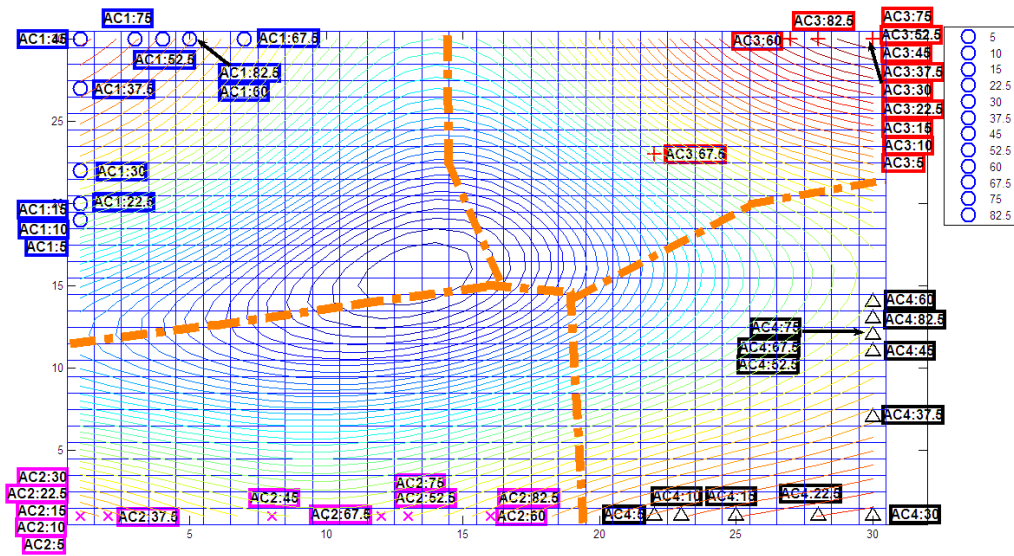


Figure 4.83 SOM Classifier #17 tested by noisy feature vectors of the aircraft AC1 (blue circles), AC2 (magenta crosses), AC3 (red plus signs) and AC4 (black triangles) at 20 dB SNR level.

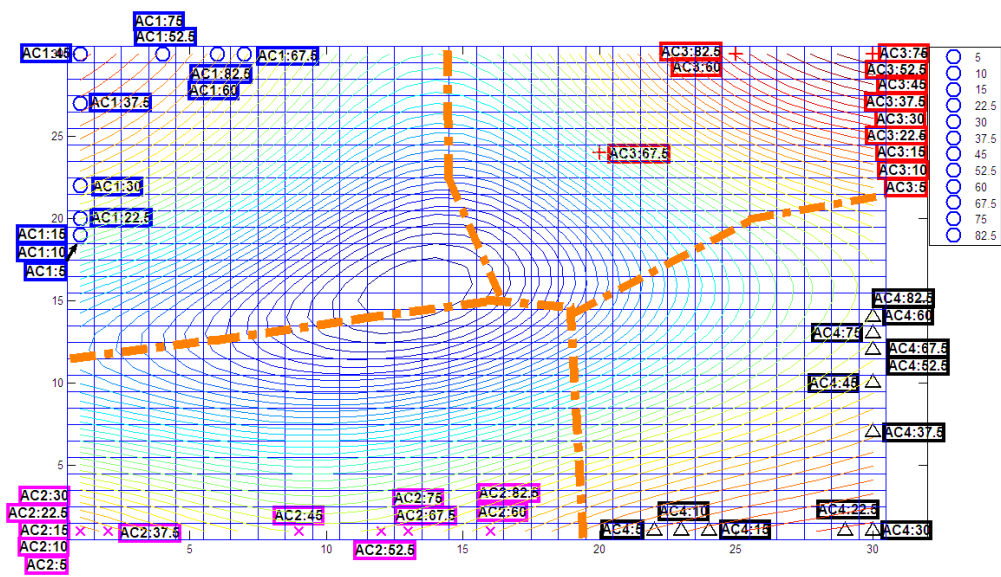


Figure 4.84 SOM Classifier #17 tested by noisy feature vectors of the aircraft AC1 (blue circles), AC2 (magenta crosses), AC3 (red plus signs) and AC4 (black triangles) at 15 dB SNR level.

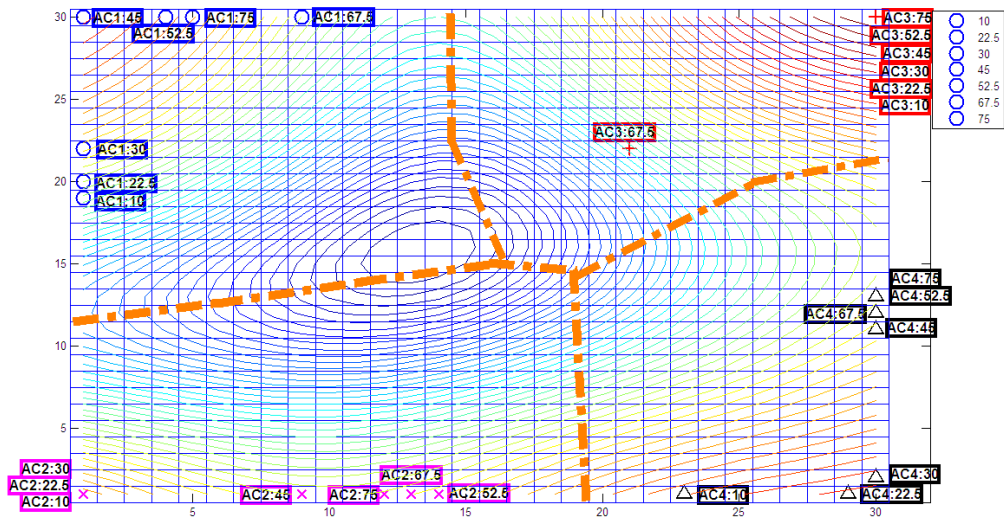


Figure 4.85 SOM Classifier #17 tested by noisy feature vectors of the aircraft AC1 (blue circles), AC2 (magenta crosses), AC3 (red plus signs) and AC4 (black triangles) at 10 dB SNR level.

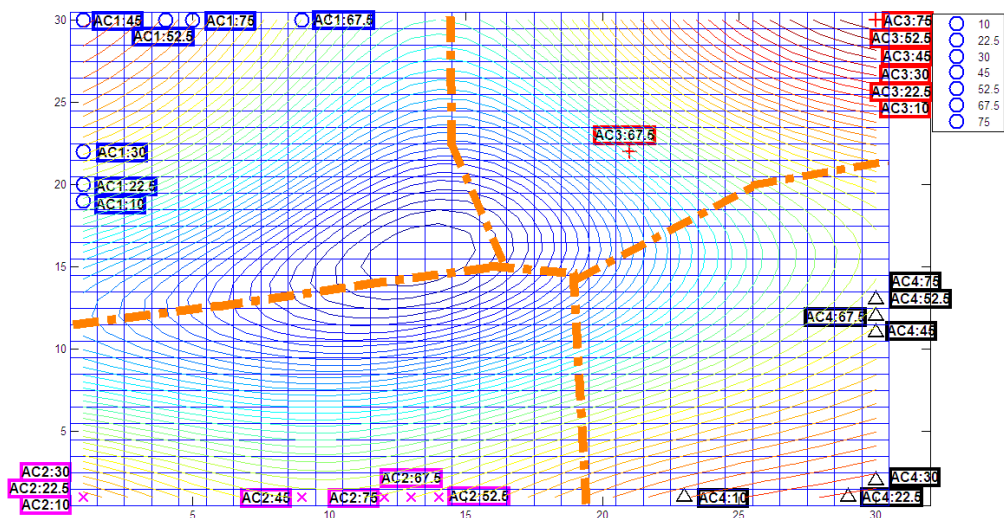


Figure 4.86 SOM Classifier #17 tested by noisy feature vectors of the aircraft AC1 (blue circles), AC2 (magenta crosses), AC3 (red plus signs) and AC4 (black triangles) at 5 dB SNR level.

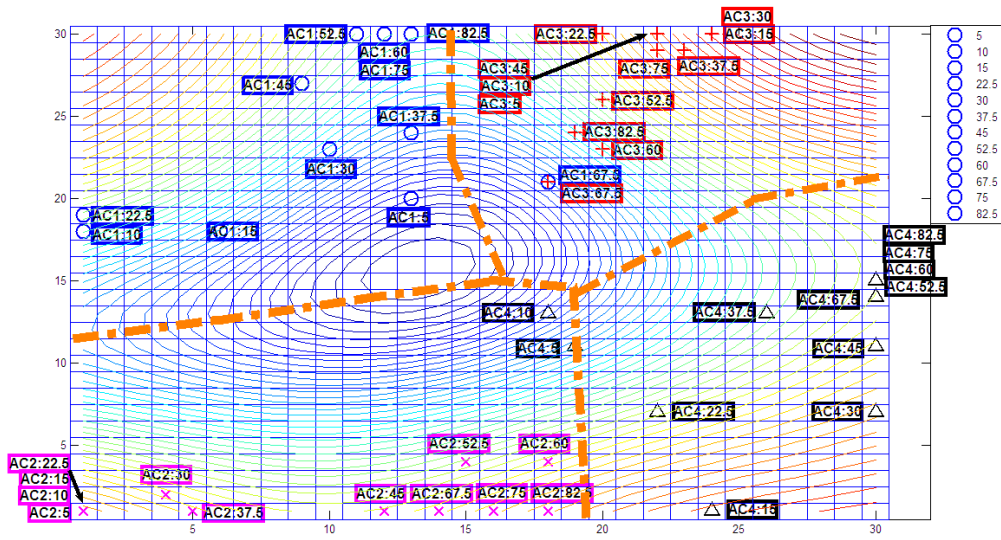


Figure 4.87 SOM Classifier #17 tested by noisy feature vectors of the aircraft AC1 (blue circles), AC2 (magenta crosses), AC3 (red plus signs) and AC4 (black triangles) at 0 dB SNR level.

Table 4.11 Correct decision rates for the Classifier #17 at different testing SNR levels for two different  $\theta$  range.

SNR	Type Of Boundary	
	For $5^\circ \leq \theta \leq 82,5^\circ$	For $10^\circ < \theta < 75^\circ$
Noise Free	100	100
20 dB	100	100
15 dB	100	100
10 dB	100	100
5 dB	100	100
0 dB	92	97

Accuracy rates of Classifier #17 against decreasing SNR levels are plotted in Figure 4.88.

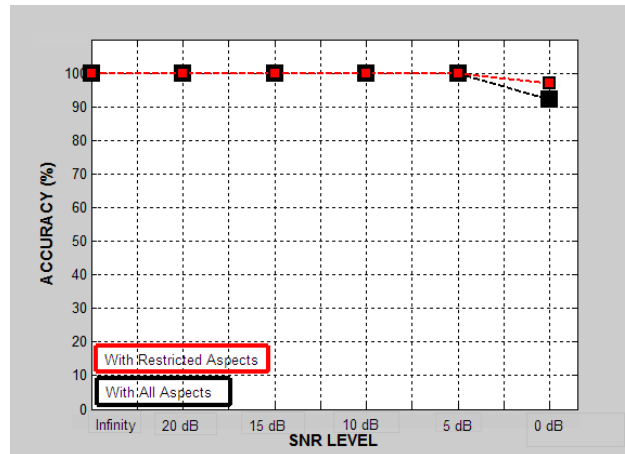


Figure 4.88 Correct classification rates computed for the Classifier #17 at various testing SNR levels for different  $\theta$  range.

The correct classification rates of both Classifier #16 and Classifier #17 are 100 percent at all testing SNR levels except the 0 dB SNR level. However, Classifier #17 actually performs better as its winning test neurons are not affected much from decreasing SNR levels. Therefore, Classifier #17 can discriminate all four model aircraft from each other by quite large safety margins. In this chapter it is demonstrated that the robustness of the SOM based electromagnetic target classifiers get much better when they are trained by slightly or moderately noisy reference database. An accuracy rate improvement of more than 40 percent is realized at 0 dB SNR levels for instance, by the classifier designs at 20 dB and 10 dB SNR levels.

## CHAPTER 5

### CONCLUSION

In this thesis, the use of SOM type neural networks and Wigner distribution based feature extraction techniques are used for electromagnetic target classification. The computer codes used to determine the optimal late-time design intervals and to test the classifiers are developed in MATLAB. The SOM Toolbox 2 [18] is used for initialization and sequential training of the SOM classifiers in the design phase. Target libraries used in design and test simulations have included two different target classes; dielectric spheres and small-scale aircraft modeled by perfectly conducting thin wires.

Target features used in SOM training are extracted by using the Wigner Distribution which is a well-known time-frequency transformation technique and its output can be interpreted as a map giving the distribution of total signal energy in the two-dimensional time-frequency plane. Hence, WD output gives valuable information about the spectral content of natural target response over an arbitrarily chosen late-time interval. Noise performance of target classifiers, which process late-time scattered signals, should be carefully tested because the effective SNR levels of the design and test data over the chosen late-time design intervals are usually much lower than the overall SNR levels of these signals. In this thesis, all of the simulated SOM classifiers are tested at various SNR levels from infinity to very low values such as 5 dB or even zero dB. Also, for each chosen target library, several classifiers are designed by using SOM techniques first by using noise-free



reference data at predetermined reference aspects, then by using slightly noisy (at 20 dB SNR) and moderately noisy (at 10 dB SNR) reference data. The simulated classifiers are extensively tested at various SNR levels changing from infinity (the noise-free case) to low SNR levels such as 10 dB or 0 dB. General trends observed in classifier performances may show variations from one target class to another as summarized below:

First of all, SOM based classifiers are designed using noise-free reference data for various target libraries containing dielectric spheres. The target libraries named TL1, TL2 and TL3 are composed of 2, 3 and 4 dielectric spheres, respectively. The lossless dielectric spheres S1, S2, S3 and S4 are very similar to each other as they have exactly the same shape and the same size with radii of 10 cm and their relative permittivity values ( $\epsilon_r = 3, 4, 5, 6$ ) are close to each other. The first target library TL1 contains two spheres S1 and S2 with radii of 10 and relative permittivities of 3, 4, respectively. The second library TL2, has 3 spheres S1, S2 and S3 with radii of 10 and relative permittivities of 3, 4, 5. Finally, the third library TL3, has 4 spheres S1, S2, S3 and S4 with radii of 10 and relative permittivities of 3, 4, 5, 6. Accuracy rates (i.e., the correct classification rates) for each one of these three libraries are computed and compared under the noise-free/noisy design and noise-free/noisy test cases.

As it seen clearly from Figure 3.10 and Table 3.2, the SOM based Classifier #1, which is designed by noise-free reference data, can successfully discriminate the spheres S1 and S2 under low noise testing conditions but its performance degrades as the testing SNR decreases. Next, Classifier #2 is designed for the same target library TL1 (of dielectric spheres S1 and S2) by using slightly noisy reference data at 20 dB SNR level to improve the classification performance at lower testing SNR values. Based on the correct decision rates reported in Table 3.2 and Table 3.3, it is clearly seen that Classifier #2 displays a much better noise performance

as compared to Classifier #1. Then, Classifier #3 is designed for the same 2-target library TL1 using moderately noisy (SNR level of 10 dB) scattered data but the resulting classifier is not found useful at all. Therefore, it is concluded that a slightly noisy training data set helps improving the accuracy rate of the SOM classifier at low SNR levels but too much noise in the training data set leads to completely unsuccessful design results.

Next, three different SOM classifiers are designed for the target library TL2 of three dielectric spheres S1 ( $r=10$  cm,  $\epsilon=3$ ), S2 ( $r=10$  cm,  $\epsilon=4$ ), S3 ( $r=10$  cm,  $\epsilon=5$ ). The first classifier, Classifier #4, is designed by using noise-free reference data and it is tested at all non-reference aspects for the SNR levels of infinity, 20 dB, 15 dB and 10 dB. Then the same task is repeated with slightly noisy reference data at 20 dB SNR level to design Classifier #5 and also repeated with moderately noisy reference data at 10 dB SNR level to design Classifier #6. Classifier #4, which is designed by noise-free reference data, can successfully discriminate the spheres S1, S2 and S3 under low noise testing conditions but its performance degrades as the testing SNR decreases, as also observed in the case of two sphere classifiers. Classifier #5 which is designed by slightly noisy reference data can also discriminate the spheres, but its performance of accuracy as compared to Classifier #4 is poor at all testing noise levels. As the classifier #6 cannot be successfully designed by using noisy reference data at 10 dB SNR, details of test results are not reported as they are practically not meaningful.

At the last part of dielectric sphere classifiers, design and test tasks are repeated for the target library TL3, of four dielectric spheres S1 ( $r=10$  cm,  $\epsilon=3$ ), S2 ( $r=10$  cm,  $\epsilon=4$ ), S3 ( $r=10$  cm,  $\epsilon=5$ ), S4 ( $r=10$  cm,  $\epsilon=6$ ) but classifier design with reference data at 10 dB SNR level is not considered, as the use of moderately noisy data in classifier design is demonstrated to be useless in Classifier Simulation #6. Then, Classifier #7 (designed by noise-free reference data) and Classifier #8 (designed by slightly noisy reference data) are both found to

discriminate the spheres S1, S2, S3 and S4 successfully under noise free and low noise testing conditions. The performance of Classifier #8 is found even better at very low SNR levels.

In summary, after all these eight classifier simulations for dielectric spheres, it can be concluded that the SOM classifiers which are designed with noise free or slightly noisy reference data can discriminate spheres under low noise testing conditions, but their performance of accuracy degrades with decreasing SNR, as expected. Also, slightly noisy reference data for the design of dielectric sphere classifiers helps improving the noise performance of the SOM classifiers.

In Chapter 4, SOM type classifier design applications and their results are reported for target libraries TL4, TL5 and TL6 which contain two, three and four small scale aircraft, respectively. These target libraries contain model aircraft Airbus, Boeing 747, P-7 and Tu 154 which are called as AC1, AC2, AC3 and, AC4 in short. The small scale target dimensions are obtained using a factor of 100 with quite similar wire lengths for the body, wing and tail of these four conducting simplified aircraft models. The length to radius ratio of 2000 is used in all wire parts while modeling these targets.

For any given aircraft target library, the SOM classifiers are designed by using noise-free, slightly noisy (with SNR=20 dB) and moderately noisy (with SNR=10 dB) reference data at a chosen set of reference aspect angles. Then, each of the resulting classifiers is tested for its accuracy rate at the signal-to-noise ratio (SNR) levels of infinity (the noise-free testing database case), 20 dB, 15 dB, 10 dB, 5 dB and 0 dB to see if these classifiers are robust enough under noisy testing conditions.

Firstly, three different SOM classifiers are designed for the simplest target library TL4, which contains only two aircraft AC1 (Airbus) and AC2 (Boeing 747). The first classifier, the Classifier #9, is designed by using noise-free reference data and it is tested at all SNR levels of infinity, 20 dB, 15 dB, 10 dB, 5 dB and 0 dB. Then, two more classifiers, the Classifier #10 and Classifier #11) are designed first with slightly noisy reference data (at 20 dB SNR level) and then using moderately noisy reference data (at 10 dB SNR level), respectively. The SOM based Classifier #9, can successfully discriminate the aircraft AC1 and AC2 under low noise testing conditions but its performance degrades as the testing SNR decreases. On the other hand performances of Classifier #10 and Classifier #11 are perfect, at least within the SNR levels (from infinity to 0 dB) considered.

Next, three different SOM classifiers are designed for the target library TL5, which is composed of three aircraft AC1 (Airbus), AC2 (Boeing 747) and AC4 (Tu 154). The first classifier, Classifier #12, is designed by using noise-free reference data and it is tested at all SNR levels of infinity, 20 dB, 15 dB, 10 dB, 5 dB and 0 dB. Then the same task is repeated with slightly noisy reference data at 20 dB SNR level for the design of Classifier #13, and then with moderately noisy reference data at 10 dB SNR level for the design of Classifier #14. Accuracy rate of Classifier #12 becomes less than 100 percent at 5 dB SNR level, and it degrades sharply at 0 dB SNR level. Winning neuron locations of test aspects at 0 dB SNR level is gathered around cluster boundaries. On the other hand, accuracy levels of the Classifier #13 and Classifier #14 become less than 100 percent at only 0 dB SNR level, the locations of winning neurons show little changes with decreasing SNR levels as opposed to the case that is observed for Classifier #12.

At the last part of conducting aircraft classifiers, design and test tasks are repeated for the target library TL6 which contains all four aircraft AC1 (Airbus), AC2 (Boeing 747), AC3 (P-7), AC4 (Tu 154). Classifier #15 which is designed by noise-free reference data, can successfully discriminate the aircraft AC1, AC2,

AC3 and AC4 under low noise testing conditions but its performance degrades as the testing SNR decreases, more importantly the safety margins of classification seriously degrades as the SNR level gets lower. The correct classification rates of both Classifier #16 and Classifier #17 are 100 percent at all SNR levels except 0 dB. However, Classifier #17 actually performs better as the locations of its winning and test neurons are not affected much from decreasing SNR levels.

In this thesis, usefulness of SOM based electromagnetic target classifiers is demonstrated for both dielectric and conducting targets. It is also demonstrated that use of noisy target features in SOM training improves the noise robustness of the resulting classifiers. The classifiers for dielectric spheres can discriminate these targets even under low SNR testing conditions only when they are designed with noise free or slightly noisy reference data although their accuracy rates degrade with decreasing SNR, as expected. For the class of spheres, use of slightly noisy training features (at 20 db SNR) is found definitely advantageous but the same is not true for using moderately noisy (at 10 dB SNR) training features. The classifiers for conducting aircraft, however, show their best performance when they are designed by 10 dB SNR reference data.

In summary, the SOM based target classifiers are designed with very high accuracy rates for both dielectric spheres and conducting aircraft models. The classifiers are found perfectly robust under low SNR levels especially when they are designed by using tolerably noisy reference target features.

Performance of the SOM classifiers are dependent on the optimal late-time design interval over which the input vectors are computed prior to SOM training. A fully automatic method for the selection of this optimal time interval in a completely unsupervised manner, i.e. without knowing anything about the identity of targets, needs to be suggested in a future work. In other words, not only the learning algorithm of the SOM network but also the feature extraction process should be made unsupervised to get the full benefit of this self-organizing approach in electromagnetic target recognition problems.

## REFERENCES

- [1] D.L. Moffatt, J.D. Young, A.A. Ksienski, H. Lin and C.M. Fhoads, "Transient Response Characteristics in Identification and Imaging", IEEE Trans. Antennas and Propagation, AP-29, pp.192-205, 1981.
  
- [2] E.M. Kennaugh, "The K-Pulse Concept", IEEE Trans. Antennas and Propagation, Vol.AP-29, pp. 327-331, March 1981.
  
- [3] G. Turhan-Sayan, "Natural Resonance-Based Feature Extraction with Reduced Aspect Sensitivity for Electromagnetic Target Classification", Pattern Recognition, Vol.36, No. 7, pp. 1449-1466, July 2003.
  
- [4] G. Turhan-Sayan, "Real Time Electromagnetic Target Classification Using a Novel Feature Extraction Technique with PCA-Based Fusion", IEEE Transactions On Antennas and Propagation, Vol. 53, No.2, pp. 766-776, February 2005.
  
- [5] D.P.Nyquist, K.M.Chen, E.Rothwell and B.Drachman, "Radar Target Discrimination Using the Extinction-Pulse Technique", IEEE Transaction on Antennas and Propagation, vol. AP-33, pp. 929-937, Sept. 1985.
  
- [6] Emre Ergin, "Investigation of Music Algorithm Based and WD-PCA Method Based Electromagnetic Target Classification Techniques For Their

Noise Performances", M. Sc. Thesis, Middle East Technical University, October 2009.

- [7] G. Turhan-Sayan, S. Inan, T.Ince, K.Leblebicioğlu, "Applications of Artificial Neural Networks and Genetic Algorithms to Electromagnetic Target Classification", The Application of Information Technologies (Computer) Science to Mission Systems, Monterey, USA, April 1998.
  
- [8] G. Turhan Sayan, K.Leblebicioğlu and T.Ince, "Electromagnetic target Classification Using Time-Frequency Analysis and Neural Networks", Microwave and Optical Techn. Lett., vol.21, no.1, pp. 63-69, Apr.1999.
  
- [9] Azimi-Sadjadi.M.R, De Yao, QiangHuang, Dobeck.G.J "Underwater target classification using wavelet packets and neural networks ", Neural Networks, IEEE Transactions on, Volume:11, Issue:3, pp. 784-795, May 2000
  
- [10] Jouny, I. Garber, F.D. Ahalt, S.C. "Classification of radar targets using synthetic neural networks ", Aerospace and Electronic Systems, IEEE Transactions on, Volume:29, Issue:2, pp. 336-344, April 1993
  
- [11] Xi Miao; Azimi-Sadjadi, M.R. Bin Tan; Dubey, A.C.; Witherspoon "Detection of mines and mine-like targets using principal component and neural-network methods", Neural Networks, IEEE Transactions on, Volume: 9, Issue: 3, pp. 454-463, May 1998
  
- [12] R.Soleti, L.Cantaini, F.Berizzi, A.Capria, D.Calugi, "Neural Network For Polarimetric Radar Target Classification", Unpublished Notes.

- [13] Mehmet Serol Doğaner, "Target Classification by Using SOM Type Neural Networks". M. Sc. Thesis, Middle East Technical University, 2000.
- [14] T. Kohonen, Self-Organization and Associative Memory, Springer-Verlag, Berlin, 1989.
- [15] T. Kohonen, "The Self-Organizing Maps " Springer-Verlag,1995
- [16] Jose Alfredo Ferrira Costa, "Data Clustering using Self-Organizing Maps with 3-D Output Grids ", Unpublished Notes.
- [17] Juha Vesanto,Esa Alhoniemi, "Clustering Of The Self Organizing Map" Unpublished Notes.
- [18] Juha Vesanto, Johan Himberg, Esa Alhoniemi and Juha Parhankangas, "SOM Toolbox for Matlab 5"
- [19] M. O. Ersoy, "Application of a Natural-Resonance Based Feature Extraction Technique to Small-Scale Aircraft Modeled by Conducting Wires for Electromagnetic Target Classification," M. Sc. Thesis, Middle East Technical University, September 2004.
- [20] L. Cohen, Time–Frequency Analysis, Prentice-Hall, Englewood CliBs, NJ, 1995.
- [21] T. Germano, "Self Organizing Maps", Unpublished Notes, March 1999.
- [22] Juha Vesanto, "Data Mining Techniques Based on the Self-Organizing Map", Ms. Thesis, Helsinki University of Technology, May 1997



- [23] Alfred Ultsch, Fabian Morchen, "ESOM-Maps: Tools for Clustering, Visualization and Classification with Emergent SOM" Unpublished Notes.
  
- [24] J. Himberg, J. Ahola, E. Alhoniemi, J. Vesanto, O. Simula, "The Self Organizing Map as a Tool in Knowledge Engineering", Unpublished Notes.
  
- [25] M. Gastine, L. Cortois and J. L. Dormann, "Electromagnetic resonances of free dielectric ", *Microwave Theory and Techniques*, IEEE Transactions on, Volume:15, pp. 694-700, 1967.
  
- [26] M. Kerker, "The Scattering of Light and other Electromagnetic Radiation", New York Academic Press, 1969.
  
- [27] K.T. Kim, L.S. Choi and H.T. Kim, "Efficient Radar Target Classification Using Adaptive Joint Time-Frequency Processing", *Antennas and Propagation*, IEEE Transactions on, Volume:48, pp. 1789-1801, December 2000.
  
- [28] M. Secmen, "A Novel Music Algorithm Based Electromagnetic Target Recognition Method in Resonance Region for the Classification of Single and Multiple Targets", Ph.D. Thesis, Middle East Technical University, February 2008.
  
- [29] M. Secmen and G. Turhan-Sayan, "Radar target classification method with reduced aspect dependency and improved noise performance using multiple signal classification algorithm", *IET Radar Sonar Navig.* Volume 3, Issue 6, Pages 583–595, December 2009.

## APPENDIX

### A SAMPLE PROGRAM CODE WRITTEN IN MATLAB FOR DESIGNING SOM CLASSIFIERS

```
%THIS PROGRAM IS FOR CLASSIFYING DIFFERENT SPHERES BY  
USING SOM
```

```
%There are 5 Steps In Program Body  
%1.Construct The DATA  
%2.Initialize Map  
%3.Training Step  
%4.Visualize Map  
%5.Analyze Map
```

```
%=====
```

```
                                %1.Construct The DATA
```

```
%=====
```

```
clear;  
%For Taking The Date From the desired interval  
% 2*512=1024 variables are used in program
```

```
%NL=input('Enter lower band index');  
NL=11;  
%NU=input('Enter upper band index');  
NU=12;
```

```
% 2*512=1024 variables are used in program  
NLi=512*(NL-1)+1  
NUi=512*NU
```

```
%cd ('c:\My Documents\PCA_paper\sphere_data\sph10eps3')  
load fw10_3_179.dat  
f1=fw10_3_179(NLi:NUi);  
load fw10_3_165.dat  
f2=fw10_3_165(NLi:NUi);  
load fw10_3_150.dat  
f3=fw10_3_150(NLi:NUi);  
load fw10_3_135.dat  
f4=fw10_3_135(NLi:NUi);  
load fw10_3_120.dat  
f5=fw10_3_120(NLi:NUi);  
load fw10_3_105.dat  
f6=fw10_3_105(NLi:NUi);  
load fw10_3_90.dat
```

```

f7=fw10_3_90(NLi:NUi);
load fw10_3_75.dat
f8=fw10_3_75(NLi:NUi);
load fw10_3_60.dat
f9=fw10_3_60(NLi:NUi);
load fw10_3_45.dat
f10=fw10_3_45(NLi:NUi);
load fw10_3_30.dat
f11=fw10_3_30(NLi:NUi);
load fw10_3_15.dat
f12=fw10_3_15(NLi:NUi);
load fw10_3_5.dat
f13=fw10_3_5(NLi:NUi);

% %cd ('c:\My Documents\PCA_paper\sphere_data\sph10eps4')
load fw10_4_179.dat
f14=fw10_4_179(NLi:NUi);
load fw10_4_165.dat
f15=fw10_4_165(NLi:NUi);
load fw10_4_150.dat
f16=fw10_4_150(NLi:NUi);
load fw10_4_135.dat
f17=fw10_4_135(NLi:NUi);
load fw10_4_120.dat
f18=fw10_4_120(NLi:NUi);
load fw10_4_105.dat
f19=fw10_4_105(NLi:NUi);
load fw10_4_90.dat
f20=fw10_4_90(NLi:NUi);
load fw10_4_75.dat
f21=fw10_4_75(NLi:NUi);
load fw10_4_60.dat
f22=fw10_4_60(NLi:NUi);
load fw10_4_45.dat
f23=fw10_4_45(NLi:NUi);
load fw10_4_30.dat
f24=fw10_4_30(NLi:NUi);
load fw10_4_15.dat
f25=fw10_4_15(NLi:NUi);
load fw10_4_5.dat
f26=fw10_4_5(NLi:NUi);

% The aim is clustering two types of spheres
% First one is 10_3 the other is 10_4

% ftotal is the whole data set which will be divided into
Train&Test Sets
ftotal=[f1
        f2
        f3
        f4
        f5
        f6
        f7
        f8
        f9

```

```

f10
f11
f12
f13
f14
f15
f16
f17
f18
f19
f20
f21
f22
f23
f24
f25
f26];

%the components of the data set are usually normalized,
% in this program example each component will have unit variance.

for i=1:26
    a=0;
    for j=1:1024
        a=a+(ftotal(i,j)*ftotal(i,j));
    end
    payda=sqrt(a);
    ff(i,:)=ftotal(i,:)/payda;
end

%8 vectors chosen from desired data groups for training
% 135',105',75',30' data for each group will used for training

ftrain=[ff(4,:)
ff(6,:)
ff(8,:)
ff(11,:)
ff(17,:)
ff(19,:)
ff(21,:)
ff(24,:)] ;

%
%=====
%
%                %2.Initialize Map
%
%    %The following parameters have to be set;
%
%    %i) the topology (rectangular or hexagonal)
%
%    %ii) the size of the map (X,Y dimensions)
%
%    %iii)the initializatio of map units
%
%                %som_randinit
%=====

```

```

% %The [12*12] map is initialized randomly
sM=som_randinit(ff,'msize',[12 12],'rect');

%=====

                %3.Training Step
                %At the training step,parameters are;
                %i) learning type (batch or sequential)
                   % som_batchtrain, som_seqtrain
                %ii) neighborhood function type
("bubble,gaussian,cutgauss,")
                %iii)neighborhood radius
                %iv) learning rate
                %v ) learning_lenght (number of samples /epochs)
                   %som_randinit or som_lininit
%=====

%In this program, sequential learning is used , with [12*12]map,
%neighborhood radius decreased from 7 to 3 , initial learning rate
set as
%0.5 , training lenght is 500 epochs, the samples from data is
chosen
%randomly step by step, bubble is used as neighborhood function

sM = som_seqtrain (sM, ftrain, 'msize', [12 12], 'radius',[7 3],
'alphaini', 0.5, 'trainlen',500, 'trainlen_type', 'epochs',
'sample_order','random','neigh','gaussian')

ftrain=[ff(1,:)
        ff(4,:)
        ff(6,:)
        ff(8,:)
        ff(11,:)
        ff(13,:)
        ff(14,:)
        ff(17,:)
        ff(19,:)
        ff(21,:)
        ff(24,:)
        ff(26,:)]];

sM = som_seqtrain (sM, ftrain, 'msize', [12 12], 'radius',[7 3],
'alphaini', 0.5, 'trainlen',500, 'trainlen_type', 'epochs',
'sample_order','random','neigh','gaussian')

%We will try to see the 'U Matrix'.It shows distances between
neighboring units and thus
%visualizes the cluster structure of the map.
%High values on the U-matrix mean large distance between
%neighboring map units, and thus indicate cluster
%borders. Clusters are typically uniform areas of low values.

```

```
%
%=====
%                               %4.Visualize Map
%
%=====

%The basic som_show_funtion is used for this purpose
som_show(sM,'umat','all')
```